1987

Hydrodynamic Study Of Bubble Column Flotation For The Recovery Of Heavy Minerals From Oilsand Tailings

Mku Thaddeus Ityokumbul

NOTICE

The quality of this microform is heavily dependent upon the quality of the original thesis submitted for microfilming. Every effort has been made to ensure the highest quality of reproduction possible.

If pages are missing, contact the university which granted the degree.

Some pages may have indistinct print especially if the original pages were typed with a poor typewriter ribbon or if the university sent us an inferior photocopy.

Previously copyrighted materials (journal articles, published tests, etc.) are not filmed.

Reproduction in full or in part of this microform is governed by the Canadian Copyright Act, R.S.C. 1970, c. C-30.

AVIS

La qualité de cette microforme dépend grandement de la qualité de la thèse soumise au microfilmage. Nous avons tout fait pour assurer une qualité supérieure de reproduction.

S'il manque des pages, veuillez communiquer avec l'université qui a conféré le grade.

La qualité d'impression de certaines pages peut laisser à désirer, surtout si les pages originales ont été dactylographiées à l'aide d'un ruban usé ou si l'université nous a fait parvenir une photocopie de qualité inférieure.

Les documents qui font déjà l'objet d'un droit d'auteur (articles de revue, tests publiés, etc.) ne sont pas microfilmés.

La reproduction, même partielle, de cette microforme est soumise à la Loi canadienne sur le droit d'auteur, SRC 1970, c. C-30.

HYDRODYNAMIC STUDY OF BUBBLE COLUMN FLOTATION FOR THE RECOVERY OF HEAVY MINERALS FROM OILSAND TAILINGS

by

Mku Thaddeus Ityokumbul

Faculty of Engineering Science

Submitted in partial fulfillment
of the requirements for the degree of
Doctor of Philosophy

Faculty of Graduate Studies
The University of Western Ontario
London, Canada

October, 1986

ISBN 0-315-40779-4

ABSTRACT

A hydrodynamic study of bubble column flotation for the recovery of titanium and zirconium minerals from oilsand tailings has been carried out in a 0.06 m (i.d.) column. A beneficiation process for these tailings was also developed which ensures the recovery of rare earth minerals.

The optimum conditions for the recovery of these minerals were found to be at a frother concentration of 0.15% (v/v) pine oil and a pH range of 8.3 to 11.7. Low recoveries were obtained at frother concentrations exceeding 0.2% (v/v) pine oil.

Individual phase hold-ups were estimated using the static pressure method. Flow regimes were identified using the changes in bubble rise velocity with gas velocity. For all the systems considered here, the liquid hold-up decreased with increasing gas velocity in the chain bubbling and bubbly flow regimes. The addition of a frother generally resulted in a decrease in the liquid hold-up, bubble size and rise velocity. The presence of solids in the column did not have any significant effect on the gas hold-up except for gas velocities at which solids were observed on the gas distributor.

The control of gangue recovery in a bubble column

flotation cell is presently accomplished with the addition of wash water near the froth-pulp interface. The results obtained here show that the height of the calming zone may be effectively used to control gangue recovery.

Liquid phase axial mixing coefficients were estimated using the pulse technique. The parameters were estimated in the frequency domain using Parseval's theorem. The isotropic turbulence theory of Baird and Rice was used to provide dimensionally consistent correlations for the chain bubbling and bubbly flow regimes. The variation of the liquid dispersion coefficient with gas velocity was found to agree rather closely with the flow regime mapping. The results obtained indicate that the gas phase Froude number is a useful criterion for characterizing flow regimes in vertical bubble columns. The addition of frother generally resulted in an increase in the liquid dispersion coefficient while the presence of solids had the opposite effect.

ACKNOWLEDGEMENTS

The author wishes to express his sincere gratitude to Drs. N. Kosaric and W. Bulani to whom he is deeply indebted for their valuable guidance and continuous encouragement throughout the course of this study. Appreciation is also expressed to Dr. W.L. Cairns for his helpful discussion in the early stages of this work.

Thanks are due to my dear friends Dr. Joshua Ndur and Mr. Isaac Imasuen for their continued support and to all the graduate students in the Chemical/Biochemical group especially Ginette Turcotte, for the long discussions on some aspects of my literature review.

The author also expresses his appreciation to the Canadian Commonwealth Scholarship and Fellowship Administration for granting him a scholarship to study in Canada.

Finally, I would like to express my deepest appreciation to my entire family especially my wife, Benedicta, and children, Seember and Aondover, for their continued support throughout the course of this study.

TABLE OF CONTENTS

LIST OF TABLES

LIST OF FIGURES

LIST OF APPENDICES

NOMENCLATURE

a	interficial area, m^2 surface/m^3 reactor volume
A	cross-sectional area, m^2
C,c	concentration, kg/m^3
C^*	volumetric ratio of solids to liquid in the column
C_s^f	concentration of solids in the feed, kg/m^3 slurry
C_s^L	solid concentration at $z = L$, kg/m^3
C_s^o	solid concentration at $z = 0$, kg/m^3
C_s^r	average concentration of solids in the column, kg/m^3 slurry
$G(0)$	solid concentration at the feed point, kg/m^3
C_∞	terminal concentration of flotable solids, kg/m^3
c_m	mass of tracer injected/system void volume, kg/m^3
D	column diameter, m
d_b	bubble diameter, m
d_p	particle diameter, m
E	eddy diffusivity coefficient, m^2/s
E_c	collection efficiency
Fr	Froude number, U_g^2/gD
$g(S)$	system transfer function
$G(t)$	normalized tracer concentration, 1/s
$\bar{G}(t)$	Fourier transformation of $G(t)$
k,k'	constant, rate or adsorption, 1/s
K	equilibrium constant
P	pressure, KPa
Pe	Peclet number $V_L L/E_L$
P_m	specific energy dissipation rate
Q	volumetric flow rate, m^3/s

S	specific bubble surface area, m^2/m^3
t	time, s
U	superficial velocity, m/s
U_r	superficial liquid velocity in the recovery zone, m/s
V_∞	interstitial velocity, m/s
V_P	particle settling velocity in the presence of gas bubbles, m/s
V	particle settling velocity in a stagnant medium, m/s
Z	axial height, m

Greek Symbols

ε	hold-up
Γ, Γ_m	bubble load and maximum bubble load, kg/m^2
δ_n	defined by equation 4.15
ρ	density, kg/m^3
θ	bubble surface coverage, Γ/Γ_m
τ	mean fluid residence time, s
ω	frequency, Hz

Subscripts

F, f	feed
g	gas
L	liquid
S, s	solid
T	tailings

Superscripts

o	$z = 0$
F, f	feed

DEFINITIONS

Enrichment Factor: Ratio of the concentration of a mineral in the froth product to its concentration in the feed stream.

Mono-dispersed Solids: Solids with a narrow particle size distribution.

Selectivity Index (SI): geometric average of the ratio of the grades of constituents A to B in the froth product, R, and of B to A in the tailings, T. Mathematically,

$$SI = \sqrt{\frac{A_R}{B_R} \cdot \frac{B_T}{A_T}}$$

CHAPTER 1

INTRODUCTION

1.1 GENERAL INTRODUCTION

Bitumen is presently recovered from the Athabasca oil-sands by the Clark (1944) hot water extraction process as shown in Figure 1.1. This process produces tailings that are approximately 40% larger in volume than the volume of mined oilsands thus presenting difficult backfill and water impoundment problems. The current tailings disposal practice involves storage in large above-ground lagoons behind dykes specially constructed for this purpose. However, this practice is not environmentally sound due to the possibility of dyke failure or overflow in times of heavy run-off (e.g. Tesero dam failure in Italy on July 19, 1985). Other tailings disposal practices have been contemplated but found to be either environmentally unacceptable (Camp, 1976; Barton and Wallace, 1979) or uneconomical (Camp, 1976; Environment Canada, 1984).

In order to improve the overall economy of any tailings management scheme, the recovery of titanium, zirconium, iron and rare earth minerals which are present in the centrifuge tailings stream has been proposed (Ityokumbul et al., 1985a-c; 1986a). The recovery mechanism for these minerals

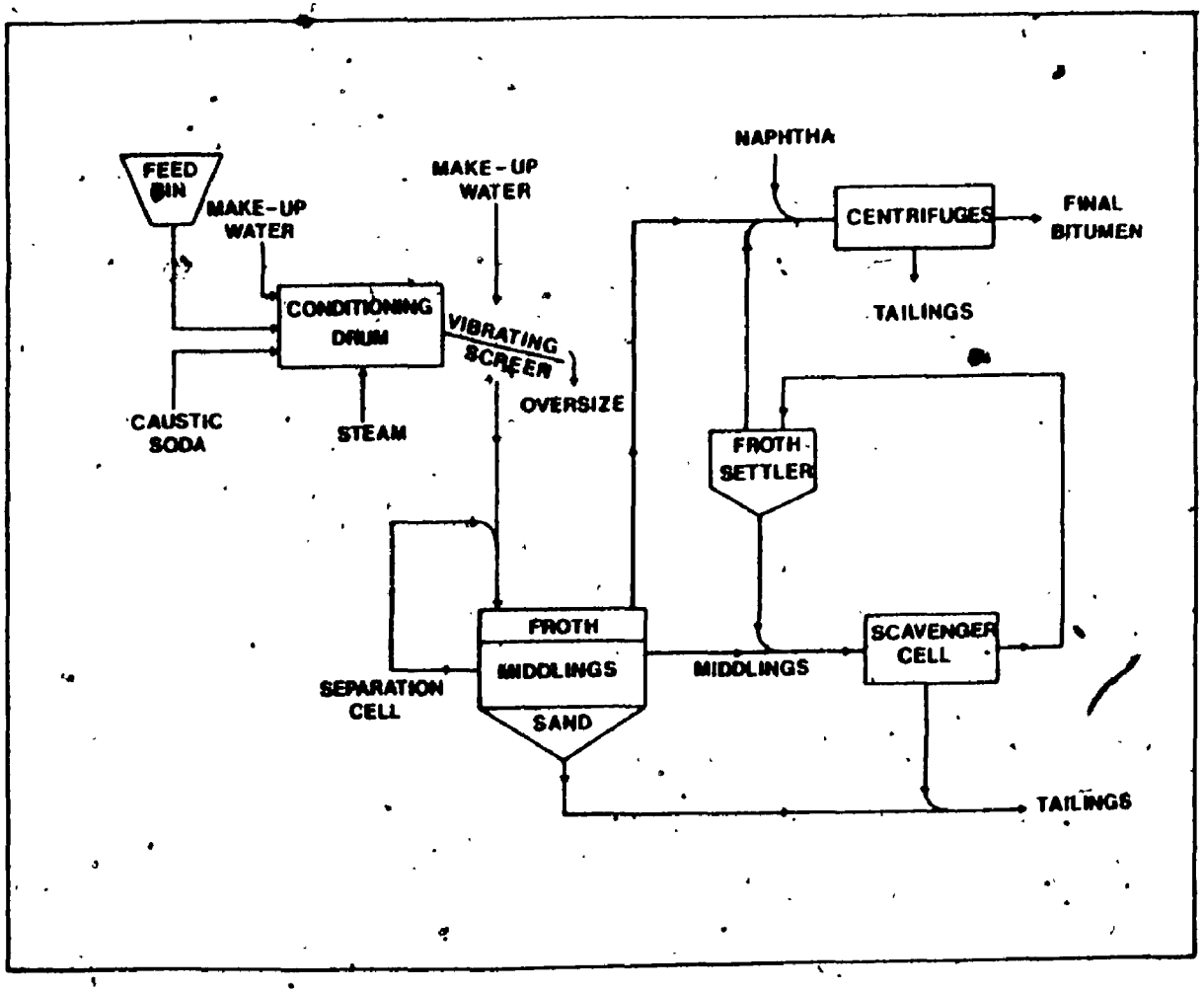

Figure 1.1 The hot water extraction process for bitumen recovery.

during the hot water extraction process has been ascribed to oil extraction and air flotation (Ityokumbul et al., 1985a). The evaluation of air flotation was selected because flotation does not interfere with the overall process objective (bitumen recovery). The reported particle size distribution of the minerals in these tailings is ideal for bubble column flotation, which was therefore chosen for a detailed study.

1.2 BUBBLE COLUMN FLOTATION

A bubble column is a multiphase contacting device in which the transport, dispersion and mixing of materials and energy is induced by the motion of the discontinuous gas phase in the form of gas bubbles in a continuous phase which may be a liquid or a homogeneous slurry (Kim, 1973; Epstein, 1981; Muroyama and Fan, 1985). A schematic of a bubble column flotation cell (flotation column) is shown in Figure 1.2.

Three zones can be identified from Figure 1.2: (1) the recovery zone extending from the feed inlet point to the base of the column, (2) the washing section which extends from the feed inlet point to the froth-pulp interface and (3) the froth zone. In the recovery section, particles suspended in the descending water phase contact a rising swarm of air bubbles produced by a sparger at the base of the column. Floatable particles collide with and adhere to the

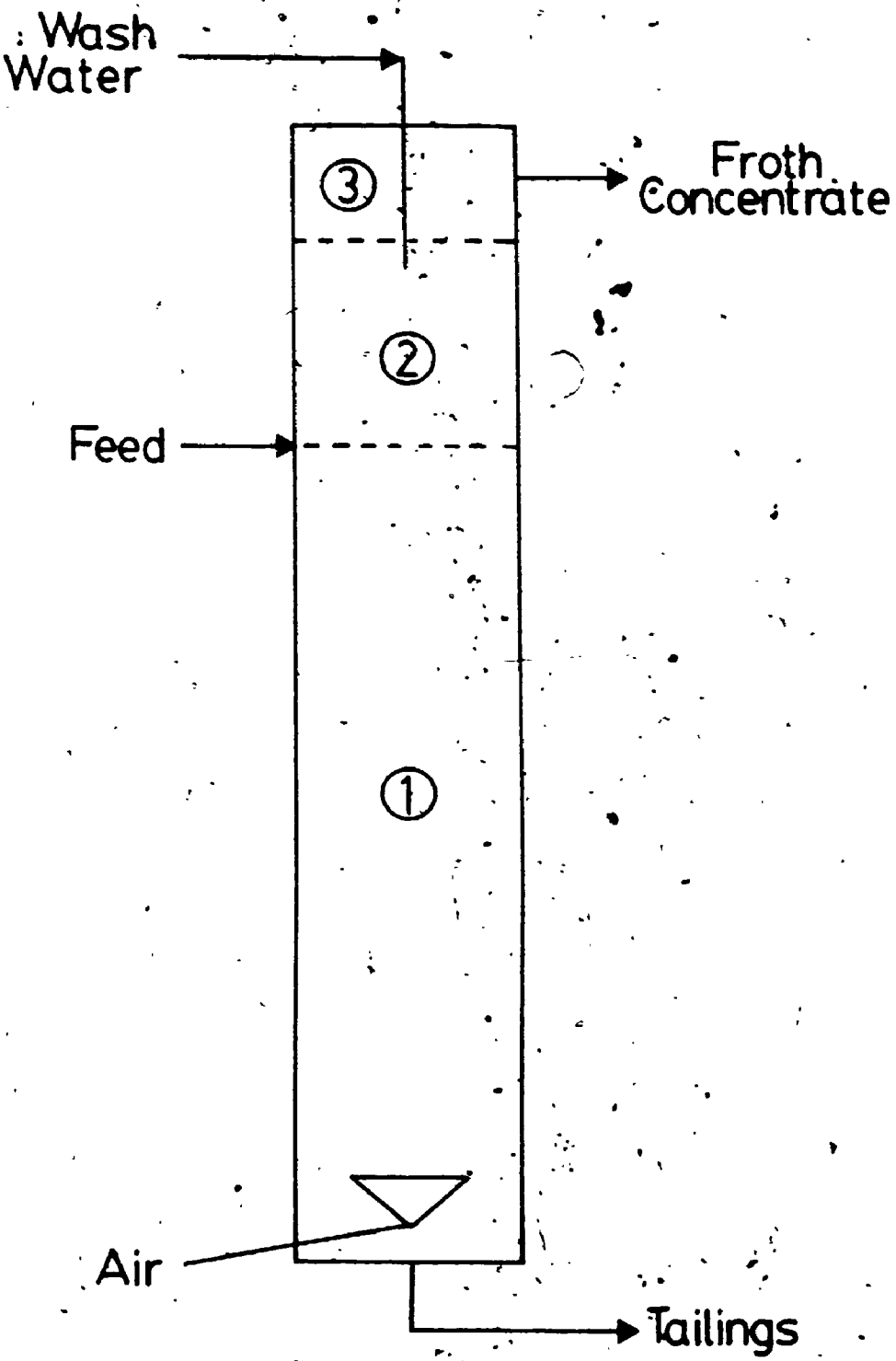

Figure 1.2 Schematic of a bubble column flotation cell showing (1) Recovery zone; (2) Washing zone and (3) Froth zone

bubbles and are transported to the washing section. Non-floatable material (gangue) is removed from the base of the column as tailings.

The washing section serves two principal functions:

(i) To wash back into the recovery zone the loosely attached or entrained gangue particles. In this way, the contamination of the concentrate by such particles is minimized.

(ii) To suppress the flow of feed slurry up the column towards the concentrate outlet. There is a net downward liquid flow in all parts of the column, thus preventing bulk flow of the feed material into the concentrate.

1.3 ADVANTAGES AND DISADVANTAGES OF USING BUBBLE COLUMN FLOTATION

The main advantages of using bubble columns in mineral flotation are:

1) A relatively simple construction since mixing in the column is obtained from the sparging action of the gas bubbles alone.

2) Operating and maintenance costs are considerably reduced due to the absence of moving parts.

3) Less floor space is required.

4) Minimal particle detachment from the bubbles since shear forces are considerably reduced compared to the mechanical

flotation cells. As a result, higher flotation rates (or space-time yields) are obtained (Flint, 1973; Dobby, 1984). This also makes flotation columns more amenable to fine particles flotation (Anon, 1965).

5) The recovery of hydrophilic (gangue) particles by mechanical entrainment is reduced since considerable distance exists between the tailings and froth removal points. As a result, higher selectivity indices (Gaudin, 1944) are obtained.

The disadvantages of bubble column flotation can be summarized as follows:

1) The pressure drop can be quite high since the current designs for industrial flotation columns are 10 m or more in height. However, for operations at pressures much above atmospheric, this effect is unlikely to be important.

2) A region of high turbulence is created around the wash water inlet point due to momentum dissipation. This important limitation arising from the use of wash water has not (to the author's knowledge) been discussed in any of the publications on bubble column flotation. The use of wash water also reduces the particle residence time in the recovery zone. In addition, the detachment of collected particles from the air bubbles in the region of the wash water entry may be promoted.

3) High gas through-puts cannot be used as slug formation

reduces the available bubble surface area, thus lowering the flotation rate. In addition, the considerable turbulence induced in the liquid phase under these conditions will enhance the detachment of mineral particles from the air bubbles, thus reducing the rate of flotation.

In spite of these drawbacks, the compelling advantages and the overall economy of bubble column flotation have led to its growing acceptance in the mineral processing industry. As an example, bubble column flotation is presently used at the Mines Gaspe, Quebec and Gibraltar Mines, British Columbia for molybdenum cleaning, and at Geco Mines, Ontario as zinc scavengers. In addition, extensive plant tests have been conducted on iron ore, coal, copper sulphide and graphite flotation (Coffin and Cienski, 1984; Wheeler, 1984; Dobby and Finch, 1986).

1.4 PROBLEM AREAS IN THE DESIGN OF FLOTATION CELLS

Even though the flotation process in general is commercially successful, problems still exist in the design and scale-up of flotation cells. For a proper design and scale-up, a mathematical model of the processes taking place is required. A procedure commonly employed for the design of chemical reactors has been presented by Shah and Deckwer (1985) and is illustrated in Figure 1.3. The application of this procedure requires detailed information

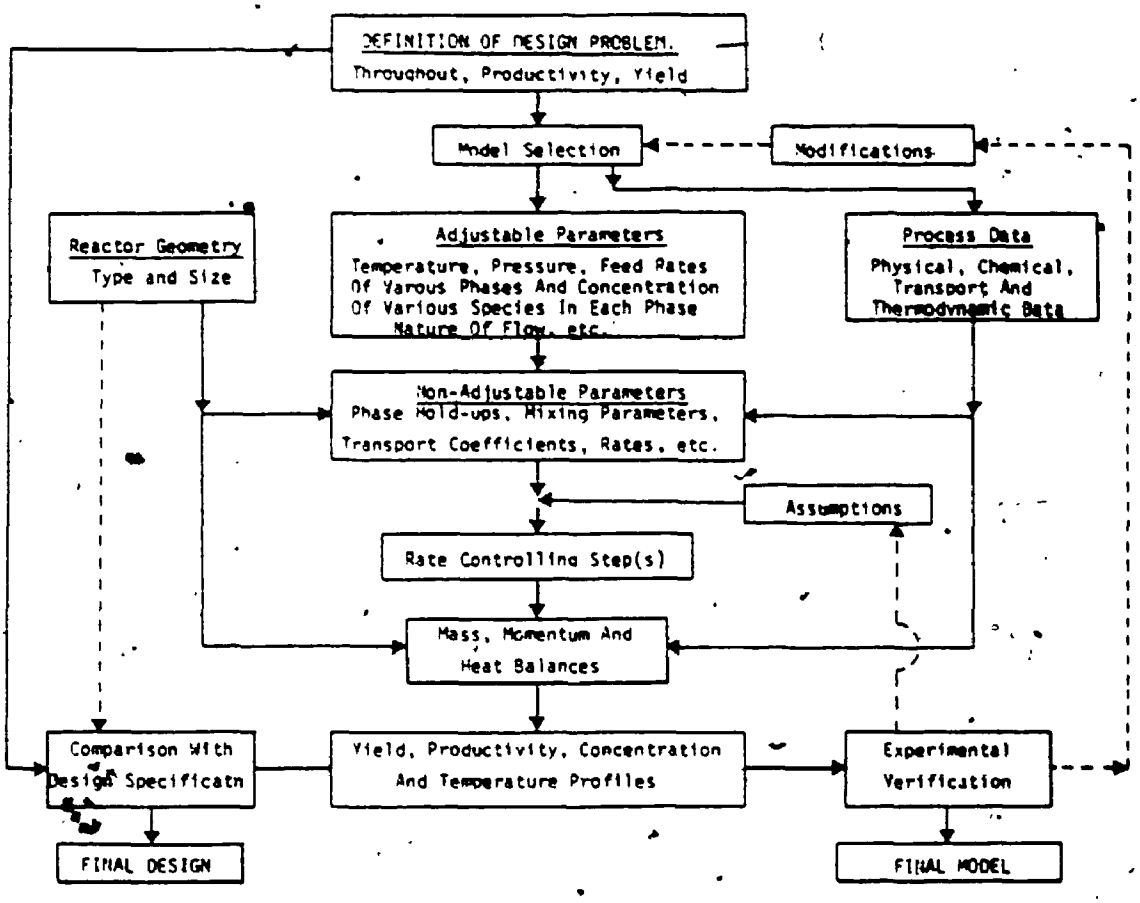

Figure 1.3 A flow path for the design and modelling of reactors (Shah and Deckwer, 1985)

on the materials-flow pattern in the reactor and a careful isolation of the important rate determining steps and how these change with the scale of the reactor. The major problem areas exist in the estimation of the non-adjustable parameters. In the case of multiphase contactors, isolation of the intrinsic kinetics from the hydrodynamic parameters may also present some problems. For example, a procedure commonly employed for the determination of flotation kinetics in a conventional mechanical cell is shown in Figure 1.4. It is evident that the kinetic data obtained from such a 'black-box' approach will be the product of the true kinetics and the hydrodynamic conditions of the cell (Laplante et al., 1985). As a result, such kinetic data are of limited utility in flotation cell design and scale-up.

Due to the complexity of the interrelationships involved in the flotation process, no satisfactory models capable of describing either the various interfacial phenomena that determine the attachment of particulates to bubbles, or the ways in which other uncontrollable factors affect the phenomena have been developed. The commercial success of flotation which has emerged as the single most important concentration process remains a triumph of enlightened 'know how' over inadequate 'know why'. Progress has been made almost exclusively by <u>empiricism</u> tempered by engineering judgement subject to the following questions: Firstly, 'Does it work?', secondly, 'Is it competitive?' and thirdly, 'What can be

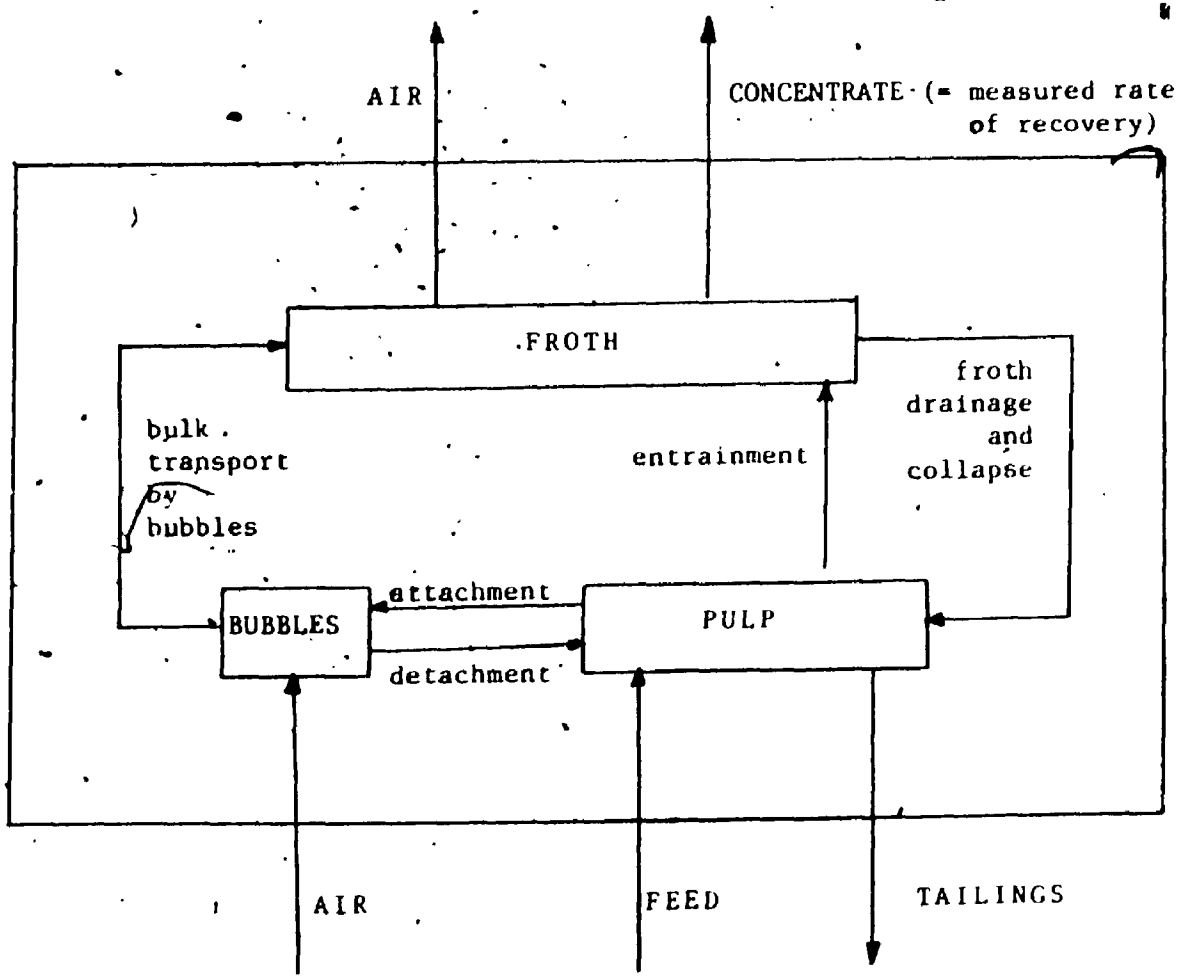

Figure 1.4 Material transport paths in flotation (Flint, 1973).

altered to make the process more attractive?' This approach has led to the slow progress in the design and/or application of new flotation cells. This progress was also hampered by the fact that flotation research in the past has been mainly directed at understanding the chemistry without adequate consideration of the physics and mechanics of this process (Flint, 1973).

The design and scale-up of a flotation column should in theory be easier than that of a mechanical flotation cell as it appears to be more amenable to the application of process models based upon fundamental physico-chemical principles. The counter-current flow of particles and bubbles provides a well defined flow regime, unlike in mechanical flotation cells where the degree of suspension of particles (particularly the larger and denser ones) is difficult to estimate and/or simulate. Also, the column has no mechanical turbulence that must be matched in a laboratory machine.

The existence of a single three-dimensional froth in the column makes froth modelling less complicated than that for a bank of mechanical cells where the froth characteristics change from cell to cell. Furthermore, the detachment and entrainment mechanisms for solids recovery in the froth are unlikely to be important in a flotation column (Flint, 1973; Dobby, 1984; Dobby and Finch, 1986). The performance of all bubble column reactors (flotation columns included)

depends quite strongly on the prevailing hydrodynamic conditions and on the transport and mixing conditions of the phases. Their accurate determination is essential for design and scale-up.

Since the object of any flotation operation is the selective recovery of hydrophobic particles by air bubbles, it is reasonable to assume that the particle collection process is also the rate determining step (Dobby and Finch, 1985; 1986). Levenspiel (1972) has shown that for simple first order kinetics, the conversion can be predicted using the value of rate constant and the two mixing parameters: the mean residence time and the vessel dispersion number. Since flotation depends on the probability of particle-bubble collision, it must be first order (Jameson et al., 1977). This means that knowledge of the hydrodynamic conditions in the recovery zone and the rate constant only will be required for design and scale-up purposes.

1.5 OBJECTIVES OF THE STUDY

The objectives of this study are:

1) To develop an upgrading process for the recovery of titanium and zirconium heavy minerals from oilsand centrifuge tailings and to compare this process with other processes that have been developed and patented. This involves an evaluation of the feasibility of using air flotation for

the initial beneficiation of these tailings.

2) To obtain hydrodynamic data relevant to the design of a bubble column flotation cell for the recovery of heavy minerals from oilsand tailings (i.e., liquid mixing, gas hold-up, particle settling characteristics under flotation conditions).

3) To investigate methods to control gangue recovery with the froth product in a flotation column. As mentioned earlier, the addition of wash water to depress gangue recovery in these units may pose serious operational limitations. Gangue recovery with the froth product depends on its concentration at the froth-pulp interface and the addition of wash water may merely reduce this concentration.

CHAPTER 2

LITERATURE REVIEW

Even though the concept of bubble column flotation was developed and patented in the early 1960s (Anon, 1965), little hydrodynamic data on it are available in the open literature (Flint, 1971; Rice et al., 1974; Dobby, 1984). This review covers the general estimation of those non-adjustable parameters for bubble column reactors that are relevant to bubble column flotation (liquid dispersion, particle and bubble dynamics) and flotation kinetics.

Over the past twenty years, numerous studies on the determination of non-adjustable parameters for bubble column reactors have appeared in the literature. Several comprehensive reviews of the subject have also been presented in the recent literature (Mashelkar, 1970; Shah et al., 1978; 1982; Shah and Deckwer, 1985). However, these reviews seldom discuss the experimental and/or mathematical methods employed by the various authors for parameters estimation. As a result, a critical assessment of the data covered in such reviews is not possible. For example, reviews on liquid phase dispersion in bubble column reactors usually cover data determined using the moments method even though Fahim and Wakao (1982) have shown that this method does not give reliable results. In addition, the application of the heat and mass

diffusivity analogy to study liquid phase mixing in three phase systems has been questioned recently (Ityokumbul et al., 1986b). In this chapter, a critical review of the literature is presented. For each design parameter, the review begins with an assessment of the experimental and mathematical methods commonly employed for its estimation. From these assessments, interpretation and/or mathematical errors that may affect the reported parameters are identified. At the end, only the literature data that have been determined with the correct experimental and mathematical method are reviewed.

2.1 LIQUID MIXING IN BUBBLE COLUMNS

2.1.1 Evaluation of Experimental Methods

Liquid mixing in bubble columns is induced by the motion of gas bubbles in the liquid. It is widely recognized that liquid mixing is detrimental to the performance of a reactor. However, in the case of bubble column flotation, the effect of liquid mixing on reactor performance is not easily discernible. While it may be argued on the one hand that it is the dispersion of the solid phase that influences flotation column performance (Dobby and Finch, 1985; 1986), it is also true that the extent of mixing of the continuous liquid phase will have an effect on the particle-detachment process. It is suggested here that the latter effect is minimal for flotation columns operating in the bubbly flow

regime. However, under other operating conditions (e.g. churn turbulence or slug flow), this effect may be important.

For studying liquid mixing in a bubble column, a mathematical model of the processes taking place is required. In many instances, the application of the one-dimensional dispersion model (plug flow with axial dispersion) has proven satisfactory. Experimental methods for studying axial mixing in bubble columns may be classified as unsteady and steady state.

2.1.1.1 Unsteady State Methods

Figure 2.1(a-c) show some of the commonly employed unsteady state methods for studying liquid mixing in bubble columns. In (a) and (b), both the liquid and gas phase flows are continuous while in (c), only the gas phase is continuous.

Assuming no radial variation in liquid velocity, the mass balance of tracer may be written as:

$$E_L \frac{\partial^2 C}{\partial z^2} - V_L \frac{\partial C}{\partial z} = \frac{\partial C}{\partial t} \qquad (2.1)$$

where E_L is the axial dispersion coefficient, C the transient tracer concentration at position z, and V_L the interstitial liquid velocity. For the special case shown in Figure 2.1(c), equation 2.1 reduces to:

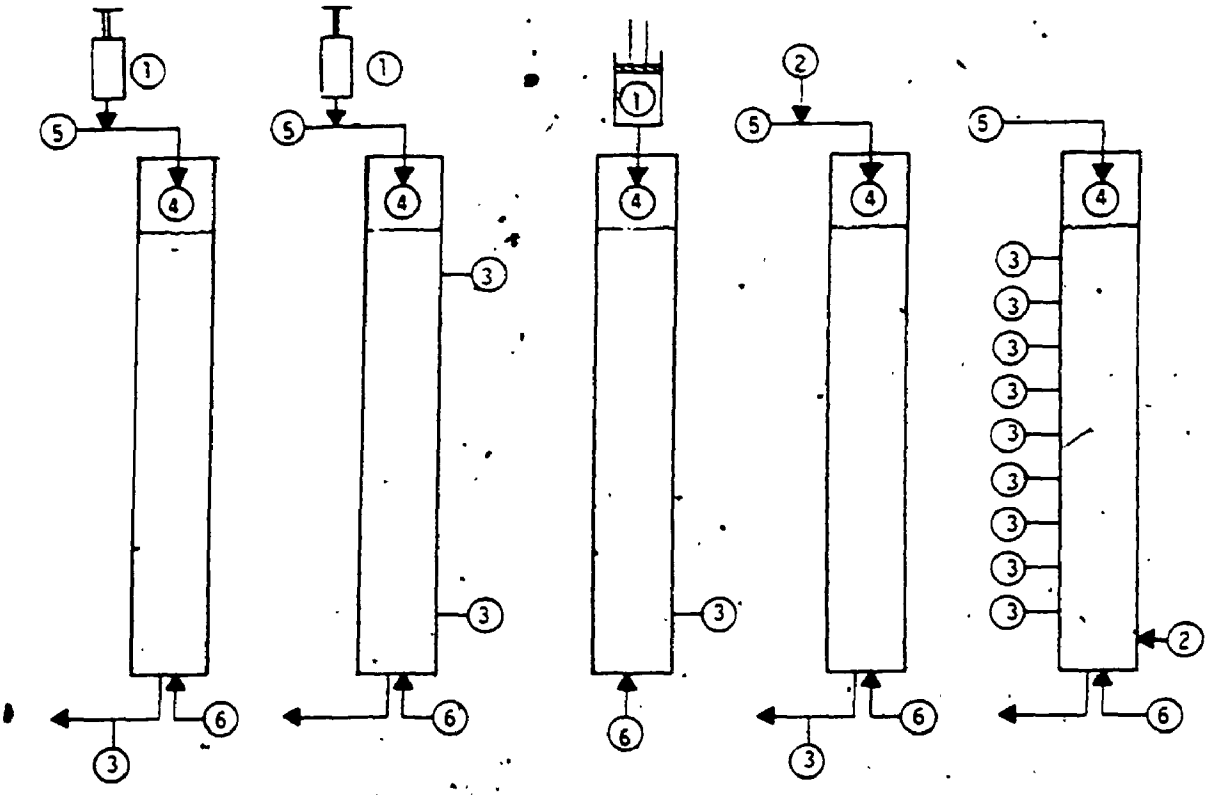

Figure 2.1 Schematic of commonly employed experimental techniques for studying liquid dispersion in bubble columns. (a) Closed-closed boundary conditions; (b) open-open boundary conditions; (c) batch-liquid unsteady state; (d) steady state flow method employing the F(t) distribution and (e) steady.state flow backmixing.. (1) Tracer pulse (2) steady tracer input (3) tracer detection (4) liquid distributor (5) liquid inlet (6) air inlet.

$$\frac{\partial^2 C}{\partial z^2} = \frac{\partial C}{\partial t} \qquad (2.2)$$

The use of the experimental methods shown in Figure 2.1(a) and (b) permit the independent determination of both fluid-dynamic parameters (E_L and V_L). Consequently, a comparison of the estimated value of V_L with that calculated using the experimental settings and the gas hold-up provides an indirect assessment of the applicability of the model. These methods can therefore be relied upon to provide diagnostic information on reactor performance (dead volumes, bypassing, etc.). By contrast, studies based on the experimental method shown in Figure 2.1(c) do not provide such diagnostic information as the only parameter determinable is the dispersion coefficient. A complete discussion of these methods has been provided recently by Ityokumbul et al. (1986b).

Even with the experimental method shown in Figure 2.1 (a) and (b), the reliability of the estimated parameters depends significantly on the mathematical method chosen. Reviews on the choice of mathematical methods have been provided by Michelsen (1972), Fahim and Wakao (1982) and Westerterp et al. (1984). As pointed out by these authors, the moments and transfer function fitting methods are suited only for providing inexpensive initial estimates of the parameters for a time domain fitting. Nonetheless, these methods have been used and continue to be used with undue reliance upon their validity.

2.1.1.2 Steady State Methods

Figure 2.1(d) and (e) show two possible configurations for studying liquid mixing by the steady state method. In both cases, the tracer, gas and liquid are introduced continuously. For the method depicted in (d), the response is measured in the tailings stream as a function of time. This dynamic response represents the F(t) curve which can be easily transformed into the E(t) curve by differentiation (Danckwerts, 1953; Levenspiel, 1978). Methods for estimating E_L and V_L from the F(t) curve can be found in the literature (Levenspiel, 1978; Westerterp, 1984), suffice to say that both parameters are determinable from such a response.

The procedure outlined in Figure 2.1(e) is by far the most popular in the literature today (Argo and Cova, 1965; Aoyama et al., 1968; Reith et al., 1968; Towell and Ackerman, 1972; Deckwer et al., 1974; Konig et al., 1978; Holcombe et al., 1982; Wendt et al., 1984; Devine et al., 1985). In this method, the axial concentration (or temperature) is determined under steady state conditions and the liquid dispersion coefficient is estimated from the equation:

$$E_L \frac{d^2C}{dz^2} - V_L \frac{dC}{dz} = 0 \qquad (2.3)$$

An integration of equation 2.3 gives

$$\ln C/C_o = - \frac{V_L}{E_L} z \qquad (2.4)$$

where C and C_o are the tracer concentration at z and z = 0 respectively. Thus a plot of $\ln(C/C_o)$ vs z should give a straight line with a slope of $-(V_L/E_L)$. With this method, the independent determination of V_L and E_L is not possible since there is only one relationship with two unknowns. As a result, verification of the model from a comparison of the calculated value of V_L (from the experimental settings) with that determined from the curve fitting of the tracer response curve (as was the case with the dynamic methods shown in Figure 2.1a, b and d) is not possible. In all such studies, the experimentally calculated value of the interstitial liquid velocity is substituted into the expression for the slope to obtain E_L.

In some studies employing the steady state method shown in Figure 2.1e, the occurrence of two distinct slopes has been reported (Deckwer et al., 1973). This phenomenon has been interpreted to be due to a change in the liquid dispersion coefficient as a result of bubble coalescence in the upper section of the column. Implicit in this statement is the assumption that the interstitial liquid velocity remains constant in both regions. However, this assumption is not valid. With bubble coalescence, the gas hold-up in the upper section will decrease. As a result, the interstitial liquid velocity in this section will decrease when compared to the lower section. This means that the change in the slope of the concentration profile is due partially

to a decrease in the liquid interstitial velocity. The current interpretation which ascribes this phenomenon to the liquid dispersion coefficient alone is therefore not a valid one.

The use of the schematic shown in Figure 2.1e presents some serious experimental difficulties which to the author's knowledge have not been discussed before. For example, if the tracer detection probes are introduced into the column, the following assumptions are implied:

(i) the liquid flow pattern in the unit is not altered, and

(ii) the probe and instrumentation yield the true liquid phase tracer concentration.

For small probes, assumption (i) may be valid. However, as the number of probes introduced increases, this assumption may well cease to hold. Similarly, assumption (ii) will hold only for probes with sensing elements which are much smaller than the average bubble size.

The withdrawal of samples from the column for analyses also presents some experimental problems. For example, in order to obtain a representative sample at any given height in the column, an elaborate sample collection device may be required. Its introduction may influence the liquid flow pattern. It is common practice to hear of "isokinetic"

sampling techniques for such systems. In actual fact, isokinetic sampling is only possible with a single phase flow!

In addition to these experimental problems, there is the fundamental question as to what the liquid phase dispersion coefficient determined with the experimental method shown in Figure 2.1e actually represents. As explained earlier by Schugerl (1967), the backmixing coefficient determined in this way was not equivalent to the axial dispersion coefficient. In reactor design, it is the axial dispersion coefficient which is required and not the backmixing coefficient. Schugerl suggested that the two parameters were related by a Taylor-Aris relationship. The implications of this are serious. For example, it means that most of the liquid phase dispersion data currently found in the literature may be underestimated. As a consequence, reactor designs based on these data may not be optimally scaled. This assessment is best illustrated from the work of Schumpe et al. (1979). These authors studied the absorption and reaction of CO_2 in NaOH solution. Their results revealed that the transition from bubbly flow to churn-turbulence was accompanied by a rapid decline in the conversion of CO_2. From fundamental principles of chemical reaction engineering, this would suggest a corresponding rapid increase in the liquid dispersion coefficient. However, none of the correlations for predicting liquid dispersion coefficients in bubble column reactors (see Shah et al., 1982) show such trends.

2.1.1.3 Application of Heat and Mass Diffusivity Analogy

The application of the heat and mass diffusivities analogy for studying liquid mixing in two phase (gas-liquid) bubble columns appears to be gaining in popularity (Aoyama et al., 1968; Chen and McMillan, 1982; Holcombe et al., 1982; Wendt et al., 1984; Devine et al., 1985). This analogy has been experimentally verified for the backmixing coefficient in two phase systems by all of these authors. Quite recently, Kara et al. (1982) and Kelkar et al. (1984) have extended this analogy to three phase (gas-liquid-solid) systems. The same method has been recommended recently by Shah and Deckwer (1985) for studying liquid mixing in three phase systems. The extension of this analogy to three phase systems is not valid as the transport mechanisms for heat and mass in three phase systems are different. For two phase (gas-liquid) systems, the predominant transport medium for heat and mass is the liquid phase. However, in three phase systems, heat transport will be affected by both liquid and solid phases whereas mass transport in these systems is primarily affected by the liquid phase. Clearly, as the transport media for heat and mass differ, the analogy between their diffusivities can at best be expected to hold only when the solid concentration is low. This assessment is consistent with the recent experimental observations of Chen and McMillan (1982). In view of the foregoing, the use of

this method to characterize liquid mixing in three phase bubble column reactors is not recommended.

Even in the case of two phase (gas-liquid) flow, care must be taken to avoid the effect of other unrelated factors on the mixing process. For example, the application of a steady state heat tracer at the base of a vertical bubble column may induce "gravitational mixing" as a result of liquid density variations (Chen and McMillan, 1982; Holcombe et al., 1983). As a result, the steady state axial temperature profile that is established in the column may not be related to the "true" mixing process described by the diffusion equation. However, for high liquid velocities, this effect is unlikely to be important.

2.1.2 Review of Literature Data on Liquid Dispersion

As the above discussion on experimental methods reveals, there are considerable data on liquid phase mixing in bubble column reactors. Recent reviews were provided by Mashelkar (1970), Baird and Rice (1975) and Shah et al. (1978; 1982). However, attempts at obtaining a comprehensive mixing theory applicable to bubble columns have so far met with only limited success (e.g. Baird and Rice, 1975; Joshi and Sharma, 1976; Joshi, 1980; Riquarts, 1981; Lehrer, 1984). The reason for this may be attributed to the wide variance of the published data which arises as a result of the following:

(i) application of wrong boundary conditions

(ii) experimental errors in the tracer measurements

(iii) mathematical and theoretical errors associated with the analysis of the tracer response measurements.

The application of wrong boundary conditions is common in the literature as authors generally try to avoid the complex analytical solutions associated with the closed-open and closed-closed boundary conditions in favour of the simpler open-open ones. Examples of this can be found in the work of Rice et al. (1974; 1981) and Dobby and Finch (1985). Experimental errors on the other hand are more difficult to spot unless the results are in violation of well established laws. For example, Awasthi and Vasudeva (1983) have reported a linearity between percent transmission and concentration which is by itself a violation of Beer-Lambert Law. In addition, the discontinuity in the axial concentration profiles reported by Deckwer et al. (1973) is in apparent contradiction with the continuity assumed by the diffusion model. The occurrence of a discontinuity in the tracer concentration profile may be due to the experimental problems already discussed for this method.

The errors associated with the mathematical treatment of the data are dependent on the accuracy obtainable by the method (moments, weighted moments, transfer function fitting, Fourier analysis and time domain fitting). A

review of the mathematical methods currently used for the estimation of liquid mixing parameters in bubble columns has been provided by Michelsen (1972), Fahim and Wakao (1982) and Westerterp et al. (1984). These reviews have shown that the most reliable methods were the time domain fitting and the Fourier analysis. As a result, the present review will be limited to studies in which the liquid phase mixing parameters were determined from transient measurements using the appropriate mathematical method.

Murphy and Timpany (1967) measured liquid dispersion data in a rectangular aeration tank with dimensions of 1.52 m x 0.91 m x 0.76 m. Their results were well represented by the expression

$$E_L = 0.053\ U_g^{0.406} \qquad (2.5)$$

Flint (1971) determined liquid dispersion coefficients in a 0.082 m (i.d.) bubble column operating under flotation conditions. His results were represented by the expression:

$$E_L = 0.0012 + 0.281\ U_g \qquad (2.6)$$

For gas velocities used in his study (0.003-0.017 m/s), this expression is well approximated by:

$$E_L = 0.0117\ U_g^{0.731} \qquad (2.7)$$

Gondo et al. (1973) measured liquid mixing in cylindrical bubble columns with diameters of 0.05 m and 0.10 m.

These columns were equipped with devices for generating small and large bubbles. Their results with the large bubbles alone showed that for gas velocities of less than 0.01 m/s, the liquid phase dispersion coefficient was well represented by

$$E_L = 0.028\ U_g^{0.52} \tag{2.8}$$

and by

$$E_L = 0.055\ U_g^{0.52} \tag{2.9}$$

for the 0.05 m and 0.10 m columns respectively. Their results also revealed that for intermediate gas velocities (0.007-0.04 m/s), the liquid dispersion coefficient could be represented by

$$E_L = 0.0068 \pm 0.0005\ m^2/s \tag{2.10}$$

For the same gas velocity and bubble column, these authors also reported that the device for generating small bubbles gave higher liquid dispersion values. This observation appears to suggest that the quality of the dispersion depends on the bubble size. Furthermore, their results also showed that the dispersion coefficient varies linearly with column diameter.

Schugerl et al. (1975) measured liquid dispersion data in a two and three phase bubble column with a diameter of 0.14 m. Their results showed that the liquid dispersion

coefficient increased with increasing liquid and gas velocities. However, the final correlations were presented as complex functions of the gas velocity, the liquid superficial and interstitial velocities.

Sangnimnuan et al. (1984) measured liquid dispersion coefficients in a 0.019 m bubble column operating under hydroliquefaction conditions. For superficial gas velocities less than 0.011 m/s and liquid velocities less than 0.005 m/s, their results were well represented by

$$E_L = 1.77\ U_g^{1.55} \qquad (2.11)$$

Since there was no mention of the operating flow regime, the slug flow regime is assumed as most hydroliquefaction reactions are carried out under these conditions.

Houzelqt et al. (1985) reported liquid dispersion data for a 0.05 m bubble column. For gas velocities ranging from 0.0025-0.0058 m/s and liquid velocities ranging from 0.00025-0.001 m/s, they found that their air-water dispersion data were represented by

$$E_L = 0.04\ U_g^{0.47} \qquad (2.12)$$

These authors also investigated the influence of liquid viscosity, surface tension (addition of surfactants), pressure, distributor design, baffles and gas properties. They found that liquid viscosity, pressure and gas properties had no

effect on the liquid dispersion coefficient, while surface tension and baffles had an effect. However, only a qualitative assessment of the effects was presented by these authors. The effect of surfactant addition on liquid mixing is of particular interest in bubble column flotation where frothers and/or residual collector molecules are added to control bubble size.

From the preceding review of liquid dispersion data in bubble columns, the following preliminary conclusions may be drawn:

1) Liquid mixing varies with the gas velocity according to the flow regime:

$$E_L \propto U_g^n \qquad (2.13)$$

For chain bubbling, 'n' = 0.4-1.0 (Flint, 1971; Gondo et al., 1973; Houzelot et al., 1985), while for bubbly flow, 'n' = 0 (Gondo et al., 1973). On the other hand, it appears that 'n' = 1.0-2.0 for the churn-turbulence flow regime (Gondo et al., 1973; Sangnimnuan et al., 1984).

2) The extent of liquid mixing depends on the column diameter and bubble size but it is not affected by the physical properties of the gas.

2.2 PARTICLE DYNAMICS IN BUBBLE COLUMN REACTORS

Knowledge of particle dynamics (settling characteristics and dispersion) is important in predicting flotation column performance. For example, the mean solid residence time in the recovery zone which is an indirect measure of the number of particle-bubble collisions in this zone may be estimated from particle dynamics (Dobby and Finch, 1985; 1986).

For an accurate estimation of these parameters, a mathematical model of the process is required. In this respect, the one-dimensional sedimentation-dispersion model has emerged as the dominant mathematical model for studying particle dynamics (Cova, 1966; Imafuku et al., 1968; Farkas and Leblond, 1969; Kato et al., 1972; 1985; Kojima and Asano, 1981; Smith and Ruether, 1985; Smith et al., 1986; Kubota et al., 1986). While several correlations for predicting particle dynamics in bubble columns exist, a critical review of the experimental methods will reveal that most of these correlations have limited use for reactor design purposes.

2.2.1 Experimental Methods For Studying Particle Dynamics

The commonly employed experimental procedures for studying particle dynamics in bubble column reactors are shown in Figure 2.2. According to the one-dimensional sedimentation dispersion model, the flux of solid particles is described

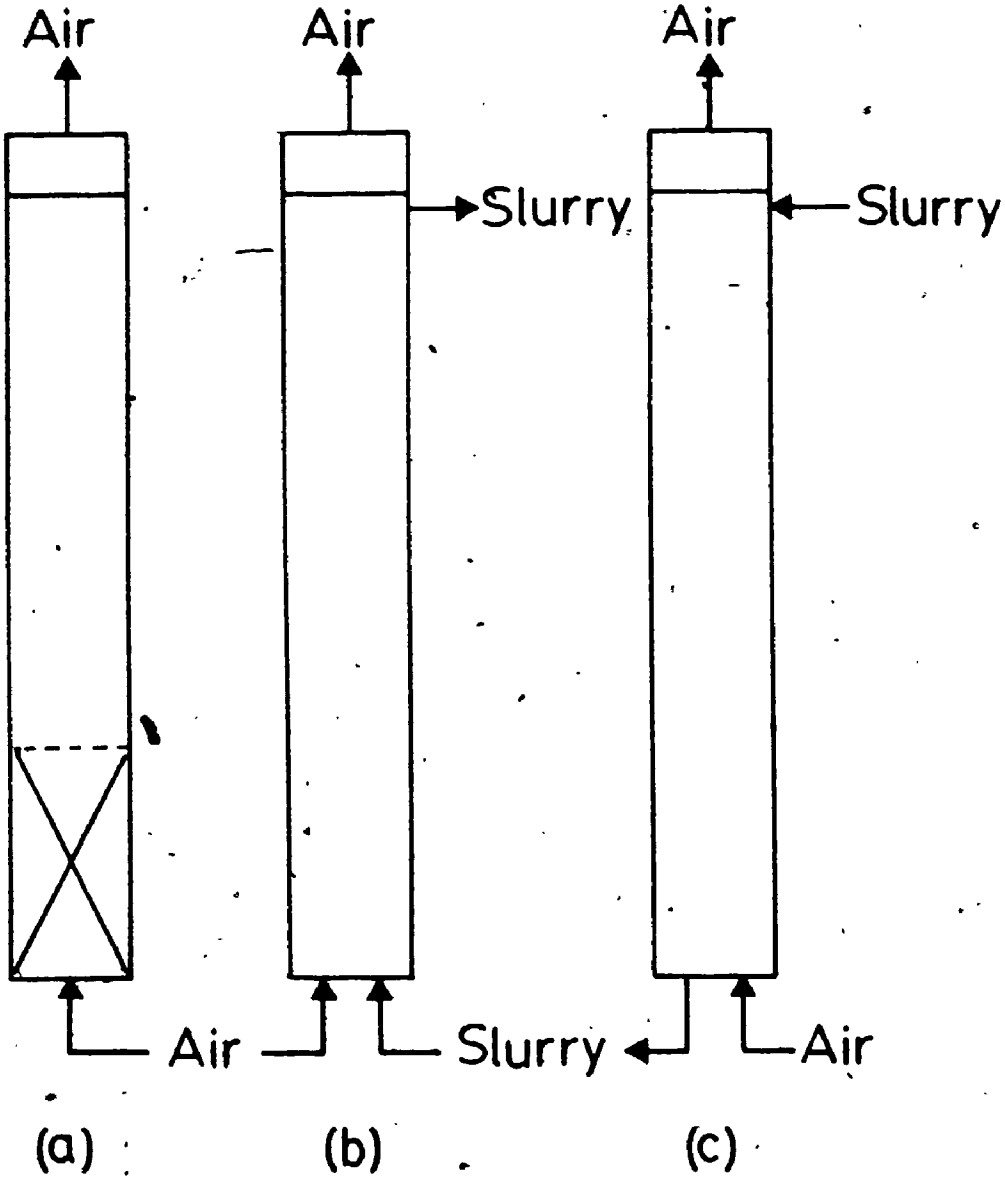

Figure 2.2 Experimental procedures for studying particle dynamics (a) semi-batch; (b) cocurrent flow and (c) countercurrent flow of slurry and gas.

by a Fickian expression of the form

$$E_s \frac{\partial^2 C_s}{\partial z^2} - (V_L \pm V_p) \frac{\partial^2 C_s}{\partial z} = \frac{\partial C_s}{\partial t} \qquad (2.14)$$

where E_s and C_s are the solid dispersion coefficient and concentration at position z, respectively, and V_L and V_p are the liquid interstitial and particle settling velocities respectively. The (+) and (-) signs in equation 2.14 refer to the countercurrent and cocurrent flow of slurry and gas respectively. Let us consider the semi-batch operation shown in Figure 2.2(a). At steady state, equation 2.14 will reduce to:

$$E_s \frac{d^2 C_s}{dz^2} + V_p \frac{dC_s}{dz} = 0 \qquad (2.15)$$

As with the non-dynamic steady state methods already discussed under liquid mixing (see section 2.1.1.2), the use of this method is not recommended. A complete assessment of this method is presented below.

An integration of equation 2.15 will yield an expression of the form:

$$C_s = C_s^o \exp(- \frac{V_p}{E_s} z) \qquad (2.16)$$

where C_s^o is the hypothetical solid concentration at z = 0. By plotting the steady state concentration profile against height on a semi-logarithmic paper, the slope 'm' may be estimated. By definition,

$$m = -V_p/E_s \qquad (2.17)$$

Since knowledge of both V_p and E_s is required and only one relationship is obtained from such a plot, another expression is required. This is exactly the same problem that was discussed earlier for the determination of the liquid phase dispersion coefficient by the steady state method given in Figure 2.1(e). Several authors have overcome this problem by determining the variation of the slope with the terminal settling velocity of a single particle in the stagnant medium (Imafuku et al., 1968; Kato et al., 1972; Kojima and Asano, 1981; Smith and Ruether, 1985; Smith et al., 1986). However, any changes in the slope can not be related directly to any one parameter comprising the slope! All of these authors assume that changes in the slope were directly related to the terminal settling velocity of a single particle. This will be true only if the solid dispersion coefficient is not a function of the particle terminal settling velocity. This would imply that a 1 μm particle which for all practical purposes may be considered to be in Brownian motion would mix to the same extent as a 1 mm particle which will settle under turbulent conditions! Therein lies the first particle dynamics paradox?

The use of the batch operation for studying particle dynamics raises several other fundamental problems. First, the existence of a big solid concentration gradient in the column all but precludes the use of a single value for the particle settling velocity (as a result of hindered settling

effect). Second, there is also the physical interpretation problem of what the variations in the slope 'm' with gas velocity "actually" represent. All of the authors who have employed this method use these variations to prepare correlations for the particle hindered settling velocity and dispersion coefficient. However, the phenomenon involved is analogous to two-phase (gas-solid) fluidization where the force of suspension for the solid particles is provided by the gas. Increasing gas velocity affects the slope insofar as it increases the energy dissipation rate which enables more solids to be maintained in suspension. It is therefore questionable if the changes in the slope can be related to the phenomenological behaviour described by the sedimentation-dispersion model. Furthermore, the use of a stationary state method to est. ate more than one dynamic parameter (in this case V_p and E_s) does not appear to be consistent.

Consider next the continuous methods for studying particle dynamics in bubble column reactors (Figures 2.2(a) and (b)). Of the two, the cocurrent upflow of slurry and gas is more popular in the literature (Imafuku et al., 1968; Kato et al., 1972; 1985; Kara et al., 1982; Kelkar et al., 1984; Smith and Ruether, 1985; Smith et al., 1986; Kubota et al., 1986; Sada et al., 1986) even though some authors have used both methods (Cova, 1966; Bhaga and Weber, 1972). With the exception of the work of Bhaga and Weber, all these authors have used the steady state axial solid

concentration to estimate their particle dynamic parameters. This method involves the integration of equation 2.15 followed by curve fitting to estimate the parameters. The integrated form of equation 2.15 subject to the correct boundary conditions is shown below:

$$C_s = [C_s^o + \frac{V_L C_s^F}{V_P - V_L}]\exp(-\frac{V_P - V_L}{E_s} z) - \frac{V_L C_s^F}{V_P - V_L} \qquad (2.18a)$$

$$= [C_s^L + \frac{V_L C_s^F}{V_P - V_L}]\exp\{\frac{V_P - V_L}{E_s}(L-z)\} - \frac{V_L C_s^F}{V_P - V_L} \qquad (2.18b)$$

where C_s^o and C_s^L are the solid concentrations at $z = 0$ and $z = L$ respectively. Curve fitting of the measured solid concentration profile using either equation (2.18(a) and (b)) is difficult owing to the huge number of parameters involved. As stated recently by Robinson and Tester (1986), a good fit of any model can be obtained if it has numerous adjustable parameters. However, if these parameters do not possess precise physical meaning, the modelling becomes an exercise in curve fitting, while the important qualitative features of the model become lost within its sophisticated mathematics. All of the authors who have used this method reduce the number of parameters to be estimated by using the experimentally set values of V_L and C_s^F. Unfortunately, neither of these may be correct. For example, the use of the experimental value of V_L implies that radial variations in the liquid and/or solid flow do not exist. While this assumption

is reasonable for columns of cylindrical configuration, it is not true for other geometries (Akita and Yoshida, 1974; Alexander and Shah, 1976). Even when this is done, the number of parameters to be estimated remains high (three). Furthermore, as the discussion below reveals, the value of C_s^F in these experiments is unlikely to remain constant with time.

This notwithstanding, there is the other fundamental issue of what constitutes steady state in the case of the cocurrent method shown in Figure 2.2(b). Because of the known particle slip phenomenon, solid build-up in the column is obtained (Cova, 1966; Bhaga and Weber, 1972; Kato et al., 1972; 1985; Smith and Ruether, 1985; Smith et al., 1986; Kubota et al., 1986). For a once through flow of slurry, steady state conditions would signal an equality of the feed and outlet solid concentrations. Cova (1966) used this method and he reported that attainment of steady state was very slow (>3 hours). It is therefore surprising to note that some of the authors have reported attaining steady states in less than one hour under similar operating conditions (Smith and Ruether, 1985; Smith et al., 1986). However, a careful evaluation of the experimental method will show how this is possible. Most of these authors have applied the slurry recirculation procedure. With this method and the solid slip phenomenon, a depletion of the solid concentration in the reservoir will result. So unless the reservoir

size is much larger than the bubble column (a situation in which the build-up of solids in the column causes only minor changes in the reservoir), attainment of steady state will be accelerated. Unfortunately, only Bhaga and Weber (1972) indicated that this important condition was met in their experiments. We note that since the majority of these authors did not even specify the feed concentrations in their experiments, it is impossible to assess the attainment of steady state in their studies. Even if this were done, the variation of the feed concentration with time would be additionally required in order to confirm the attainment of steady state.

2.2.2 Review of Literature Data On Particle Dynamics

Bhaga and Weber (1972) studied particle settling characteristics in two (liquid-solid) and three (gas-liquid-solid) phase systems in a vertical column. They employed the co-current and countercurrent flow arrangements shown in Figures 2.2(b) and (c). By plotting their solid hold-up data as:

$$\frac{U_s}{\epsilon_s} = \frac{U_s + U_L}{1-\epsilon_g} + \frac{V_\infty}{(1+C^*)^{n+1}} \qquad (2.19)$$

they obtained the particle settling velocity, V_∞. In equation 2.19, U_s and ϵ_s are the superficial solid flow velocity and average solid hold-up respectively. U_L is the superficial liquid velocity, C* the volumetric ratio of solids

to liquid in the column, and n is an exponent which is dependent on the particle Reynolds number (Richardson and Zaki, 1954). Their results revealed that for two phase flow of solids and liquid, the value of the intercepts for both cocurrent and countercurrent flow arrangement agreed rather well with the computed value of V_∞. By contrast, they found that for three phase systems, the value of the intercept was higher in magnitude than that for two phase flow. This shows that for three phase systems, the particles were settling at a much higher velocity. However, no correlations for predicting the settling velocity under these conditions were presented by these authors. Coincidently, the values of the intercepts obtained from the studies of Bhaga and Weber are well predicted by the relationships given by Ramachandran and Chaudhari (1983) for the intermediate settling regime.

Quite recently, Dobby (1984) used MnO_2 particles as a solid tracer in an attempt to measure the residence time distribution of solid particles (RTD) in an industrial flotation column. However, Dobby (1984) used only seven data points which were determined at irregular intervals over a twenty minute period for the estimation of his parameters. Considering the scarcity of the data and the relatively long residence time of the solids in the column, the reliability of the estimated parameters may be questionable. Furthermore, Dobby used the analytical solution for the open-open

boundary conditions for the estimation of his parameters even though the tracer was detected in the tailings stream.

Several of the studies already discussed here have suggested that the solid dispersion coefficient in a bubble column was the same as the backmixing coefficient of the liquid under the same operating conditions. No upper limit for particle settling velocities for which this assumption is valid has been provided to this author's knowledge. Since most of the solid and liquid dispersion data were obtained from these questionable experimental procedures, this assumption may not be valid. Moreover, it is highly unlikely that the particles will follow the liquid streamlines exactly as indicated by the equality in the two dispersion coefficients since even the finest particles have a non-zero gravitational force acting on them (Flint, 1971; Reay, 1973). Jameson et al. (1977) have shown that solid particles will follow the liquid streamlines exactly in the presence of a gas bubble only if

$$\frac{\rho_p d_p^2 U_b}{9 \mu_L d_b} << 1 \qquad (2.20)$$

In equation 2.20, d_b and U_b are the bubble size and rise velocity respectively. For typical flotation size air bubbles in a bubble column (d_b = 0.001 m and U_b = 0.12 m/s), and a solid particle with a density of 3000 kg/m^3, this condition reduces to

$$d_p << 180 \ \mu m \quad . \qquad (2.21)$$

It is clear from this that only fine particles settling in the Stoke's regime ($Re_p << 0.1$) will follow the liquid streamlines exactly. As a result of this, it is unrealistic to expect that the particle dispersion coefficient will be the same as that of the liquid. Therein lies the second paradox of particle dispersion in bubble columns.

In the absence of acceptable correlations for particle settling velocity and dispersion, the following correlations are suggested:

1) For particle settling velocity in a bubble column, the correlation presented by Ramachandran and Chaudhari (1983) for the intermediate settling velocity which is given below may be applied.

$$V_p = [0.0178 \ g^2 \frac{(\rho_P - \rho_L)^2}{\mu_L \rho_L}]^{1/3} \ d_p \qquad (2.22)$$

2) For particle dispersion, plug flow may be assumed under flotation conditions (see 2.2.2 above).

2.3 BUBBLE DYNAMICS

Since flotation is a surface phenomenon involving the selective removal of hydrophobic particles from an aqueous suspension by air bubbles, knowledge of bubble characteristics (gas hold-up, bubble size and rise velocity) is important

in predicting flotation column performance. For example, the gas hold-up and average bubble size are required in the computation of the interfacial area which is directly related to the flotation rate constant (King et al., 1976; Jameson et al., 1977). In a mechanical flotation cell, bubble characteristics are largely determined by the mechanical action of the impeller while in a flotation column, these parameters are determined by interfacial forces. As a result of the above, surface active substances (frothers and/or residual collector molecules) are present in all flotation media. A comprehensive review of the experimental methods for studying bubble dynamics in bubble columns has been presented by Shah et al. (1982) and will not be treated here.

The effect of surface active substances on bubble characteristics in a bubble column have been studied by a number of authors (Kumar et al., 1976; Schugerl et al., 1977; Oels et al., 1978; Kelkar et al., 1983). These studies have shown that the presence of short chain alcohols in the medium (water) prevented bubble coalescence and also reduced the bubble rise velocity. This effect is attributed to the accumulation of these molecules at the interface where they tend to orient themselves in such a way that the dipole layer generated prevents bubble coalescence. The gas hold-up in these systems is increased considerably when compared with the air-water system. Furthermore, the

increase in gas hold-up was found to be dependent on the chain length of the alcohol (Schugerl et al., 1977; Kelkar et al., 1983). While short chain alcohols are rarely used in flotation, increases in gas hold-up have also been reported with the frothers commonly used in these operations (Gaudin, 1957; Klassen and Mokrousov, 1963).

The mapping of hydrodynamic flow regimes for bubble column reactors is determined using the variation of gas hold-up with gas velocity. Since the addition of these surface-active substances has been shown to influence the gas hold-up, their presence is also expected to have an effect on the flow regime mapping. This has been confirmed by the results of Kelkar et al. (1983) who demonstrated that the presence of alcohols changed the gas velocities at which the transition from bubbly flow to churn-turbulence flow took place.

Flint (1971) and Rice et al. (1974) determined bubble dynamics in a 0.082 m bubble column. In order to simulate flotation conditions, these authors added reagent grade terpineol (0.004% and 0.016% respectively) to their medium (water). The authors estimated their voidages by manually withdrawing samples from the column with 50-ml syringes. Since isokinetic sampling of the column contents under these conditions is difficult, the reliability of their measurements is questionable. This is probably the reason for the

considerable scatter observed in their gas hold-up measurements.

2.5 FLOTATION KINETICS

For a successful design and scale-up of a flotation cell, knowledge of the 'true' flotation kinetics is additionally required. It represents the study of the variation in the amount of floatable material overflowing in the froth product with time, and also the quantification of the rate controlling variables or steps. The variables that affect the flotation process may be divided into three general groups: (1) the properties of the ore and its constituent minerals, (2) the reagent treatment given the pulp, and (3) the characteristics of the flotation machines and their operations. Knowledge of the physical properties of the ore and its major constituent minerals is essential in selecting the types and quantities of reagents to be added in order to maximize recoveries and selectivities. In some cases, the rate limiting step(s) may even be the physical configuration of the cell. For example, Laplante et al. (1985) have recently shown that with the conventional mechanical flotation cells, the rate limiting step may not be the particle collection step but rather the transport of material over the cell lip. The formulation of a flotation rate expression under these conditions must therefore reflect this effect if it is to bear any resemblance to the

actual flotation process. If this is not done, the results obtained will be of limited use in design and scale-up. In the treatment that follows, we assume that the optimum treatment conditions for the ore have been found.

In studying flotation as a rate process, most authors have used the analogy with chemical kinetics and utilized the following expression to represent the variation of floatable material in the cell with time

$$\frac{dC(t)}{dt} = -k\,[C(t)]^n \qquad (2.23)$$

where C(t) is the concentration of floatable material remaining in the cell, 'k' is the apparent rate constant and 'n' the order of the rate equation. The use of equation 2.23 to represent the removal of floatable material from the cell assumes that the cell contents are perfectly mixed. This may not be the case with other flotation cells (e.g. flotation columns), where the concentration of floatable material varies with the column height. Under these conditions, the single rate expression must be replaced by one that varies with axial height. As reviewed by a number of authors (Fuerstenau and Healy, 1972; Jameson et al., 1977), the general consensus is that the process is basically first order (although some authors have taken 'n' to be 2 while others have considered it to be variable). This does not necessarily mean that these studies are wrong; it may well be that the particle-bubble collision mechanism was not the

rate limiting step in these studies. The use of a modified first order rate expression of the form

$$\frac{dC(t)}{dt} = -k[C(t) - C_\infty] \qquad (2.24)$$

has been suggested by some authors (Bushell, 1962; Klimpel et al., 1982). In equation 2.24, C_∞ represents the "terminal concentration" of the mineral being floated and it physically represents the concentration of floatable material that remains in the flotation cell after long times.

The particle collection process can be thought of as occurring in a series of stages; collision, film thinning and film recession stages. In the collision stage, the trajectories of the particle and the bubble relative to each other are such that the distance between them becomes quite small. Since in most practical cases, the bubble is much larger than the particle, the particle may be considered to be approaching a planar surface. As the gap between the particle and the bubble is reduced, the liquid between them forms a film. This introduces the next stage in the collection process, the film thinning. Because of the small dimensions involved, the viscous stresses in the thin film can become quite high, thus reducing the approach velocity between particle and bubble. If these viscous stresses are quite large, they can produce particle "bounce" by virtue of their preventing the drainage of the liquid between the two objects during the time of their closest proximity. As

the separation between the particle and bubble approaches zero, it can be shown that the hydrodynamic force resisting the approach of the two bodies will become infinite thus preventing film rapture and consequent coalescence. However, as the film thickness decreases to less than 1000 nm, forces of molecular origin come into play. According to Finch and Smith (1981), double layer interactions dominate for separation distances between 1000 nm down to 30 nm while van der Waal's forces and hydration effects dominate below 30 nm. If the solid particles are hydrophobic, the thinning process is promoted thus leading to film rapture and attachment. The final part of the collection process is the film recessing stage, in which the liquid around the point of rapture or adhesion of the particle and bubble, draws back and forms a stable contact angle with the solid. If highly turbulent conditions exist in the flotation cell, detachment of particles from the bubble surface may occur as a result of powerful viscous stresses or turbulent eddies.

From their review of the various microprocesses involved in particle collection, Jameson et al. (1977) have questioned the validity of applying the analogy between chemical reaction and the flotation process. These authors have argued that the flotation process has more in common with mass or heat transfer than with chemical kinetics. However, by considering the case of a batch flotation cell of the bubble column variety, they arrived at the following rate

expression:

$$\frac{dC}{dt} = -(1.5\ U_g\ E_c/d_b)C \qquad (2.25)$$

In equation 2.25, E_c is the collection efficiency and it represents the fraction of particles contacting a gas bubble that results in a successful attachment. A comparison with equation 2.23 will reveal that the removal process is first order with the rate constant 'k' being

$$k = 1.5\ U_g\ E_c/d_b \qquad (2.26)$$

It should however be noted that the hypothetical conditions used by these authors (uniform particle concentration over the cell height) rarely exist in practice.

In the present study, we derive a rate expression for flotation by assuming that the particle collection process is analogous to physical adsorption for the following reason: In a flotation column, the bubble density is extremely high even at low gas velocities due to the presence of frothers and/or residual collector molecules. Under these conditions, it is reasonable to assume that particle-bubble collision will not be rate limiting. Of the two remaining processes (namely film thinning and rapture and the film recession stages) weaker interaction forces are likely to predominate in the former process. It is therefore reasonable to assume that it will be the rate determining step. The bubble loading rate may be written as:

$$\frac{d\Gamma}{dt} = k'[C(\Gamma_m - \Gamma) - \frac{\Gamma}{K}] \qquad (2.27)$$

where Γ and Γ_m are the bubble load and maximum bubble load respectively, C the mineral concentration, k' and K the adsorption rate constant and equilibrium constant respectively. The right hand side of equation 2.27 can be rearranged to give

$$\frac{d\Gamma}{dt} = k'\Gamma_m[C(1-\theta) - \frac{\theta}{K}] \qquad (2.28)$$

with the product $k'\Gamma_m$ (m/s) being equivalent to an interphase 'mass transfer coefficient' and θ the fractional surface coverage. In the absence of strong viscous stresses or turbulent eddies, the particle equilibrium constant is expected to be a function of its hydrophobicity and size.

With the exception of cleaning circuits, the availability of bubble surface is hardly rate limiting in flotation (Dobby and Finch, 1986). In addition, photographic evidence has shown that collected particles are immediately swept to the rear of the bubble (Brown, 1965). This means that for bubble surface coverages of less than 50% of the maximum coverage, the availability of bubble surface is unlikely to influence the particle collection process. For the particles made selectively hydrophobic, the equilibrium constant will be considerably larger than the surface coverage. Under these conditions, equation 2.28 reduces to:

$$\frac{d\Gamma}{dt} = k'\Gamma_m C \qquad (2.29)$$

The feed to flotation circuits usually contain mineral particles with varying surface properties. For flotation column modelling under these conditions, equation 2.29 may be written for each mineral component. The total bubble loading rate will be obtained by summing the individual loading rates as shown below:

$$\frac{d\Gamma}{dt} = \sum_i \left(\frac{d\Gamma_i}{dt}\right) = \Gamma_m \sum_i (k_i' C_i) \qquad (2.30)$$

Equation 2.30 is similar to that derived by King et al. (1977) for single bubble loading. They presented the following relationship for the maximum bubble load

$$\Gamma_m = 3.535 \times 10^{-3} / d_b^{0.875} \qquad (2.31)$$

where Γ_m and d_b are in kg/m^2 bubble surface and m respectively.

CHAPTER 3

FLOTATION COLUMN MODELLING AND SIMULATION

A mathematical model of the flotation column is required for the prediction of recoveries and grades. As mentioned earlier, the present designs for flotation columns have three zones: the recovery, cleaning and froth zones. All the mathematical models that have been developed to date use a probability term in their rate expression (Flint, 1971; Rice et al., 1974; Jameson et al., 1977; Dobby and Finch, 1986) and as such may be of limited utility for design and scale-up purposes. The probability term in these rate expressions is equivalent to the use of a "fudge factor" since its relationship to the hydrodynamic conditions prevailing in the column is largely unknown. In some of these studies, the assumptions invoked do not appear to be valid. For example, Rice et al. (1974) assumed that the particle settling velocity was small compared to the liquid interstitial velocity for the estimation of the probability of attachment in their studies. For the sand particles used in their study (d_{p_o} = 70 μm), the particle settling velocity was estimated by equation 2.22 to be 0.011 m/s compared with liquid interstitial velocities of 0.006 m/s and 0.001 m/s for the recovery and washing sections respectively.

For the development of a mathematical model for bubble

column flotation, the following assumptions were made:

1) Particle collection takes place in the recovery zone only (Flint, 1973; Rice et al., 1974).

2) The rate limiting step is the particle collection process. The effect of the froth phase on the recovery and grade is likely to be small unless the froth height is excessive (Engelbrecht and Woodburn, 1975; Laplante et al., 1985).

3) The availability of bubble surface is not rate limiting. This is especially true for columns employed in scavenger operations. Under these conditions, equation 2.28 may be applied.

4) The behaviour of solid particles in a flotation column may be described using a plug flow model. This assumption is reasonable for particles which do not follow the liquid streamlines (i.e. particles settling outside the Stokes' regime).

5) There is no wash water addition to the column. It is assumed here that the concentrate grade can be controlled by varying the height of the "calming section" above the feed inlet point. The recovery of gangue minerals in flotation depends on their concentration at the froth-pulp interface. The addition of wash water only serves to decrease this concentration. The same effect can be obtained by varying the height of the calming section since there is no bulk transport of gangue minerals up the column. Since the gangue concentration at the froth-pulp interface will

decrease with increasing height of this zone, this assumption appears to be reasonable.

It follows from (1) and (2) that the modelling of the flotation column reduces to one of the recovery zone only. In practice, it would be important to establish the conditions under which the other zones would not interfere with the particle recovery process. From (4) and section 2.3.3, the motion of solid particles is assumed to be by convection and sedimentation only.

3.1. MATHEMATICAL MODEL FOR BUBBLE COLUMN FLOTATION

We begin our analysis by considering the flotation of a single mono-dispersed mineral. This is followed by the general case of a single mineral displaying a wide particle size distribution. This procedure is finally extended to the general case of a mixed mineral flotation.

3.1.1 Flotation of a Mono-Dispersed Mineral Fraction

Consider the schematic of the flotation column shown in Figure 3.1. A material balance for an element in the recovery zone for the case of a mono-dispersed mineral fraction may be written as:

$$\text{Input} - \text{output} + \text{rate of production} = \text{rate of accumulation} \qquad (3.1)$$

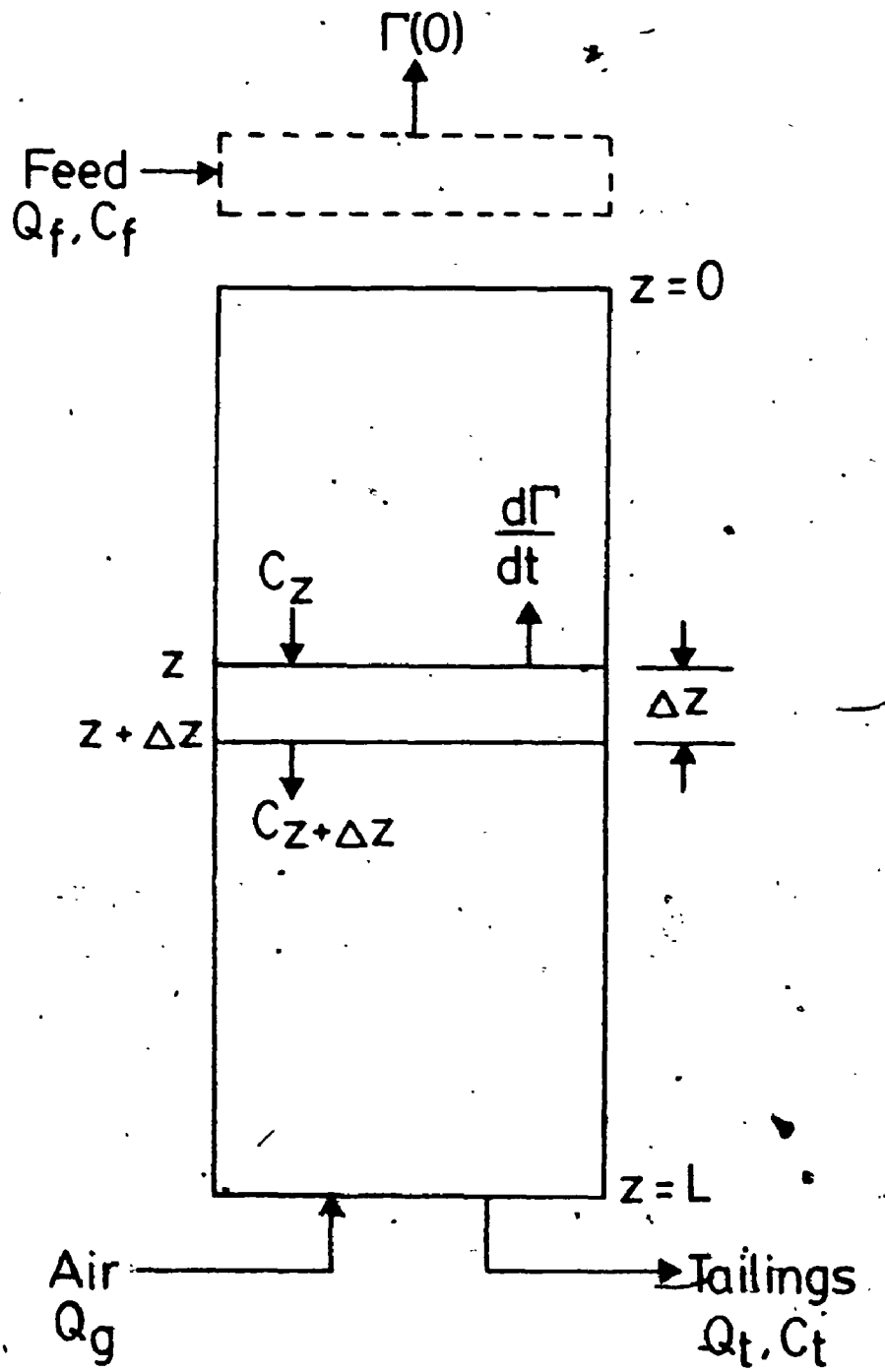

Figure 3.1 A material balance for the recovery zone.

The rate of production is given by

$$-\frac{dC}{dt} = a\frac{d\Gamma}{dt} \qquad (3.2)$$

Equation 3.2 merely states that the rate of loss of particles from the liquid phase in the element is equal to the rate at which the bubbles pick them. This equation differs in a most significant way from those presented by Flint (1971), Rice et al. (1974), and Dobby (1984): Equation 3.2 considers the bubble loading process to be dynamic while the others do not. Substituting the appropriate mathematical terms into the general material balance expression 3.1 and applying assumption (4), we get

$$A\left(\frac{V_P+U_R}{1-\varepsilon_g}\right)\{C_z - C_{z+\Delta z}\} - aA\Delta z\frac{d\Gamma}{dt} = A\Delta z\frac{\partial C}{\partial t} \qquad (3.3)$$

In equation 3.3, A is the cross-sectional area of the column, U_R the superficial liquid velocity in the recovery zone and C_z the concentration of floatable material at position z. Note that the convention used here is plus for co-gravity motion with z = 0 at the feed inlet point. Dividing throughout by $A\Delta z$ and taking the limits as $\Delta z \to 0$, we obtain

$$\frac{V_P+U_R}{1-\varepsilon_g}\frac{\partial C}{\partial z} - a\frac{d\Gamma}{dt} = \frac{\partial C}{\partial t} \qquad (3.4)$$

At steady state, $\frac{\partial C}{\partial t} = 0$, thus reducing equation 3.4 to

$$\frac{dC}{dz} = -\frac{a(1-\varepsilon_g)}{V_P+U_R}\frac{d\Gamma}{dt} \qquad (3.5)$$

Since both C and Γ are height dependent, a relationship

between the two is additionally required for the solution of equation 3.5. This is done by using the bubble loading rate (equation 2.28) which gives on rearrangement

$$\frac{dC}{dz} = - \frac{ak'\Gamma_m(1-\varepsilon_g)}{V_p+U_R} C \qquad (3.6)$$

For the solution of equation 3.6, the boundary conditions are required. A mass balance at the feed inlet point will give

$$\left(\frac{V_p+U_R}{1-\varepsilon_g}\right) A\ C(0) = Q_f C_f \qquad (3.7)$$

Equation 3.7 merely states that the solids entering the column at the feed point leave by convection and sedimentation. The underlying assumption here is that the particles are at their terminal settling velocity upon entering the column. This is clearly an oversimplification as the liquid jet will dissipate its momentum in a finite zone upon entering the column. It would therefore be more appropriate to consider the particles as starting with a zero terminal settling velocity which increases to V_p in a finite height.

Integration of equation 3.6 gives

$$C = C(0)\exp\left\{- \frac{ak'\Gamma_m(1-\varepsilon_g)}{V_p+U_R} z\right\} \qquad (3.8)$$

where

$$C(0) = \frac{Q_f C_f (1-\varepsilon_g)}{A(V_p+U_R)} \qquad (3.9)$$

For the estimation of the recovery, an overall mass balance

over the recovery zone may be written as:

$$\text{Recovery} = \frac{Q_F C_F - Q_T C_T}{Q_F C_F} \qquad (3.10)$$

where Q_T, Q_F are the tailings and feed flow rates respectively and C_T is the concentration of floatable material at $z = L$. It should be noted that in equation 3.10, Q_T differs from Q_F due to the entrainment of liquid by the rising air bubbles.

The bubble load at $z = 0$ may be estimated from an overall mass balance over the recovery zone as shown below

$$\Gamma(0) = \frac{Q_F C_F - Q_T C_T}{Q_G S} \qquad (3.11)$$

where Q_G and S are the gas flow rate and bubble surface to volume ratio respectively. The bubble load estimated from this mass balance may then be used to verify assumption 3. If the assumption does not hold (e.g. the fractional coverage of the bubble exceeds 0.5), the bubble loading rate should be replaced by the more general expression for the bubble loading rate (i.e., equation 2.28).

3.1.2 Flotation of a Poly-Dispersed Mineral

The procedure presented above for the mono-dispersed mineral can be extended to the general case of a mineral with a wide particle size distribution. Consider the flotation of a single mineral having j fractions each with an

adsorption rate constant k_j. Equation 3.6 may be written for each of the j fractions.

$$\frac{V_{P_j}+U_R}{1-\varepsilon_g}\frac{dC_j}{dz} = -a\Gamma_m k_j' C_j \qquad (3.12)$$

In general, what is required for the prediction of recoveries is the variation of the total concentration of floatable material with height and not the individual fractional concentrations. This is obtained from a summation of equations 3.12 as shown below:

$$\sum_j \left(\frac{V_{P_j}+U_R}{1-\varepsilon_g}\cdot\frac{dC_j}{dz}\right) = -a\Gamma_m C \sum_j (k_j' x_j) \qquad (3.13)$$

where x_j is the weight ratio of fraction j to the total weight of the mineral at position z. The integration of equation 3.13 is complicated by the dependence of C and x_j on the height and of k_j' and V_{P_j} on the particle size. At the present time, the dependence of k_j on the particle size is largely unknown. This dependence should not be confused with that of the collection efficiency which has been determined for mechanical-type flotation cells (e.g. Imaizumi and Inoue, 1963; Tomlinson and Fleming, 1963; Jameson et al., 1977; etc.). Under these conditions some additional simplifying assumptions are required. It should be noted that the right hand side of equation 3.13 represents the total bubble loading rate at position z.

For bubble column flotation, the bubble rise velocity

will normally be much larger than the sum of V_{P_j} and U_R for typical flotation size particles. Under these conditions, it may be reasonable to assume that the bubble residence times in the recovery zone will be much shorter than the time over which k_j and x_j change significantly in the flotation column (King et al., 1975). Consequently, these quantities may be taken as being constant over the lifetime of the bubble. As a result, equation 3.13 reduces to

$$\sum_j \left(\frac{V_{P_j} + U_R}{1-\varepsilon_g} \cdot \frac{dC_j}{dz}\right) = -a\,\bar{k}'\,\Gamma_m C \qquad (3.14)$$

where

$$\bar{k}' = \sum_j (k_j' x_j) \qquad (3.15)$$

It is desirable to express the left hand side of equation 3.14 in the same form as equation 3.6. If U_R is much larger than the settling velocity of most of the solid particles, the use of a weight average value defined by equation 3.16 may suffice.

$$\bar{V}_P = \sum_j (V_{P_j} x_j) \qquad (3.16)$$

By applying these simplifications, equation 3.12 may be reduced to the familiar relationship derived earlier for the flotation of the mono-dispersed mineral.

$$\frac{dC}{dz} = -\frac{a\bar{k}'\Gamma_m(1-\varepsilon_g)}{\bar{V}_P + U_R} C \qquad (3.17)$$

The values x_j used in this case may be those of the feed material.

3.1.3 Mixed Mineral Flotation

In practice, the feed to a flotation circuit is usually made up of several minerals each displaying a wide particle size distribution. Consider a feed containing i minerals each with j fractions. The mathematical treatment presented for the flotation of a poly-dispersed mineral may be readily extended to the general case of a mixed minerals flotation. First, equation 3.17 may be written for each of the minerals.

$$\frac{dC_i}{dz} = - \frac{a\bar{k}'_{i\,m}(1-\epsilon_g)}{V_p+U_R} C_i \qquad (3.17)$$

Integration of these equations subject to the correct boundary conditions may be used to compute the concentration profile of each mineral in the column. With this information, the recoveries can be estimated using the modified form of equation 3.10.

$$\text{Recovery}_i = \frac{Q_F C_{F_i} - Q_T C_{T_i}}{Q_F C_{F_i}} \qquad (3.18)$$

In mixed mineral flotation, information on the concentrate grade is also required. This may be done by performing an overall balance on the liquid and gas phases in the recovery zone as shown below

$$\text{Grade}_i = \frac{Q_F C_{F_i} - Q_T C_{T_i}}{\sum_i (Q_F C_{F_i} - Q_T C_{T_i})} \qquad (3.19a)$$

$$= \frac{\Gamma_i(0)}{\sum_i \Gamma_i(0)} \qquad (3.19b)$$

3.2 FLOTATION COLUMN SIMULATION

For flotation column simulation, the hydrodynamic parameters and the integrated form of equations 3.6 or 3.17 are required. We begin our analysis by considering the flotation response of a single poly-dispersed mineral. This may be extended to the flotation of a mixture of minerals using the procedure presented above for modelling such systems.

3.2.1 Flotation of a Poly-Dispersed Mineral

If we consider the flotation of a poly-dispersed mineral having j fractions, equation 3.17 may be written for the recovery zone

$$\frac{dC}{dz} = - \frac{a\bar{k}' \Gamma_m (1-\varepsilon_g)}{\bar{V}_p + U_R} C \qquad (3.17)$$

An integration of equation 3.17 gives

$$C = C(0) \exp \left\{ - \frac{a\bar{k}' \Gamma_m (1-\varepsilon_g)}{\bar{V}_p + U_R} \cdot z \right\} \qquad (3.20)$$

where $\bar{V}_p$ and $\bar{k}'$ are as previously defined.

For a numerical simulation of the flotation column performance, knowledge of the following kinetic and hydrodynamic parameters is required: $\bar{K}'$, Γ_m, $\bar{V}_p$, a, ε_g, U_R, d_b, U_b and Q_T/Q_F. For the purpose of this exercise, only the order of magnitude for the kinetic parameters are used. For example, even though King et al. (1975) reported a $\bar{K}'$ value of 7.7×10^{-3} for their adsorption rate constant only a value of 10^{-3} is used in this simulation. The superficial gas velocity assumed here (0.02 m/s) is the optimum value that has been determined experimentally by Dobby and Finch (1986) for copper flotation at Gibraltar Mines, B.C. For the purpose of the simulation, the following hydrodynamic and kinetic data were used:

$\bar{K}' = 0.001\ m^3/kg\ s$ $\qquad$ $\Gamma_m = 3.54\times10^{-3}\ /d_b$

$d_b = 0.001\ m$ $\qquad$ $U_b = 0.1\ m/s$

$\bar{V}_p = 0.015\ m/s$ $\qquad$ $U_g = 0.02\ m/s$

$\varepsilon_g = 0.2$ $\qquad$ $C_F = 50\ kg/m^3$

and

$$a = 6\varepsilon_g/d_b$$

Substituting and solving for C(z) gives

$$C(z) = 25.4\ \exp(-40.5\ z) \qquad (3.21)$$

This shows that for highly floatable material, only a small recovery height may be required for high recoveries. Since

the particle collection process takes place in a fairly narrow zone, the assumption that k_j and x_j do not change appreciably with height appears to be a logical one. However, this observation is in apparent contradiction with the present practice of designing flotation columns with recovery zones of over 9 m in height! While it is possible that the mathematical model presented here may be in error, this does not appear to be the case. For example, recent communications with the original inventor of the flotation column have confirmed that in the flotation of strongly hydrophobic minerals, only a small recovery zone was required (Wheeler, 1984). While the reasons for this discrepancy are not entirely clear at the present time, they have been attributed to the additional turbulence created by the addition of wash water near the froth-pulp interface which may promote mineral detachment. The same effect may also be explained by considering the role of frother co-adsorption on the mineral surface on flotation response (Ityokumbul et al., 1985b). Since the wash water used in these operations does not contain frothers, it is probable that some frother (or even collector) molecules may be removed from the mineral surface thus promoting the detachment of the mineral particles from the air bubbles. The mineral particles removed in this way are then transferred back into the recovery zone as a result of the positive bias which exists in these columns. This would suggest that present-day

industrial flotation columns may not be optimally operated.

3.2.2 Effect of Gas Velocity On Flotation Response

The effect of gas velocity on flotation response is required for scale-up purposes. In theory, there should be an optimum gas velocity for bubble column flotation: at zero gas velocity, there will be no recovery, while at extremely high gas velocities, there will be a 100% recovery of the feed (equivalent to no recovery). The optimum in flotation recovery has been reported by some authors to be in the gas velocity range of 0.01-0.03 m/s (Van Ham et al., 1983; Dobby and Finch, 1986). For the systems considered, this gas velocity corresponds to the bubbly flow regime. The same hydrodynamic flow regime has been determined for other bubble column reactor applications as well (Schumpe et al., 1979). It will therefore be desirable to see if this optimum can be predicted from theoretical considerations.

Consider first the flotation rate expression presented by Jameson et al. (1977) and used by Dobby and Finch (1985, 1986) in their modelling work.

$$\frac{dC}{dt} = -(1.5\ U_g\ E_c/d_b)C \qquad (2.25)$$

This expression shows that flotation is a first order rate process with the rate constant being

$$k = 1.5\ U_g\ E_c/d_b \qquad (2.26)$$

The data of Anfruns and Kitchener (1977) for fine particles flotation ($Re_p < 0.1$) indicate that

$$E_c \propto d_b^{-1.69} \qquad (3.22)$$

On substituting into equation 2.25, the following is obtained

$$k \propto U_g / d_b^{2.69} \qquad (3.23)$$

For bubbly flow conditions, the bubble size will not change appreciably with gas velocity (Kumar et al., 1976). Under these conditions, the rate constant will increase linearly with gas velocity. Since the transition from bubbly flow to the churn turbulence flow regime is accompanied by a rapid increase in bubble size with gas velocity, the rate constant will decrease with increasing gas velocity thus confirming the existence of an optimum gas velocity for bubble column flotation. However, as explained in Chapter 2, the derivation of this rate expression does not consider the bubble loading rate to be height dependent.

Consider next the rate expression presented in this study (i.e., equation 3.2). The rate constant on substituting for the bubble loading rate under free flotation conditions becomes

$$\frac{d\Gamma}{dt} = - ak' \Gamma_m C \qquad (3.24)$$

Equation 3.24 also shows that flotation is a first order rate process with the rate constant being

$$k = ak'\Gamma_m \tag{3.25}$$

For spherical bubbles,

$$a = \frac{6\epsilon_g}{d_b} \tag{3.26}$$

On substituting for Γ_m (i.e., equation 2.31) and a, we obtain

$$k \propto \epsilon_g / d_b^{1.875} \tag{3.27}$$

For bubbly flow, the gas hold-up increases linearly with gas velocity. A comparison of equation 3.26 with equation 3.23 shows similar trends, with the major difference being the bubble diameter exponent. However, it is not entirely clear at the present time if the same bubble diameter exponent will be applicable for flotation of particles settling outside the Stoke's regime. Since the present treatment assumes the bubble loading rate to be height dependent, its use is recommended. This treatment also shows that for transition to the churn turbulence flow regime, the flotation rate will decrease rapidly with increasing gas velocity since both ϵ_g and Γ_m decreases with increasing bubble size (King et al., 1975; Shah et al., 1982).

In all the treatments considered here, it was assumed that the dependence of the rate constant on the gas velocity is only through the effect of the latter on the various hydrodynamic parameters comprising the former. In practice,

increases in gas velocity even if the bubbly flow regime may be expected to increase particle detachment thus reducing the rate constant.

CHAPTER 4

MATERIALS AND METHODS

4.1 MATERIALS

The solids used in this study were Ottawa sand (Weldron Plant Designation 705 and 505) and centrifuge tailings samples obtained from the Syncrude Canada Limited operations in Fort McMurray, Alberta. The particle size distribution of the Ottawa sand was determined by sieving using a Rotap device and is shown in Figure 4.1.

Air and water were the gas and liquid phases respectively. In order to simulate flotation conditions, pine oil was added to the tap water in the model experiments in varying concentration. In the flotation experiments with the centrifuge tailings, pine oil and surfactants of the alkyl aryl sulphonates (available under the trade names Tretolite F-46 and Tretolite E-3453 supplied by the Petrolite Corporation, Calgary, Alberta) were also used even though the tailings have been shown to contain surface active compounds (Bowman, 1967; Baptista and Bowman, 1969; Hocking, 1977).

All the experiments were carried out at 25°C ± 1°C.

4.2 EQUIPMENT

The bubble column had an internal diameter of 0.06 m

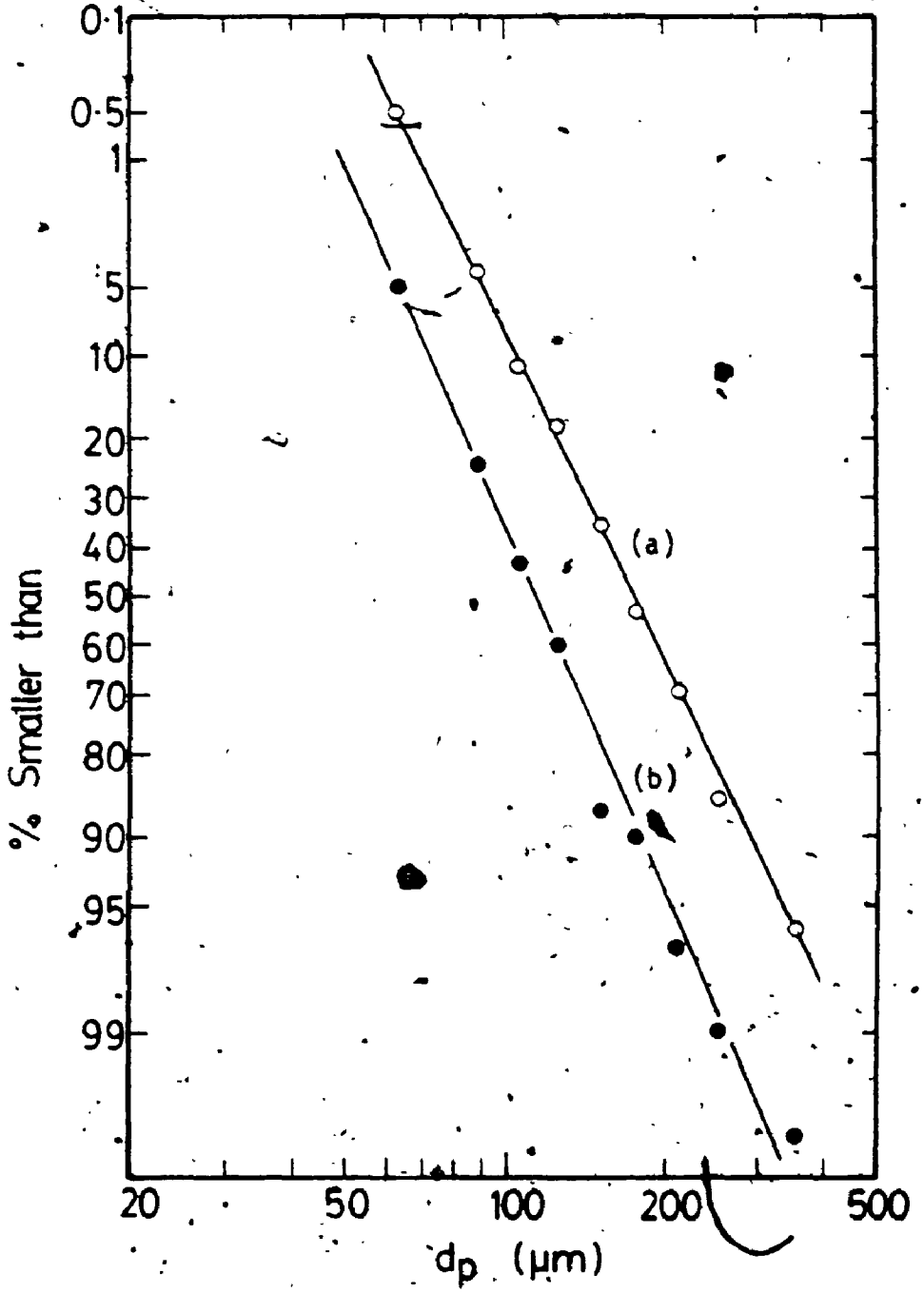

Figure 4.1 Particle size distribution of the Ottawa sand (a) Weldron Plant Designation 505 and (b) Weldron Plant Designation 705.

and was made of transparent acrylic. It had an overall height of 0.96 m. However, owing to its sectionalized nature, this height could be varied. Air which had been passed through an oil filter and a pressure regulator was introduced into the column through a porous stainless steel plate located at the base of the unit. The average pore size of the plate was determined by the method of Houghton et al. (1957) to be 134 μm (Ityokumbul et al., 1985a). A schematic of the experimental set-up is shown in Figure 4.2. Details of the design of the column bottom for the batch flotation experiments and the continuous experiments are shown in Figures 4.3(a) and (b) respectively.

The flow rates of the feed and tailings streams were regulated by two identical peristaltic pumps (Cole Palmer Model 7553-00). The calibration of the pumps was performed daily to check for drifts which arise as a result of tubing wear. For the two-phase (gas-liquid) experiments, the feed stream was uniformly distributed at the top of the column with the aid of a 0.019 m polypropylene ball having 16 holes (diameter 1 mm) covering the lower chord forming an obtuse angle of 120° at the centre of the ball.

The air fed to the column was passed through one of two identical rotameters (or both) which were initially calibrated against a wet gas test meter (Precision Scientific Co.). Details of the calibrations are shown in

Appendix A.

Ten brass pressure and sample taps were mounted along the column axis. Each pressure tap was connected to a manometer containing the same liquid as the column.

Three different reservoirs were used in these experiments. For the two phase experiments, the reservoir was a 12 L stainless steel bucket equipped with a large magnetic stirring bar. For the phase hold-up experiments, the reservoir was a 25 L steel container while a 25 L plastic carboy was used in the three phase liquid dispersion experiments. For all the three phase experiments, the reservoir was equipped with a Lightnin Mixer (Gray Mixing Equipment Model 10).

4.3 PROCEDURE

In the present study, the superficial liquid and gas velocities ranged from 0.0 to 0.007 m/s and 0.0 to 0.04 m/s respectively. As shown in Figure 4.2, only the counter-current flow arrangement of gas and liquid (or slurry) was used in the continuous experiments reported here.

4.3.1 Batch Flotation Experiments

About 200 litres of diluted centrifuge tailings containing approximately 15% solids and 3% bitumen were obtained from the Syncrude Canada Limited operations in Fort McMurray,

Figure 4.2 Schematic of the experimental set-up

(1) Prefiltered utility air at 115 KPa
(2) Gas flow meters
(3) 25L reservoir
(4) 0.06m (i.d) bubble column
(5) Static pressure taps
(6) Sampling taps
(7) Canlab solid state combination pH electrode (Model H5503-21)
(8) Fisher Accumet Digital pH meter (Model 425)
(9) Variable speed recorder (Servegor 210)

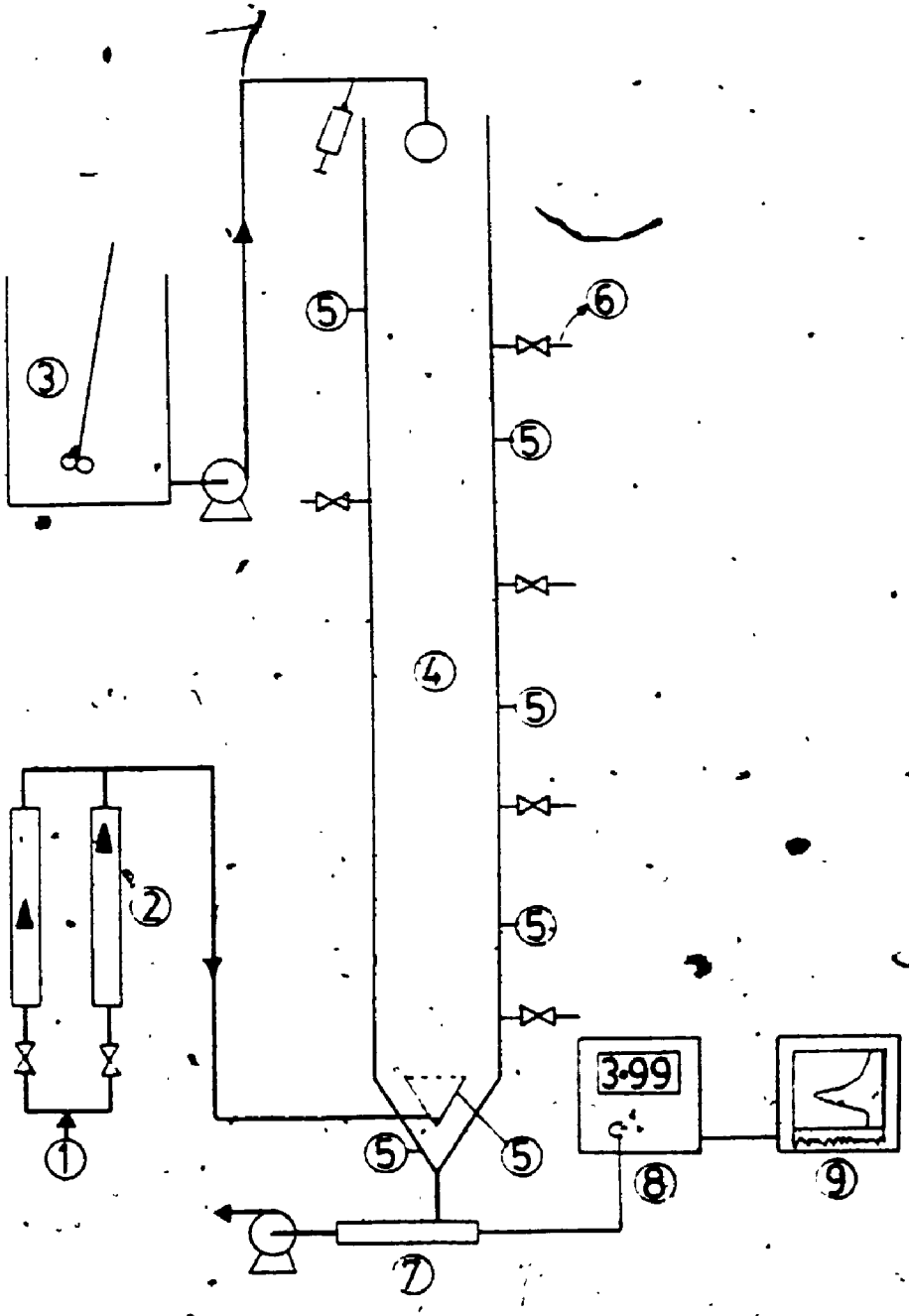
3·99
1
2
3
4
5
6
7
8
9

Alberta in 25-litre containers. As received, the solids in these samples settled to the bottom of the container while an oil film (bitumen/naphtha) floated on top of the partially clarified water. This oil film was skimmed off manually and the solids redispersed by mechanical agitation.

For these experiments, the geometry shown in Figure 4.3a for the column bottom arrangement was employed. In addition, only a 40 cm test section of the column was used. Preliminary experiments were carried out to test the air flotation mechanism proposed here for the recovery of these minerals. These involved the transfer of approximately 1100 ml of the homogenized slurry into the column followed by aeration and recovering the froth that was produced. Figure 4.4 shows that only approximately 40% of the solids initially present in these tailings were floatable. X-ray powder diffraction analysis of the feed and flotation concentrate solids (Figure 4.5) revealed that gangue rejection was effective.

For the subsequent experiments aimed at determining the optimum physico-chemical factors likely to affect the flotation recovery of the minerals present in these tailings, the batch flotation time was fixed at 10 min since preliminary results (Figure 4.4) revealed that approximately 90% of the floatable solids were recovered in this time interval. In these experiments, approximately 1100 to 1200 ml of the

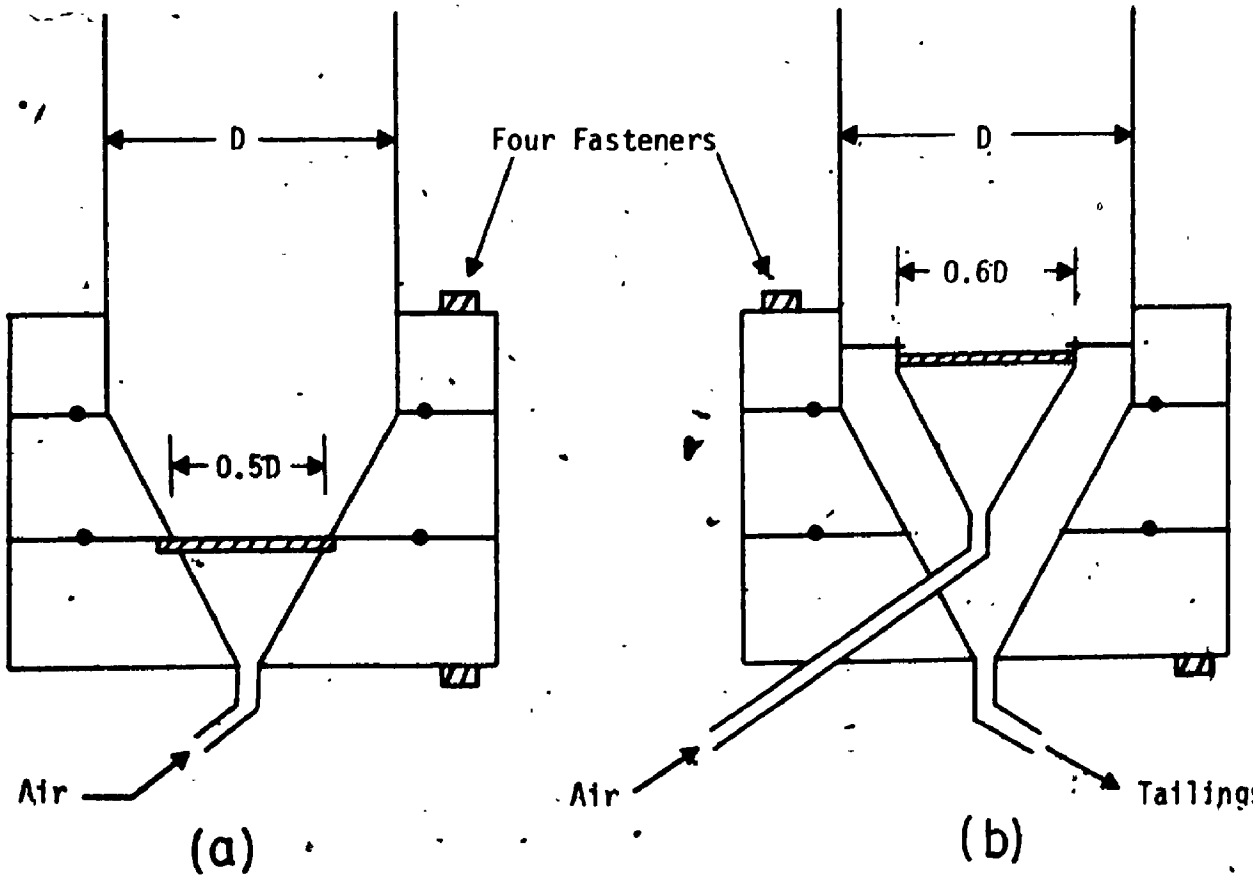

Figure 4.3: Design for column bottom (a) for batch flotation experiments and (b) for the continuous experiments.

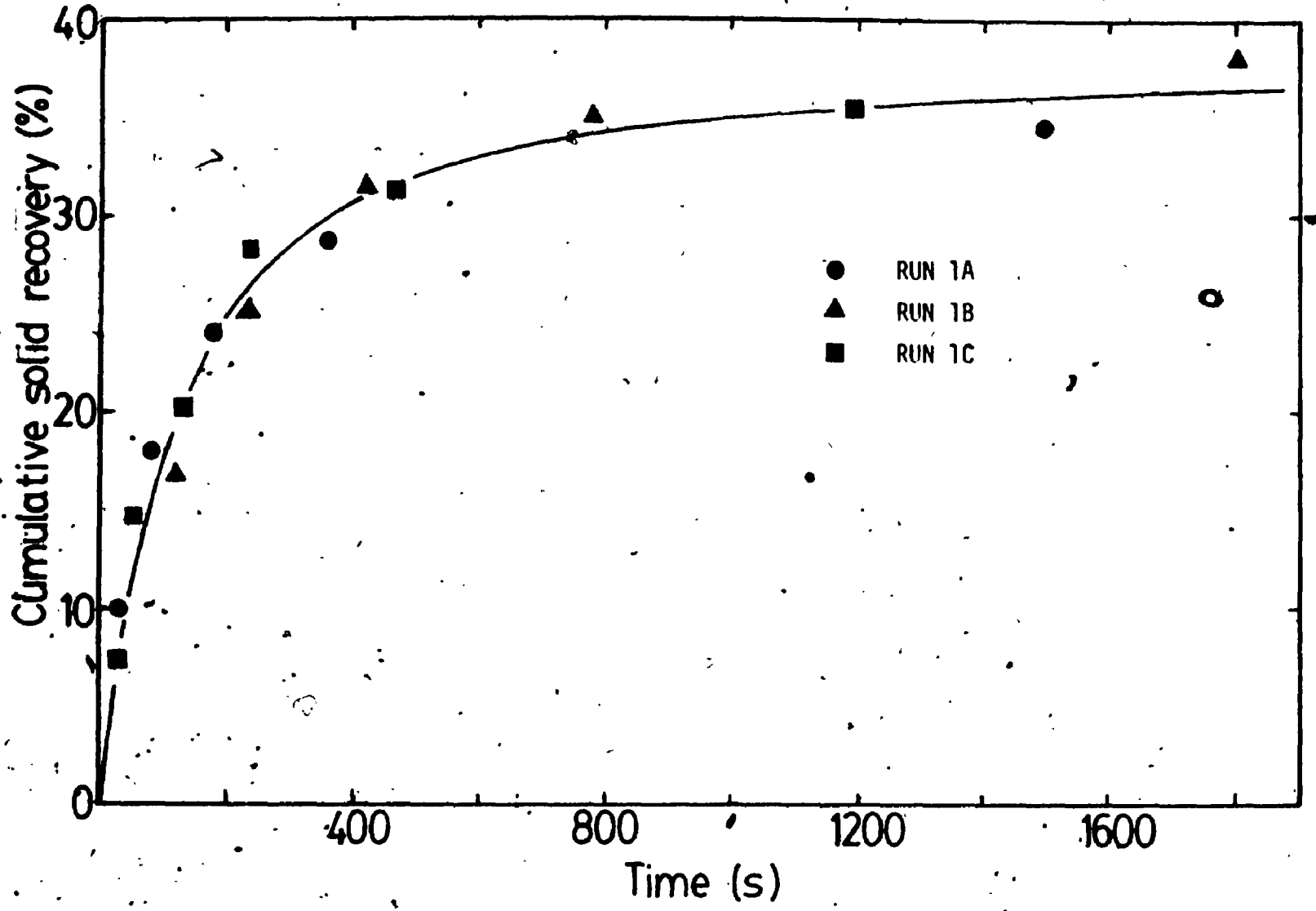

Figure 4.4 Fraction of solids recovered as a function of batch flotation time.

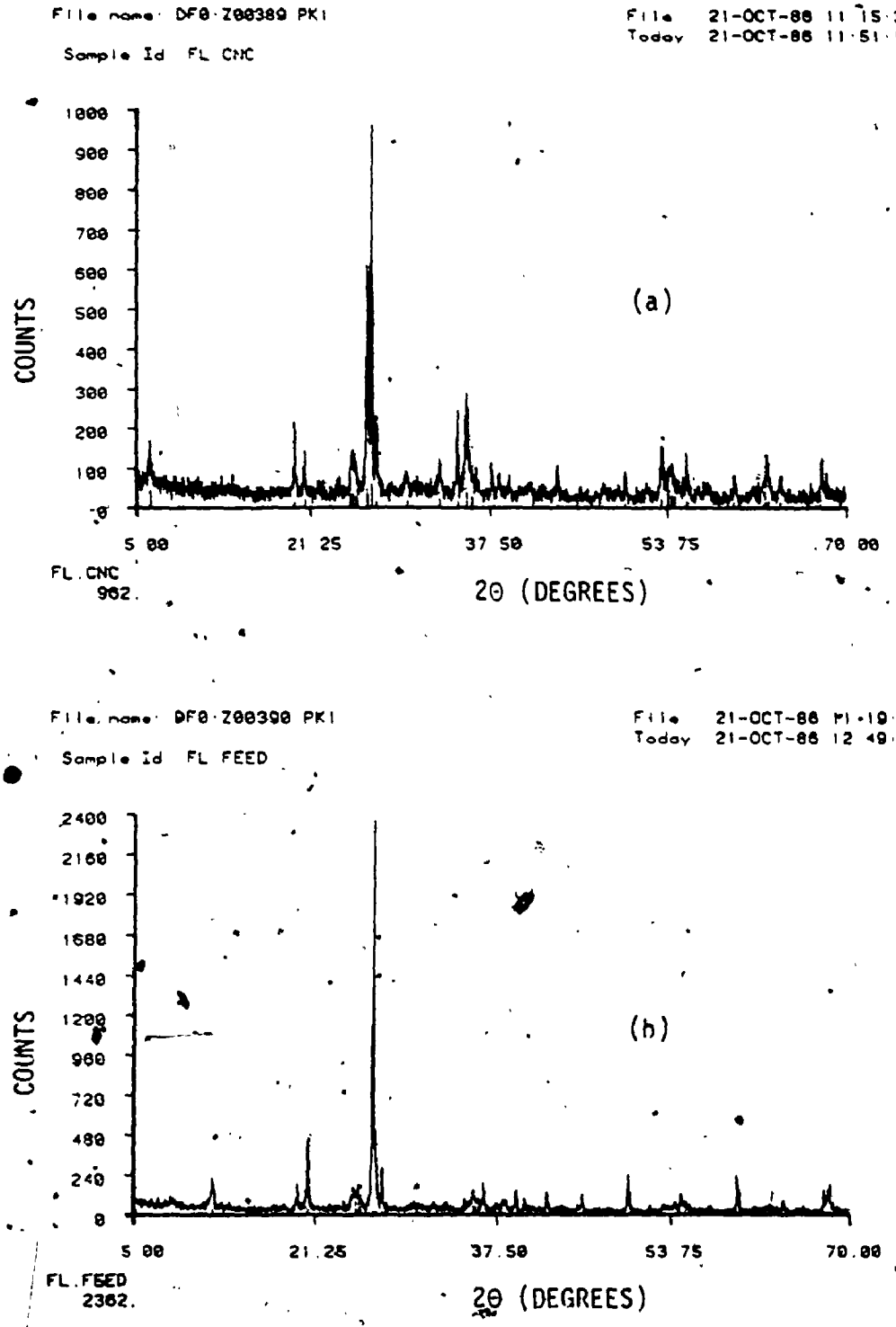

Figure 4.5 X-Ray Diffraction pattern of (a) flotation concentrate and (b) crude centrifuge tailings (Cu Kα λ = 1.5405 A).

homogenized slurry were transferred into a large beaker. Additives as required were blended with continuous agitation at this stage. Starch was added in the soluble form as causticized starch for the depression of iron minerals (Glembotskii et al., 1963) since enriched concentrations of iron minerals were observed in our flotation concentrate (Ityokumbul et al., 1985a). Hydrochloric acid and sodium hydroxide were used for pH modification. Except for experiments involving pH changes, agitation was continued for a further 5 minutes. After this period, samples were taken for analyses (pH, solids content, surface tension, bitumen content and elemental analysis for the heavy minerals), and the remaining slurry was transferred into the column. The air flow rate was quickly adjusted to give a superficial gas velocity of 0.013 m/s. The froth samples produced were recovered as a function of batch flotation time. The choice of the gas velocity was based on estimates for the complete suspension of the solids present in the column (Imafuku et al., 1968; Koide et al., 1983).

For experiments involving pH modifications, attainment of a constant pH was slow owing in part to the presence of the hydrocarbon phase on the solid particles. For example, in titration experiments, it was found that at least 5 hours of standing were required after the initial agitation to achieve a steady pH. As a result, all experiments involving pH effects were allowed to equilibrate for 24 hours prior

to sampling.

The surfactants initially tested were of the alkyl aryl sulphonates type (available under the trade names Tretolite F-46 and Tretolite E-3453) since Kovaric et al. (1981) have shown that they were effective in the deemulsification of oil in water and water in oil emulsions respectively. In the end, pine oil was selected because of ease of availability and its superior properties. For example, the presence of residual oil in these tailings will produce froths with low drainage properties. This means that any trapped gangue particles would not be rejected in the froth phase. According to Taggart (1945), this condition can be easily overcome by the addition of pine oil.

In addition to these batch bubble column flotation experiments, some experiments were also conducted in a 2.5 L mechanical flotation cell (Denver Laboratory Flotation Machine Model D-1). The aim of these experiments was to test if the same recoveries and concentrate grades (as from the batch bubble flotation column) could be obtained in such cells.

From the composition of the feed and the concentrate, the recoveries of these minerals were calculated.

The development of an upgrading process for the flotation concentrate was based on differences in physical

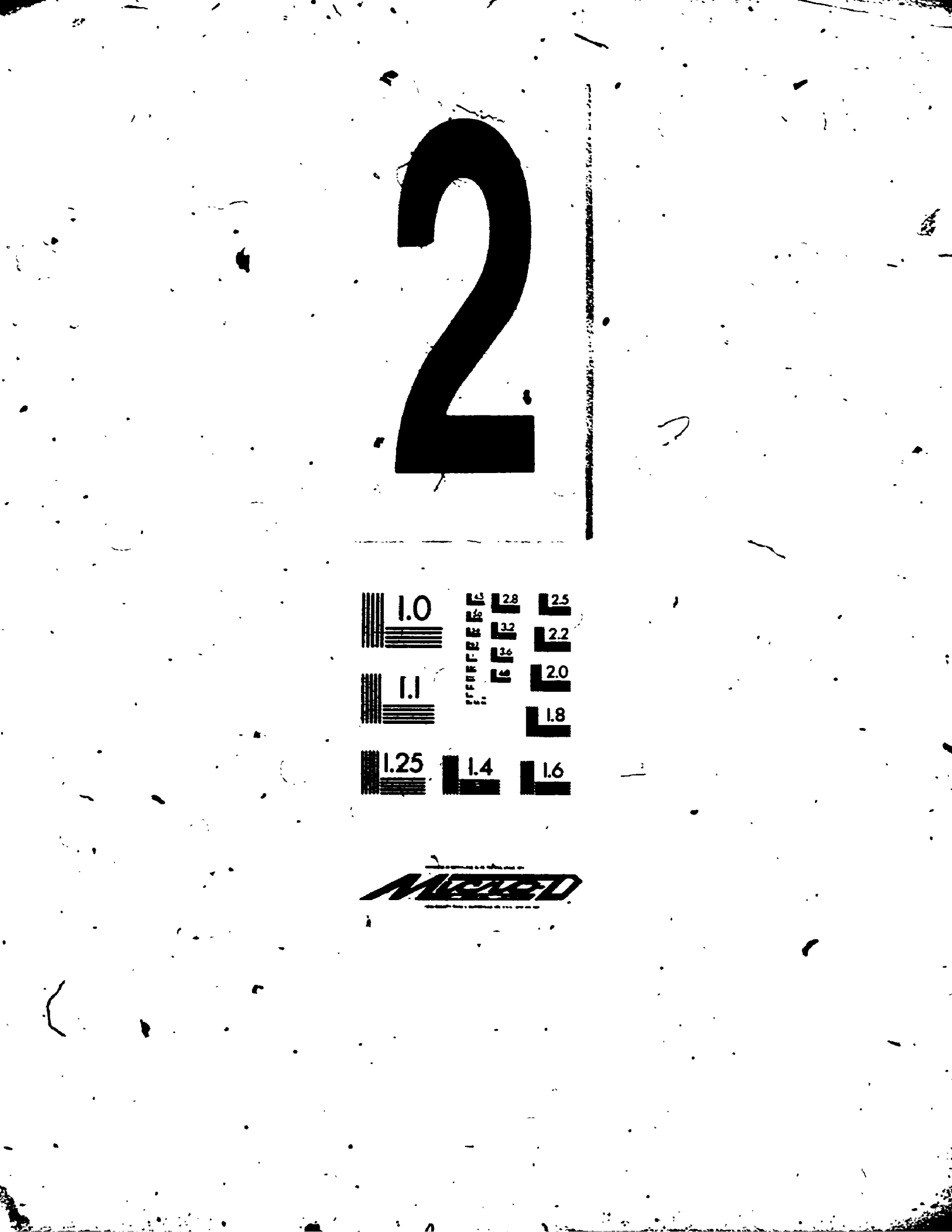
2
1.0
1.1
1.25
1.4
1.6
2.0
2.2
2.5
2.8
3.2
3.6
MICRO

properties of the minerals found in these centrifuge tailings. The physical properties tested were:

(i) Size: this was done by sieving using a Rotap device.

(ii) Low intensity magnetic susceptibility: this was done by repeatedly passing a magnetic bar over the solids and separating the mineral particles that remained attached to the magnet.

(iii) Density: Meriam fluid #5 (density 2950 kg/m^3) was used to separate the lighter minerals from the heavy minerals.

(iv) High intensity magnetic susceptibility: a Frantz Isodynamic Separator Model L-1 was used for these tests. The magnetic intensity of the unit was varied by changing the current through its armature. The equipment setting (forward and side slopes) and armature current employed were those required to give the following fractions:

Armature Current	Major Mineral Fraction
0.35A	Ilmenite
0.70A	Xenotime
0.95A	Monazite
1.50A	Rutile
Non-magnetic fraction at 1.50A	Zircon

4.3.2 Analyses

Reported values for pH and surface tension are those of the supernatant obtained after centrifugation of the samples

at a relative centrifugal force (RCF) of 13,800 g for 20 minutes. pH was determined using a Fisher Accumet Digital pH meter (Model 425) while the surface tension was determined using a Fisher Autotensiomat.

Bitumen was determined by the weight loss method of Hocking (1977). This method entails drying the sample at 105°C for 24 hours and then heating it in a muffle furnace at 340°C for a further 48 hours. Despite the simplicity of the method, it has been shown to yield results which were comparable to those obtained using elemental analysis and to be superior to both solvent extraction and oxygen plasma oxidation (Hocking, 1977). The upper temperature was selected to avoid kaolinite dehydroxylation which has been determined to commence at 400°C (Ityokumbul et al., 1985a,b).

The solids remaining at 340°C were ground in a tungsten carbide mill. Qualitative analysis of the solids (to identify the minerals present) was by infra-red (IR) spectroscopy using a Beckman double beam spectrometer (AccuLab 2). In addition, x-ray powder diffraction (XRD) analysis using a Rigaku Geigerflex computer oriented diffractometer attached to a microprocessor was also used. The IR samples were prepared as a 1% to 2% solid solution in a potassium bromide matrix and the transmittance recorded over the range of 4000-600 cm^{-1}. The XRD pattern obtained with a CuKα (λ = 1.5405Å) radiation was recorded over the 2θ range of 5° to

70°. Identification of the phases present in the sample (from the XRD patterns) was done with the aid of the microprocessor.

Quantitative analysis of the solids for titanium, zirconium, silicon, aluminium and iron was by x-ray fluorescence (XRF) using a Phillips x-ray generator (Model LZ 5) with standards of known composition. Briquets for XRF analysis were prepared by pressing the powder in a hydraulic press at a pressure of 900 MPa. These analyses were found to be in good agreement with those obtained from independent laboratories employing neutron activation, XRF and plasma emission spectroscopy (Barringer Research, Toronto and X-Ray Assays Limited, Toronto).

4.3.3 Phase Hold-Up Measurements

For the phase hold-up experiments, the fluids were introduced into the column at the desired flow rates. The static pressure profile over the entire column height was measured several times with manometers until there was no change in the pressure drop across the bed. During this period, the manometers were carefully checked to ensure that no air bubbles were trapped in them. At the point where the bed pressure drop remained constant, the attainment of steady state was assumed. The static pressure profile along the column axis was measured two or more times

depending on the amplitude of the oscillations observed in the manometer readings and the average values recorded. These oscillations became pronounced at the onset of slugging conditions in the column (i.e., transition from bubbly flow to churn turbulence flow regime). Typical pressure profiles are shown in Figure 4.6.

In the case of gas-slurry operations, the solid to liquid ratio in the column was determined independently by simultaneously stopping the feed and tailings pumps. The contents of the column were removed and the solids separated from the liquid. By measuring the volume of liquid in the column and the weight of the dried solids, the solid to liquid ratio was determined. In these experiments, the manometers were not connected to the column. This was necessary to avoid the solids which were observed in these connections and also the liquid contained in them. Typical solid to liquid ratios in the column are shown in Figure 4.7. These experiments were also used in the estimation of the solid settling velocity.

Experiments were also carried out to evaluate the possibility of using the 'calming section' above the feed inlet point to control gangue recovery. In these experiments, the total liquid level in the column was fixed while the feed inlet point was varied.

For the estimation of the phase hold-ups, the following

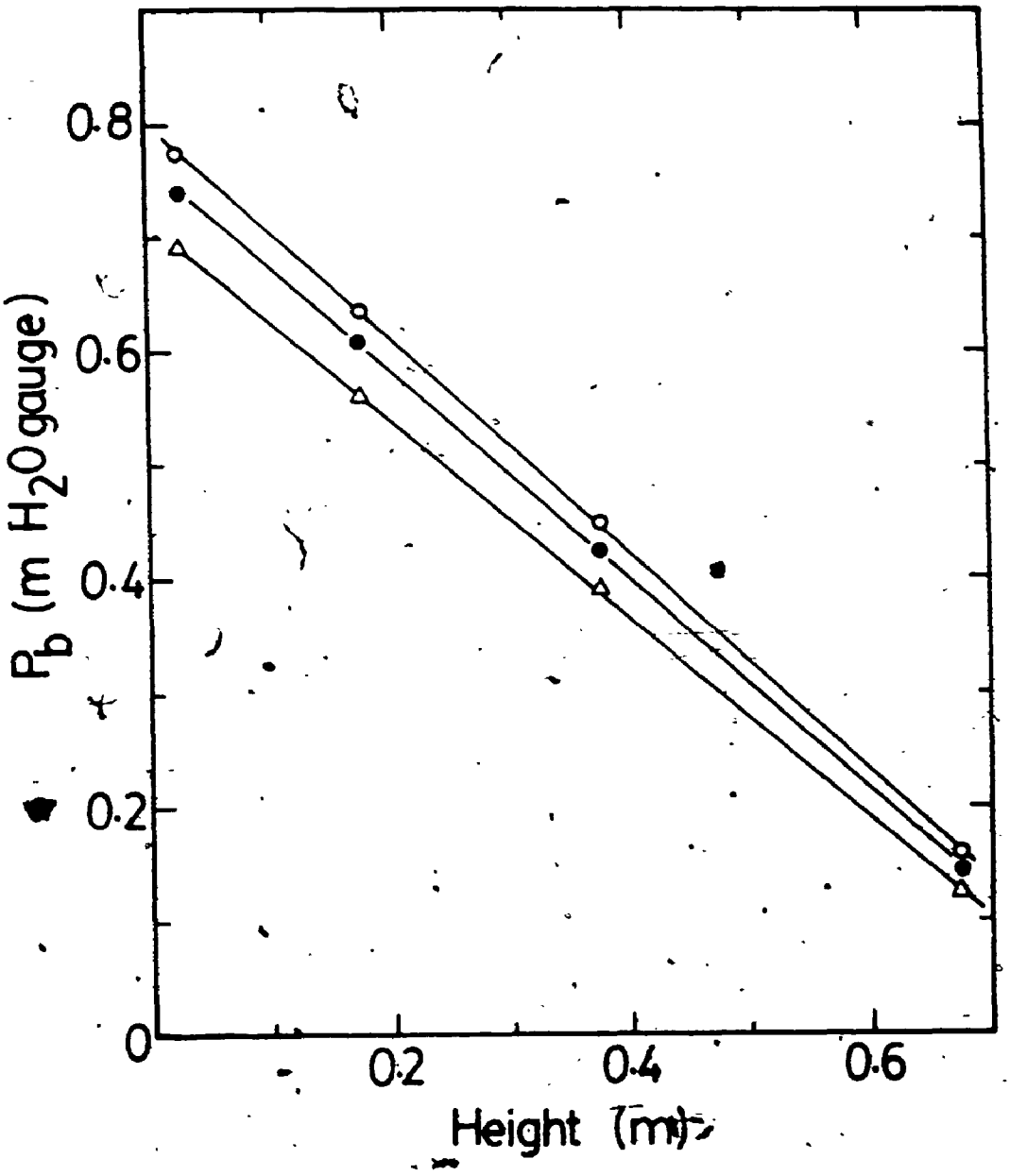

Figure 4.6 Typical static pressure profiles at a liquid velocity of 0.0043 m/s. (O) Air water U_g = 0.01 m/s (●) Air water with frother (10ppm pine oil) U_g = 0.01 m/s and (Δ) Air water solids (18 wt. %) U_g = 0.021 m/s.

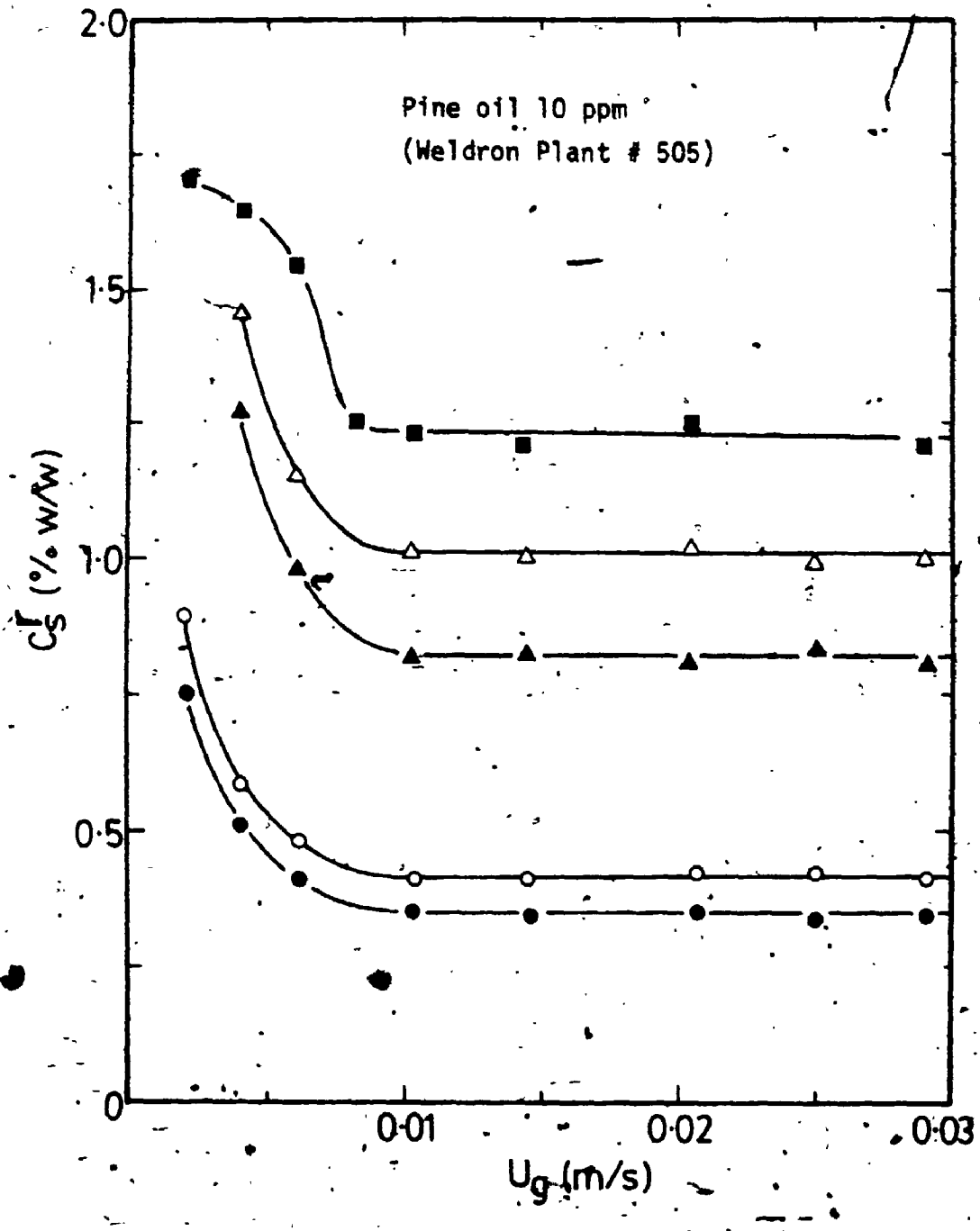

Figure 4.7 Variation of solid to liquid ratio in the column with feed solid concentration: (○, ●) 2.4 wt. %; (△, ▲) 5.0 wt. % and (■) 8.4 wt. %. The open and closed symbols represent liquid velocities of 0.0043 m/s and 0.0063 m/s respectively.

relationships were applied:

1) The sum of the liquid, solid and gas hold-ups (ε_L, ε_s and ε_g respectively) is unity.

$$\varepsilon_L + \varepsilon_s + \varepsilon_g = 1 \qquad (4.1)$$

2) The slope of the static pressure with height is given by

$$-\frac{dP}{dh} = \rho_L\varepsilon_L + \rho_s\varepsilon_s + \rho_g\varepsilon_g \qquad (4.2)$$

Since for most practical cases, $\varepsilon_g\rho_g$ is much smaller than the other terms, equation 4.2 reduces to

$$-\frac{dP}{dh} = \rho_L\varepsilon_L + \rho_s\varepsilon_s \qquad (4.3)$$

3) By taking the ratio of solid to liquid determined from Figure 4.7 (taken to be the flat portion of the curve), the three holdups can be determined. The use of this method assumes that a uniform solid concentration profile exists in the column. Since the correlation coefficient for the static pressure measurements (i.e., equation 4.2) was normally greater than 0.9999, this assumption appears to be valid (Kara et al., 1982; Kelkar et al., 1984).

For the case of two-phase (gas-liquid) flow, only equations 4.1 and 4.3 are required in the estimation of the hold-ups since $\varepsilon_s = 0$.

4.3.4 Liquid Phase Dispersion

For the study of liquid phase dispersion, the pulse technique was used. The tracer employed was 6N hydrochloric acid. The pH of tap water was initially adjusted to 4.00 ± 0.10 in order to avoid the natural buffer of the water. The gas and liquid flow rates were carefully adjusted to the desired values. Approximately 1 ml of the tracer was injected into the liquid feed stream and the response measured in the tailings stream with a Canlab solid state combination electrode (Model 5503-21). The pH electrode was connected to a Fisher Accumet Digital pH meter (Model 425), and the output from the pH meter was recorded on a variable speed chart recorder (Servegor 210). In order to test the calibration of the chart recorder, pH values were read from the meter at regular intervals of 15 s to 20 s depending on the liquid flow rate. Prior to the introduction of the tracer, the feed and tailings pumps were carefully adjusted to the same flow rates. With this arrangement, the boundary conditions can be considered to be closed-closed (Levenspiel, 1972). From the recorded pH-time response and the background hydrogen ions concentration, the concentration-time curve was obtained.

For the estimation of the fluid-dynamic parameters, a mathematical model of the processes taking place is required. The mixing of fluid in a bubble column is normally represented

by the axially dispersed plug flow model. The mass balance of tracer yields the following continuity equation for cylindrical co-ordinates:

$$E_{zL} \frac{\partial^2 c}{\partial z^2} + \frac{1}{r} \frac{\partial}{\partial r} \left(D_r \, r \, \frac{\partial c}{\partial r}\right) - V_r \frac{\partial c}{\partial z} = \frac{\partial c}{\partial t} \qquad (4.4)$$

For a uniform distribution of tracer at the top of the column, radial dispersion may be neglected. Under these conditions, equation 4.4 reduces to the familiar one-dimensional dispersion model expressed in dimensionless form as

$$\frac{1}{Pe} \frac{\partial^2 C}{\partial Z^2} - \frac{\partial C}{\partial Z} = \frac{\partial C}{\partial \theta} \qquad (4.5)$$

where

$$Pe = \frac{V_L L}{E_L} \qquad (4.6)$$

$$c = c/c_m \qquad (4.7)$$

c_m = mass of tracer injected/system void volume (4.8)

$$\theta = t/\tau \qquad (4.9)$$

$$Z = z/L \qquad (4.10)$$

The boundary conditions necessary for solving equation 4.5 are

$$C_i(\theta) = C(0^+, \theta) - \frac{1}{Pe} \frac{\partial C}{\partial Z}\Big|_{Z>0^+} \qquad (4.11)$$

$$\left.\frac{\partial C}{\partial Z}\right|_{Z=1} = 0 \qquad (4.12)$$

$$C(Z,0) = 0, \qquad (4.13)$$

Equations 4.11 and 4.12 arise from mass balances at the planes of injection and measurement respectively, and equation 4.13 arises from the definition of C as a deviation variable from the steady state.

The analytical solution of equation 4.5 subject to the boundary conditions, equations 4.11-4.13, has been given by Westerterp et al. (1984) as

$$C(\theta) = \exp\left[\frac{Pe}{2}\left(1 - \frac{\theta}{2}\right)\right] \sum_{n=1}^{\infty} \frac{\delta_n [Pe\sin\delta_n + 2\delta_n \cos\delta_n]}{\left[\delta_n^2 + \left(\frac{Pe}{2}\right)^2 + Pe\right]} \cdot \exp\left(-\frac{\delta_n^2 \theta}{Pe}\right) \qquad (4.14)$$

where δ_n is the nth root of the transcendental equation

$$\cot\delta_n = \frac{\delta_n}{Pe} - \frac{Pe}{4\delta_n} \qquad (4.15)$$

It can be readily seen that the application of a least-squares criterion to equation 4.14 to estimate the fluid-dynamic parameters (Pe and τ) requires the summation of an infinite series that converges poorly for certain values of Pe and θ. In the present study, the conflict of computational requirements is resolved by expressing the least-squares

criterion in the frequency domain using Parseval's theorem (Guillemin, 1963):

The measured concentration-time data was normalized as shown below

$$G(t) = \frac{c(t)}{\int_0^\infty c(t)dt} \qquad (4.16)$$

The denominator of equation 4.16 represents the mass balance of tracer material:

$$\int_0^\infty c(t)dt = \tau c_m \qquad (4.17)$$

The general criterion for an unweighted least-squares fit is given by a minimization of the integral

$$\phi = \int_0^\infty [G(t) - G_d(t)]^2 dt \qquad (4.18)$$

By Parseval's theorem, ϕ can be expressed in the frequency domain as

$$\phi = \frac{1}{\pi} \int_0^\infty [(\Delta R)^2 + (\Delta I)^2] d\omega \qquad (4.19)$$

where

$$\Delta R = \text{real}[\bar{G}(j\omega)] - \text{real}[\bar{G}_d(j\omega)] \qquad (4.20)$$

$$\Delta I = \text{imag}[\bar{G}(j\omega)] - \text{imag}[\bar{G}_d(j\omega)] \qquad (4.21)$$

The barred quantities in equations 4.20 and 4.21 represent

the Fourier transforms

$$\bar{G}(j\omega) = \int_0^\infty G(t)e^{-j\omega t}\,dt \qquad (4.22)$$

$$\bar{G}_d(j\omega) = \int_0^\infty G_d(t)e^{-j\omega t}\,dt \qquad (4.23)$$

The real and imaginary parts of $\bar{G}(j\omega)$ can be derived from

$$\bar{G}(j\omega) = \bar{G}_i(s)\ \bar{g}(s)\Big|_{s=j\omega} \qquad (4.24)$$

where G_i is the normalized inlet concentration, and $\bar{g}(s)$ is the transfer function between G and G_i. $\bar{g}(s)$ can be easily obtained by Laplace transformation of equation 4.5 and the application of the desired boundary conditions.

In this study, the normalized response data were numerically Fourier transformed and compared in the frequency domain with the pulse response of a closed-closed system. The Peclet number and t were chosen to minimize the error between the two responses using the Simplex minimization procedure of Nelder and Mead (1967). The numerical integration of the equations was done using Filon's quadrature (Clements and Schnelle, 1963). Since the system response is much larger than the injection time, it was assumed that $\bar{G}_i(j\omega)/\bar{G}_i(0) = 1.0$ over the entire range of ω for which the magnitude of $\bar{g}(j\omega)/\bar{g}(0)$ remains greater than the experimental error involved in measuring $G_i(t)$. As a result, no

attempt was made to transform the input numerically. Details of the method and the Simplex minimization program for the closed-closed boundary conditions are given in Appendix B. Upon convergence, the program prints out the estimates of Pe and τ as well as the magnitude of the frequency response as a function of the frequency. Typical frequency responses for the highest and lowest values of Pe encountered in this study are shown in Figure 4.8. As a result of the recommendations of Clements and Schnelle (1963), the frequency responses were not pursued beyond frequencies for which the magnitude of the responses fell below 0.2 to 0.3. This procedure was adopted in order to avoid numerical errors that may arise at higher frequencies.

4.3.5 Bubble Characteristics

For the estimation of bubble size, the photographic technique was employed. The gas and liquid (or slurry) were introduced into the column at the desired flow rates. When steady state was reached, still photographs were taken with a Konica camera at a shutter speed of 1/125 s. The slides obtained were projected onto a large sheet of graph paper and the bubble size estimated by comparison to a 2 cm black strip fixed on the column wall. In addition, a comparison of the projected bubble size to the column dimensions was also used in the estimation of bubble size. The photographic technique has the disadvantage of providing

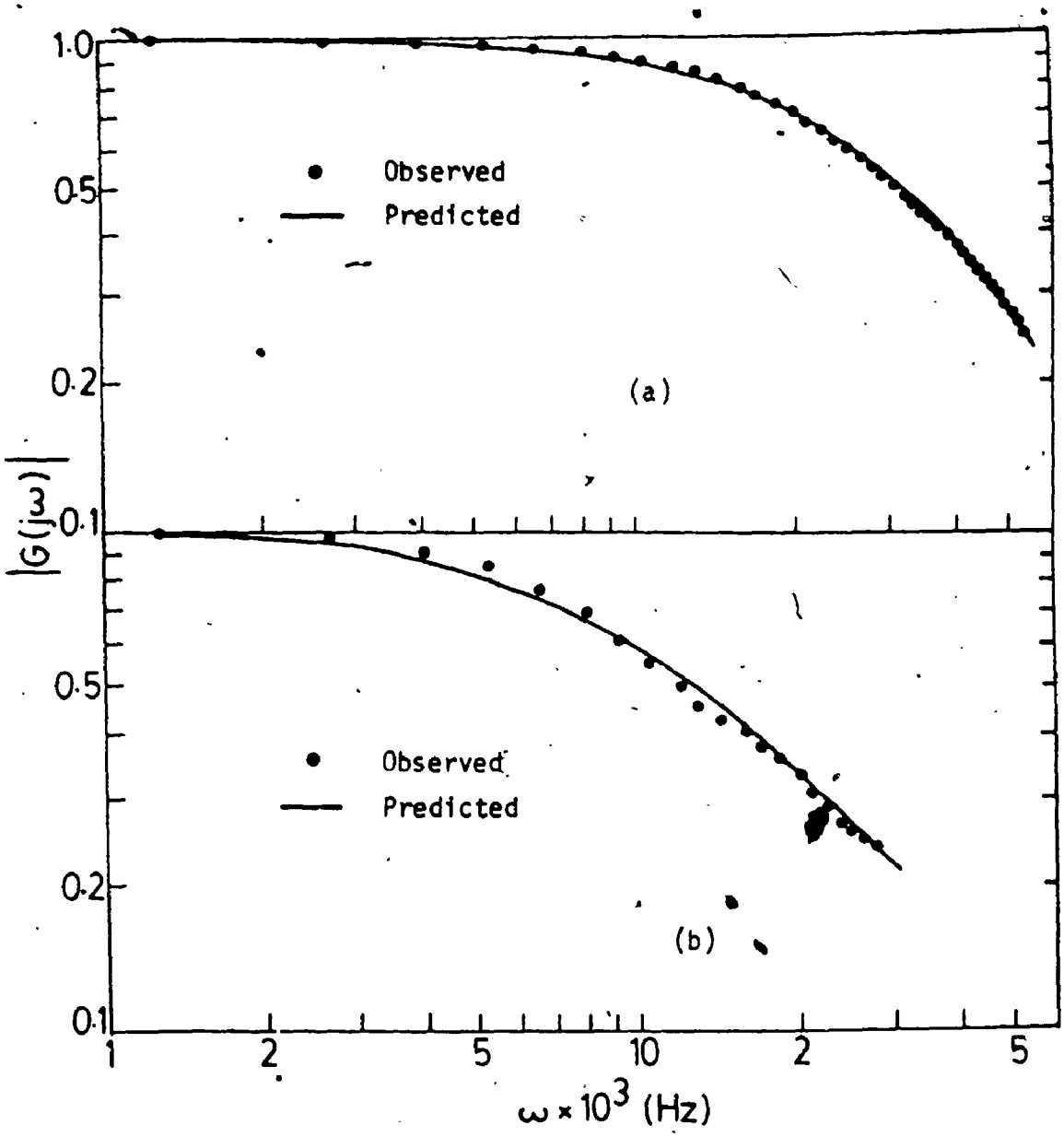

Figure 4.8 Typical frequency response of the axial dispersion equation for closed-closed boundary conditions:
(a) Pe = 4.88 τ = 90 s
(b) Pe = 0.34 τ = 188 s.

estimates for the bubbles in the vicinity of the column wall only but not the larger bubbles which tend to rise in the central part of the column at high gas velocities. Consequently, the method is limited to the chain bubbling and bubbly flow regimes for which the bubbles are of uniform size. This method was used to provide a qualitative estimate of the effect of frothers and/or solids on the bubble size. Visual observations of such phenomena as slug formation, solids on the grid etc. were also recorded.

The bubble rise velocity, U_r, was estimated from the superficial gas velocity and gas hold-up using the relationship

$$U_r = \frac{U_g}{\epsilon_g} \qquad (4.25)$$

Changes in the bubble rise velocity with superficial gas velocity together with the visual observations were used to establish the operating flow regimes for the bubble column.

CHAPTER 5

RESULTS AND DISCUSSION

5.1 FLOTATION RESULTS AND HEAVY MINERALS UPGRADING PROCESS

5.1.1 Effect of pH

For equilibrium pH values below 7.0 and above 11.5, flocculation of these tailings was observed. The supernatant observed in the former case was clear while that from the latter had an orange colour. Flocculation of oilsand tailings at these extreme pH values has been reported before (Kessick, 1979) and will not be discussed at length here.

The variation of heavy mineral recovery and heavy minerals to gangue selectivity index (Gaudin, 1930) with pH is shown in Figure 5.1. The feed and concentrate grades obtained at these pH values are shown in Table 5.1. The parallel shape of the two curves suggests that the separation of these heavy minerals is strongly dependent on pH. The results show that the optimum conditions for the recovery of heavy minerals were obtained for pH values in the range 8.3 to 11.7. Since the pH at which these tailings are produced during the course of the bitumen extraction process is in this range, the tailings can be upgraded by flotation as produced. Low recoveries were obtained for pH values

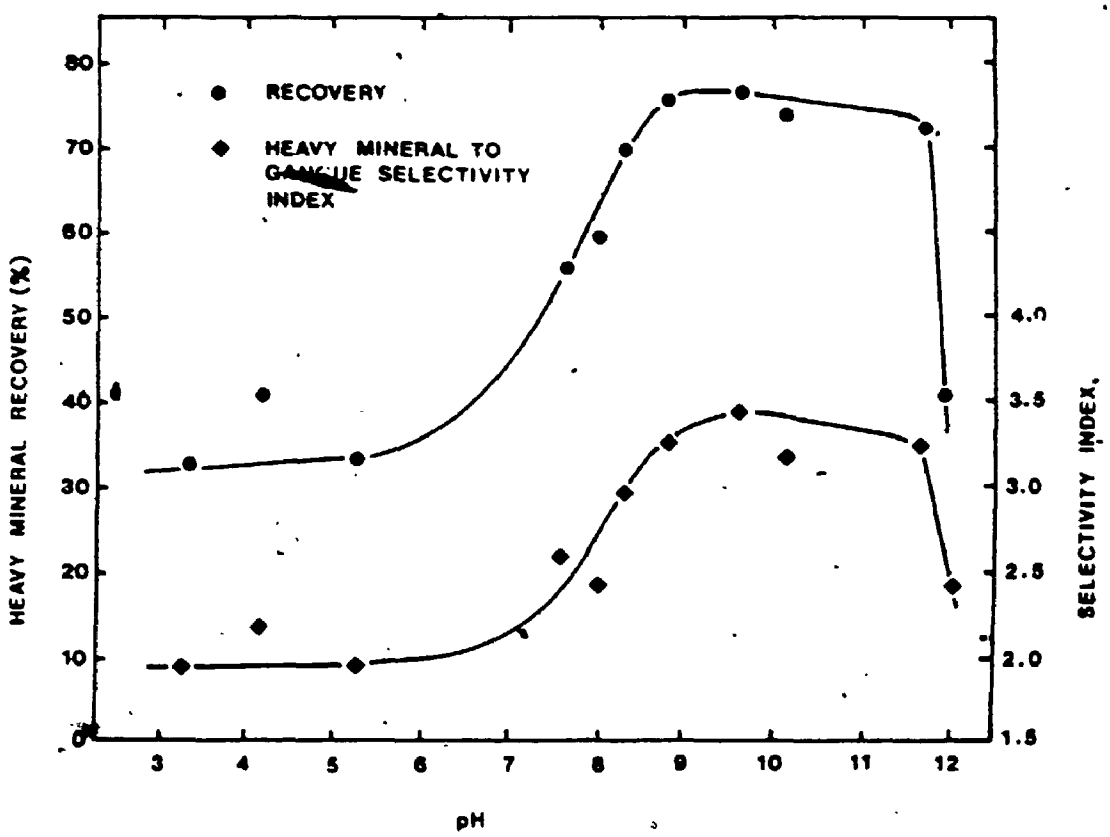

Figure 5.1 Variation of heavy mineral recovery and selectivity index with pH.

TABLE 5.1 SUMMARY OF pH EFFECT

pH	Feed Grade		Concentrate Grade		Overall Recovery (%)	
	%TiO_2	%ZrO_2SiO_2	%TiO_2	%ZrO_2SiO_2	%TiO_2	%ZrO_2SiO_2
3.3	11.4	5.0	22.9	13.3	30	39
4.2	11.6	4.4	25.8	12.8	38	50
5.3	12.8	5.3	24.1	13.2	30	40
7.6	11.2	4.5	28.4	11.8	56	53
8.0	11.3	4.9	26.3	11.3	60	59
8.3	10.8	4.2	27.0	10.7	69	71
8.8	10.7	4.4	27.3	10.0	79	70
9.6	11.0	4.2	29.0	10.6	79	75
10.1	11.1	4.2	27.4	9.8	75	71
11.7	10.7	4.3	28.1	10.8	74	68
11.9	10.1	4.2	27.3	12.1	50	53

lower than 6.6 and above 11.7, with the recovery curve increasing rapidly with pH in the range of 6.6 to 8.3.

In order to explain the effect of pH on the flotation recovery, titration of the supernatant obtained after centrifugation at 13,800 g was carried out (Figure 5.2). Figure 5.2 reveals the presence of a functional group with an apparent pKa of 6.5 which is consistent with the findings of Kessick (1979). In addition to this functional group, another more weakly dissociating group is also present as seen from the diffuse nature of the titration curve above pH 9. On the basis of the findings of Gewers (1968), Baptista and Bowman (1969) and McKinnon and Boerger (1986), the organic constituent with the lower pKa is assumed to be a naphthenic acid with the higher pKa representing the dissociation of a phenolic functional group (Moschopedis et al., 1977).

The results shown in Figures 5.1 and 5.2 reveal that the sharp increase in the heavy minerals recovery/selectivity index for pH values in the range of 6.6 to 8.3, corresponds to the region in which the naphthenic acid is present in the dissociated state. These results are in agreement with the findings of Kulkarni and Somasundaran (1975) who demonstrated that with anionic collectors, best recoveries were obtained at pH values which favoured the formation of acid soap complexes.

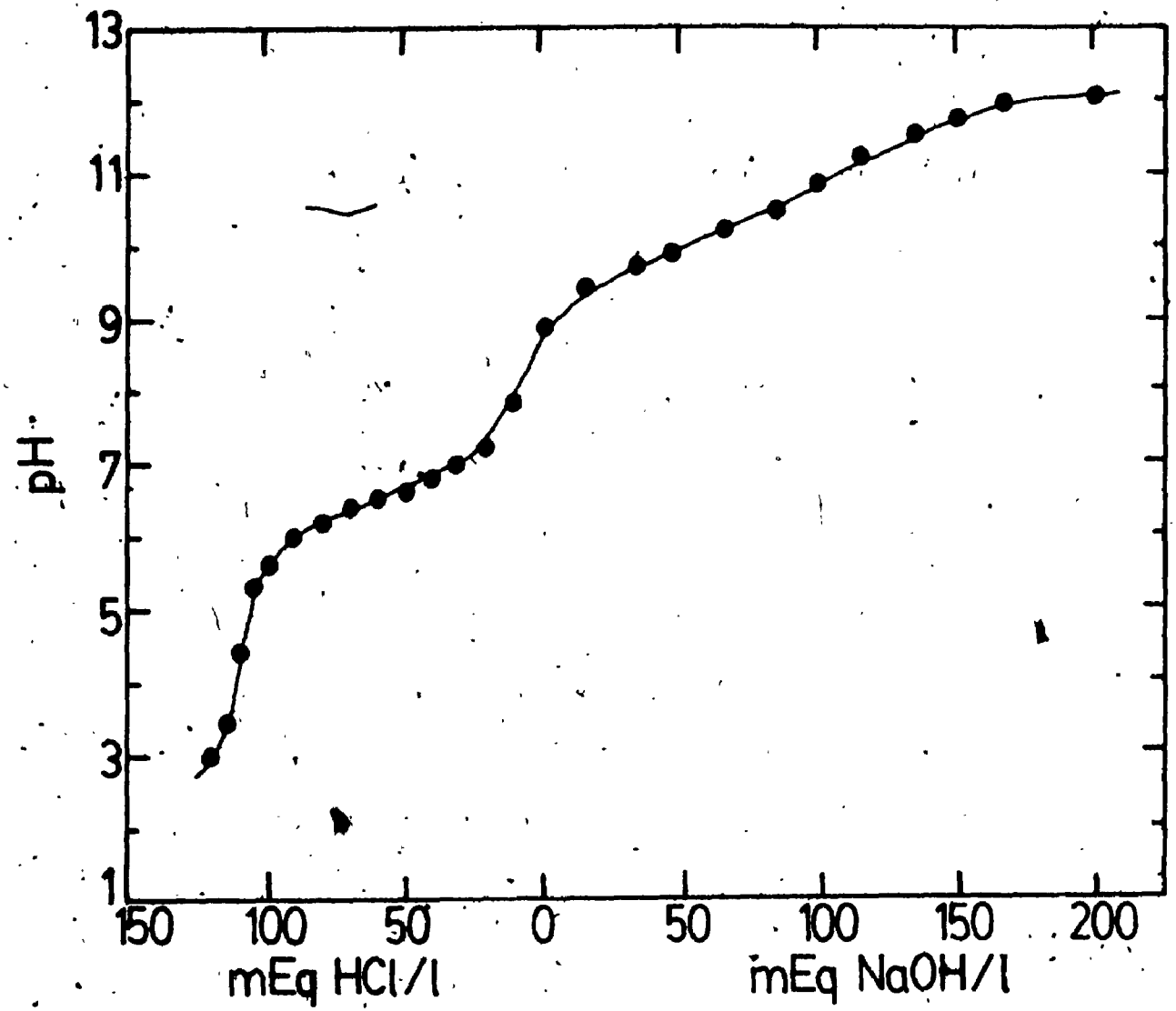

Figure 5.2 Titration curve of the extraction cell water.

The low recoveries obtained at both low and high pH values (pH $\leq$ 6.6 and pH $\geq$ 11.7 respectively) is attributed to surfactant removal from the mineral surfaces (Baptista and Bowman, 1969; Kessick, 1979). However, the observed flocculation of these tailings at these extreme pH values can not be adequately explained on the basis of surfactant displacement from the mineral surface (Ityokumbul et al., 1985b). Since H^+ and OH^- ions are potential determining ions for minerals which occur in the oilsands (oxides, silicates, carbonates, etc.), their adsorption in the Stern plane (Kruyt, 1954) will bring about changes in the surface charge of the minerals. For example, investigations by Eigeles (1950) have shown that the suppression action of H^+ ions takes place without a decrease in the amount of adsorbed collector.

The pH optimum obtained in this study differs from that reported earlier by Baptista and Bowman (1969) for tailing solids from oilsand operations. This difference may be attributed to the differences in the nature and particle size distribution of the solids used in the two studies. For example, the solids used in this work represent the minerals which are preferentially recovered during the bitumen extraction process and displayed a wide particle distribution (Kramers and Brown, 1976; Trevoy et al., 1978). By contrast, the solids used by Baptista and Bowman (1979) represent the "gangue" from the hot water extraction process

and displayed a narrower particle size distribution.

5.1.2 Effect of Frother

In flotation practice, frothers are generally added to prevent bubble coalescence in the pulp and hence to increase the surface area available for collection. However, frothers are also known to decrease the hydration of mineral surfaces, thereby activating their flotation (Klassen and Mokrousov, 1963).

The variation of heavy minerals recovery with frother concentration is shown in Figure 5.3. The results presented here show that the optimum frother concentration is 0.15% (v/v pine oil). Above a frother dosage of 0.20% (v/v), frothing was depressed, and heavy minerals recovery dropped rapidly with increasing frother concentration.

The results obtained here indicate that a sharp transition in heavy minerals recovery occurs at a frother concentration of 0.20% (v/v) pine oil for which the liquid surface tension is 36 mN/m (Figure 5.3). The occurrence of this transition was first reported by Zisman (1964) who defined it as the critical surface tension for wetting and represents the maximum surface free energy of a liquid for spontaneous spreading over the solid surface. In flotation, where the liquid is water, it represents the hydrophobic/hydrophilic transition of the solid surface. This

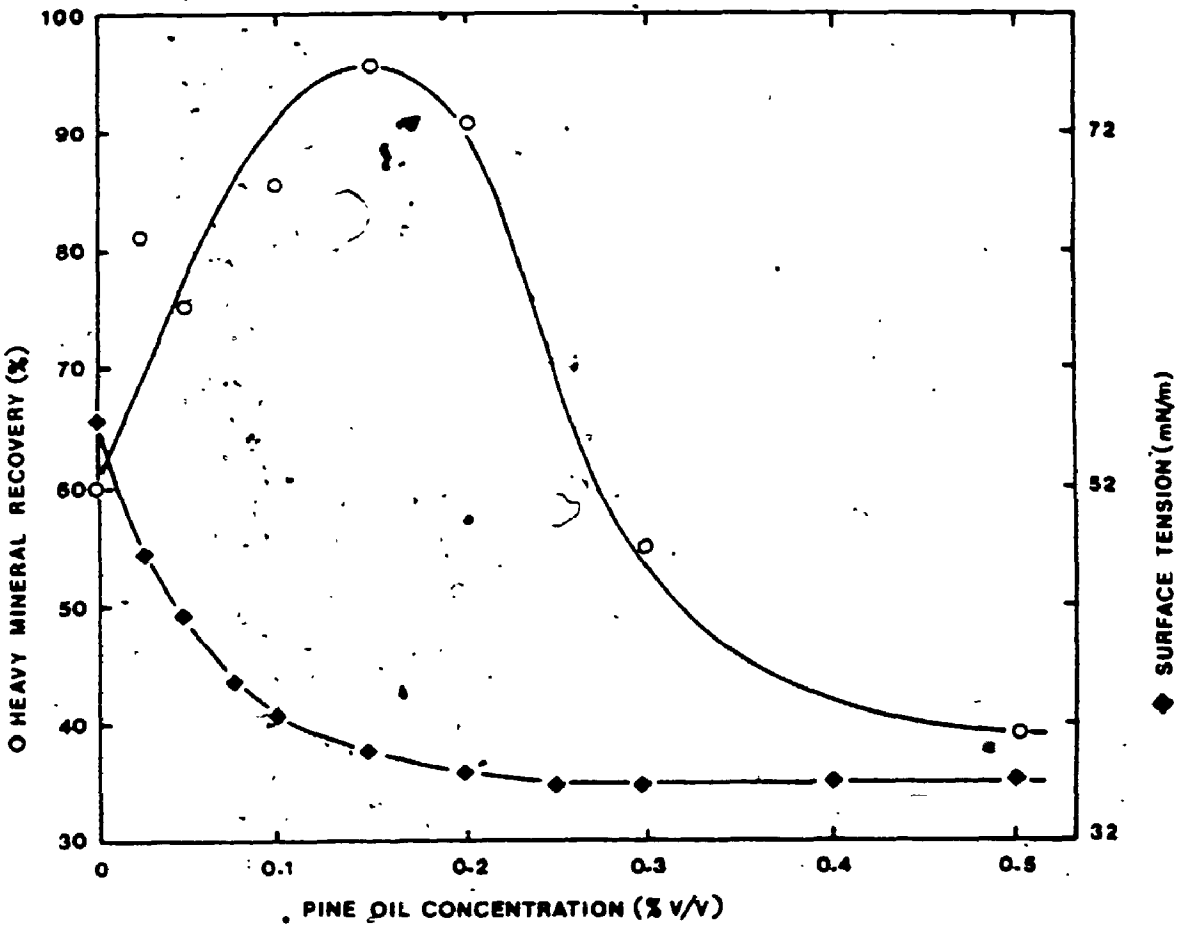

Figure 5.3 Effect of frother on heavy mineral recovery.

transition has in the past (Mackenzie, 1970; Finch and Smith, 1975) been explained on the basis of the "monolayer penetration" model of bubble-particle attachment (Leja and Schulman, 1954). This model envisages penetration of the hydrocarbon chains of the collector molecules adsorbed at the solid-liquid interface into the layer of adsorbed collector or frother molecules at the air-liquid interface. At high concentrations, the formation of a closely-packed monolayer of frother at the air-liquid interface presumably causes the bubble surface to become hydrated. Under such conditions, the penetration of the hydrocarbon chains of the collector molecules adsorbed at the mineral surface may be prevented.

For frother concentration in the range of 0.0 to 0.15% (v/v) pine oil, the liquid surface tension decreases with increasing frother concentration. The increase in heavy mineral recovery with frother concentration in this range can not be attributed to an increase in the availability of bubble surface since the amounts generally required for a reduction in the bubble size are much lower than the concentrations used here (Lindland and Terjesan, 1965; Flint, 1971; Raymond and Zieminski, 1971; Shah et al., 1982).

5.1.3 Effect of Depressant

Of the gangue minerals initially present in the oilsand

tailings, only iron was preferentially concentrated in the froth product (see Table 5.2). This suggests that the recovery mechanism for the iron was similar to that of the heavy minerals. However, as the collector species in the tailings is anionic, causticized starch was employed as a depressant for the iron minerals (Glembotskii et al., 1963). As can be seen from Figure 5.4, the depressive action of the starch was non-selective, that is, it also resulted in a corresponding depression of the heavy minerals. The effect of starch observed here suggests that both the iron and heavy minerals have similar surface properties since the depressive action of starch is related to surface reactions which lead to the formation of thick hydrated films on the mineral surfaces. As a result, separation between the iron and heavy minerals must be left to the subsequent upgrading operations.

5.1.4 Comparison of Flotation With Other Processes For Heavy Minerals Recovery

In order to establish the heavy mineral grade and recovery levels, several experiments were carried out. These results have consistently shown that with a feed containing 10-12% TiO and 4-5% ZrO_2SiO_2 (zircon), a 28-30% TiO_2 and 10-12% zircon concentrate was obtainable at 85-95% recoveries if frothers were used. These results have shown that an enrichment factor (ratio of concentrate to feed grade) of

TABLE 5.2 ELEMENTAL ANALYSIS OF FEED AND CONCENTRATE SOLIDS

Component	Feed	Concentrate
TiO_2	10-12%	28-30%
$ZrO_2.SiO_2$	4-5%	10-12%
Al_2O_3	12-15%	7-9%
Fe_2O_3	10-12%	16-18%
SiO_2	50-55%	20-25%

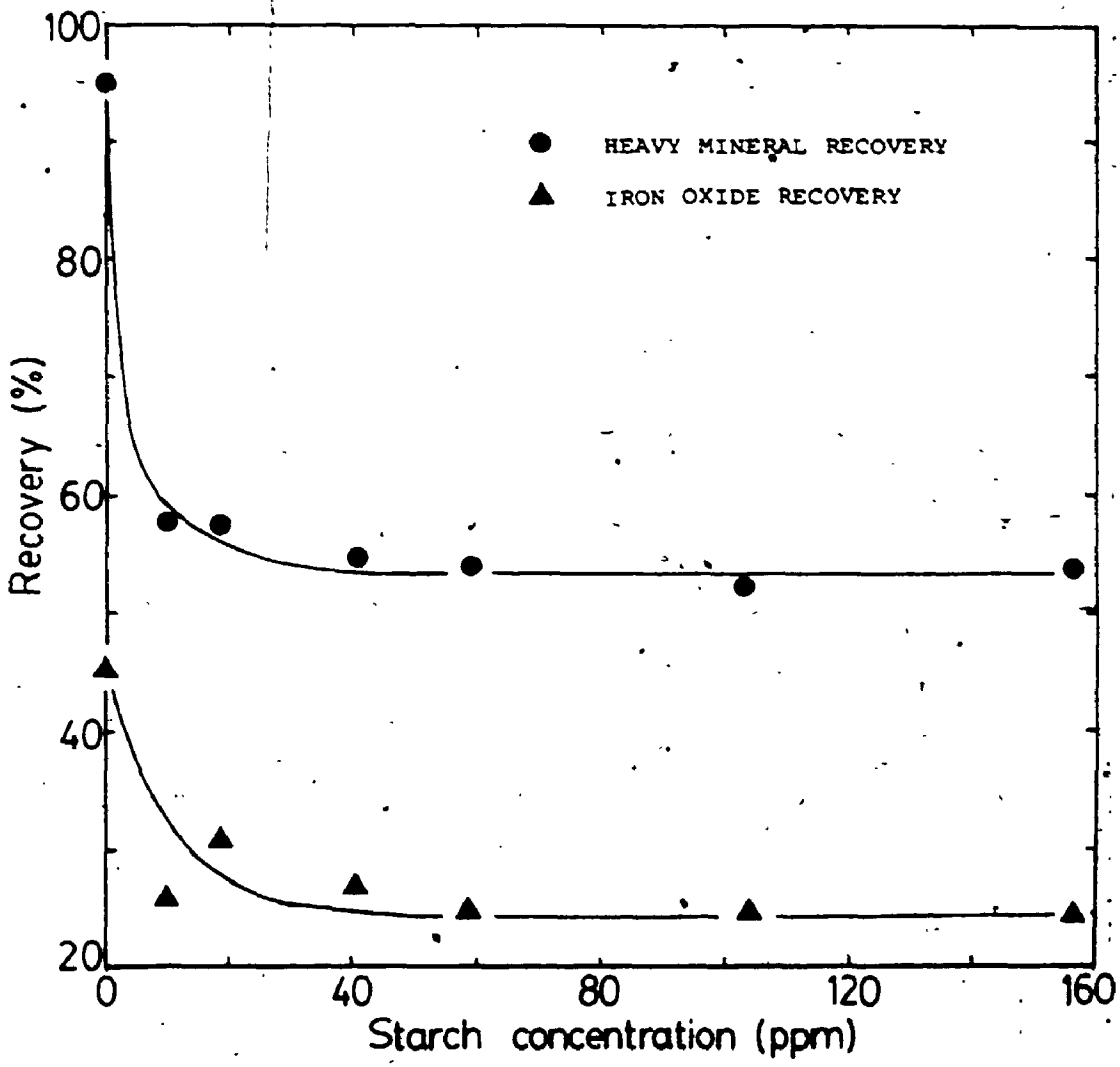

Figure 5.4 Effect of starch addition on iron and heavy mineral recovery.

2.4 to 2.7 was obtainable at the indicated recoveries (Ityokumbul et al., 1985b).

For a comparison of the effectiveness of flotation with the process that has been developed by Syncrude Canada Limited, the feedstock is assumed to be of the same grade as that given in the Syncrude process i.e., 13% TiO_2 and 8% zircon. The result of this comparison assuming an enrichment factor of 2.5 for the flotation process is shown in Figure 5.5. As can be seen, the major advantages of this flotation process over the Syncrude process are:

(i) As gangue rejection from the process occurs prior to burnoff, the size of the burnoff unit is considerably reduced - thus saving on capital expenditure. Furthermore, the need for several energy intensive steps (hydroclones, and spiral circuit) employed in the Syncrude process for gangue rejection may be eliminated.

(ii) The reported loss of low specific gravity cellular white leucoxene (density < 3300 kg/m^3) in the Syncrude process (Trevoy et al., 1978) will be minimized as the spiral circuit may no longer be required for gangue rejection if flotation is used. Even if the spiral circuit is used, the separation will be greatly simplified since the coarse sand particles will be rejected from the flotation step.

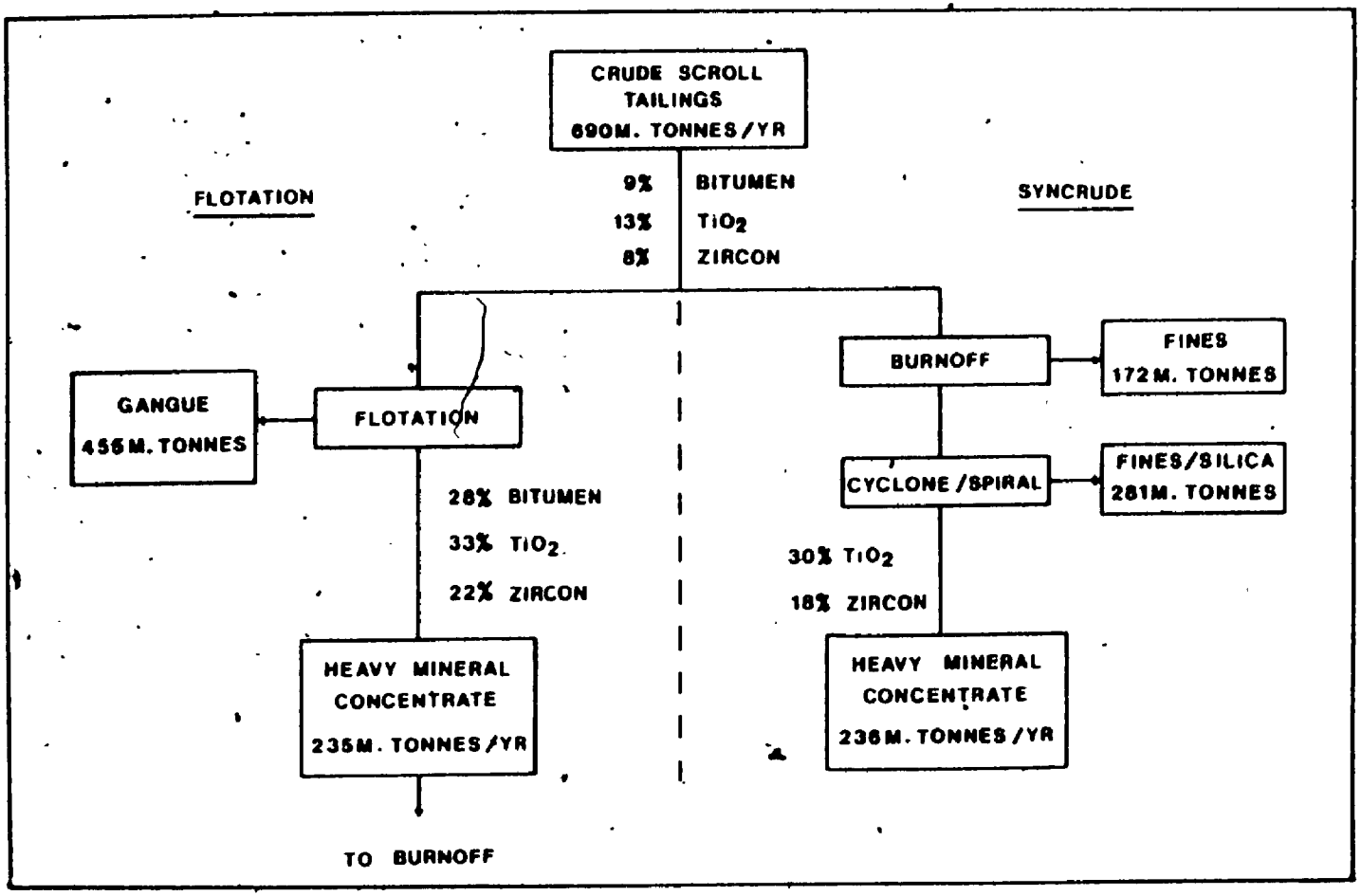

Figure 5.5 Comparison of heavy mineral recovery schemes; flotation vs Syncrude process.

5.1.5 Process for Heavy Minerals Recovery From Oilsand Tailings

In view of the advantages of using flotation for the initial recovery of heavy minerals from the centrifuge tailings, the process shown in Figure 5.6 was developed and is presently undergoing evaluation for patentability at the Canada Patents and Development Limited, Ottawa.

The fines from the froth product were removed by wet gravity classification. The burnoff solids were mixed with water to give a 20 wt% slurry. The gravity classifier was designed to separate all particles with settling velocities of less than 6 m/h. The small amounts of silica sand present in the underflow from the gravity classifier were removed by dense medium separation. In practice, this separation may be easily accomplished in a spiral circuit.

A typical mass flow and mineral enrichments obtained in this beneficiation process as outlined in Figure 5.6 are given in Table 5.3. The Ti/Fe ratio of the first three fractions from the high intensity magnetic separator (streams 6-8) was nearly constant, while the rare earth elements (REEs) were concentrated in streams 7 and 8. The last two streams to be separated from the high intensity magnetic separator (streams 9 and 10) contained mainly Ti and Zr respectively with only traces of iron. A detailed analysis of the REEs (Table 5.4) shows that in stream 7, the major

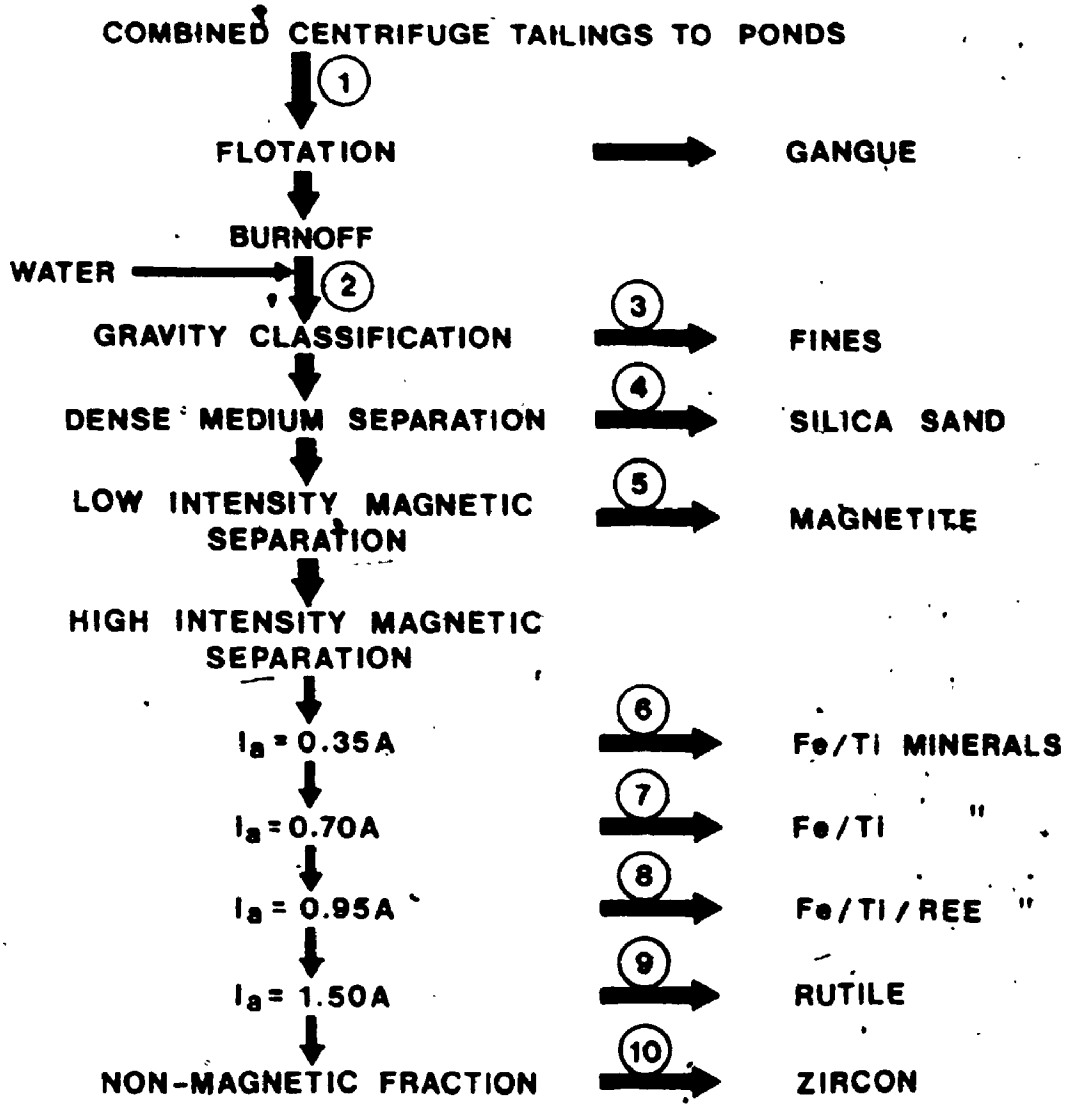

Figure 5.6 Process for heavy minerals recovery from oilsand tailings.

TABLE 5.3 MASS FLOW AND ELEMENTAL ANALYSES OF SOLID STREAMS

*Stream No.	Wt (gm)	Elemental Analyses (wt% of stream)				
		Ti	Cr	Fe	Si	REE
1	1000	7.1	2.5	12	26	0.39
2	380	17	6.0	18	14	0.94
3	133	8.4	1.0	40	13	0.15
4	37	2.4	1.0	5.6	37	0.10
5	11	4.8	1.0	18	12	<0.01
6	25	40	<0.05	14	6.1	0.21
7	27	32	<0.05	13	7.0	0.74
8	49	19	1.0	7.7	5.6	6.0
9	47	38	9.0	<1.0	10	0.40
10	51	9.6	29	<1.0	17	0.25

*For description of the stream number, see Figure 5.6

TABLE 5.4 REE ANALYSES OF FRACTIONS SEPARATED BY HIGH INTENSITY MAGNETIC SEPARATION (wt% of fraction)

Element	Magnetic Fraction at Indicated Armature Current				
	0.35A	0.70A	0.95A	1.5A	1.5A*
Ce	0.08	0.20	3.2	0.21	0.12
La	0.05	0.10	1.38	<0.01	<0.01
Y	<0.01	0.28	0.11	0.12	0.06
Gd	ND	ND	0.15	ND	ND
Nd	0.05	0.07	0.79	<0.05	<0.05
Sm	<0.01	0.02	0.29	<0.01	<0.01
Th	<0.005	0.008	0.15	0.016	0.009

*Non-magnetic fraction at indicated armature current

ND not determined

REE was Y while in stream 8, it was C_e with Y representing less than 2% of the REEs present. Clearly, another major advantage of using the upgrading process described here is the possibility of recovering the rare earth minerals which are also present in the centrifuge tailings. Their recovery has not to this author's knowledge been attempted before due to their low concentrations in this stream.

Identification of the minerals present in these streams was by XRD analysis. Typical XRD patterns are shown in Figure 5.7. The minerals identified from the XRD analysis are shown below:

Stream #	Major minerals identified From XRD
6	Ilmenite, rutile, hematite
7	Rutile, pseudorutile
8	Monazite, rutile, pseudorutile
9	Rutile, zircon
10	Zircon, rutile

Streams 6-10 may be subjected to high tension separation to remove the conductors (rutile and iron/titanium mineral) from the non conductors (monazite and zircon) but this has not been done to date.

The distribution of the heavy minerals in the flotation product by size is shown in Table 5.5. While these results show that dry screening may be employed to effect the

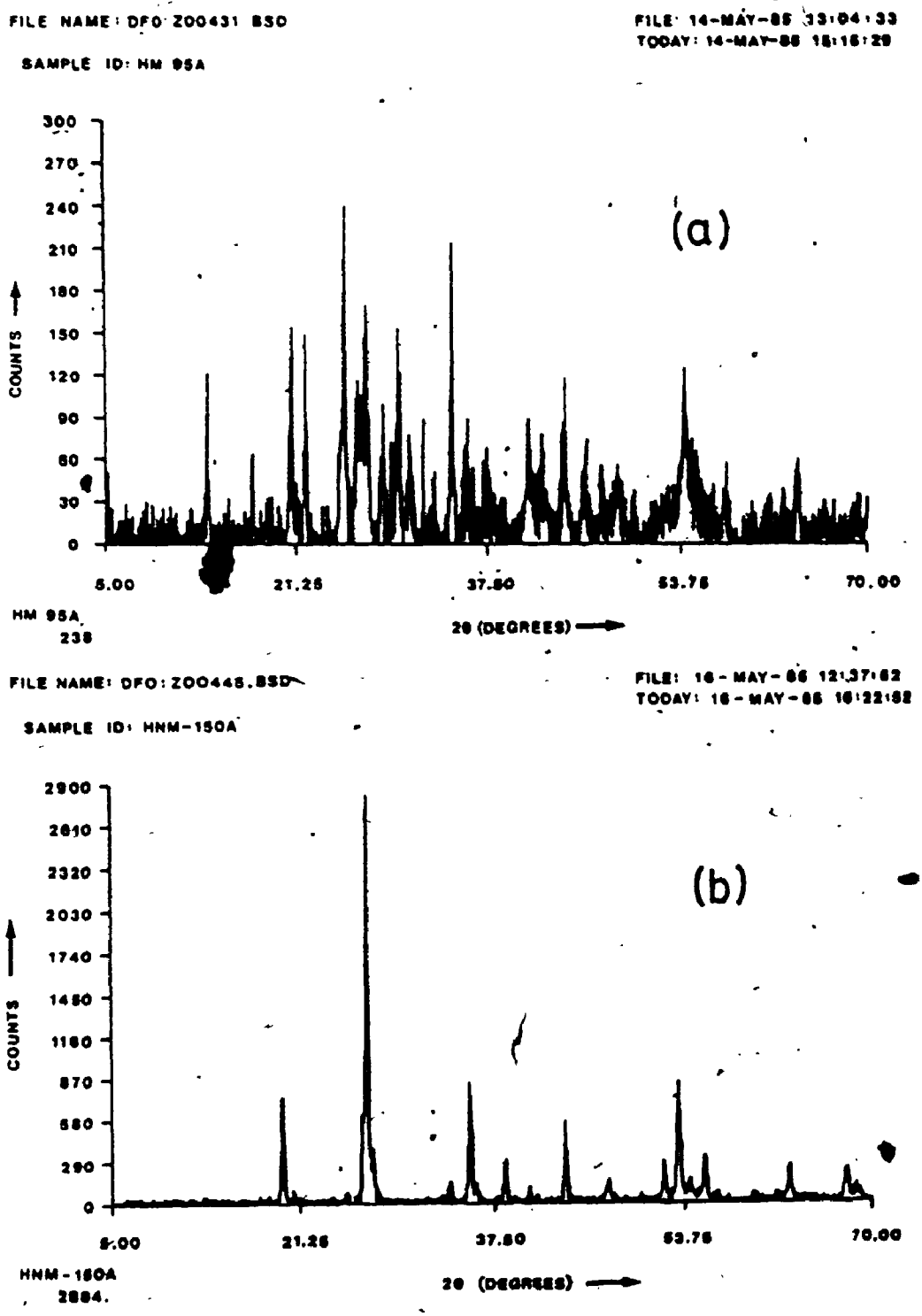

Figure 5.7 Typical X-Ray Diffraction pattern for fractions separated from the process shown in Figure 5.6: (a) stream 8 and (b) stream 10. (Cu Kα λ=1.5405 A)

TABLE 5.5 ELEMENTAL ANALYSES OF HEAVY MINERALS BY SIZE

(CDN std. Sieve)	Wt Fraction Retained (%)	Elemental Analyses (wt% of fraction)				
		Ti	Zr	Si	Fe	REE
-60 +100 mesh	6.7	13	1.5	26	9.8	0.13
-100 +200 mesh	39.5	27	4.0	16	7.7	0.68
-200 +325 mesh	21.3	19	15	14	7.7	2.70
-325 mesh	32.5	8.4	2.0	11	29	0.10

separation and concentration of the various minerals, its use is not recommended. For example, the traces of iron that would be left would coat the other mineral grains thereby altering their physical properties and consequently their efficient separation. Dry screening may however be applied to the product from the wet gravity classification prior to its upgrading.

5.1.6 Estimates of Potential Production of Heavy Minerals From Oilsand Tailings

For an oilsands plant producing 130,000 bbl/d synthetic crude oil, the combined centrifuge tailing solids production rate is estimated to be 4300 t/d (Anon, 1973). Given this and assuming average values of 7% Ti, 2% Zr, 12% Fe and 0.5% REE with recovery efficiencies of 70., 80 and 33% respectively for the Ti, Sr-REE and Fe minerals, the potential annual production rates and values are estimated to be as shown in Table 5.6. Although the iron oxide is of pigment grade, it has been priced as ore grade for major sale to the steel industry. Any markets developed for it as a paint pigment will command a price at least 10 times greater. Since current forecasts show that the demand for Ti minerals will remain strong through the 1990s (Mining Journal, Vol. 306, 7858, p. 221, 1986), the revenue from the recovery of these minerals may be expected to increase with time.

TABLE 5.6 HEAVY MINERALS PRODUCTION FROM OILSAND TAILINGS
(Based on a 130,000 bbl/day Plant)

Mineral	Production t/y	Unit Price CDN $/t	Annual Value (10^6)
Rutile	38,000	487[1]	18.50
74%TiO_2Slag	62,000	118[2]	7.25
Monazite	9,000	487[3]	4.38
Zircon	38,000	141[1]	5.36
Iron oxide (pigment grade)	80,000	36[4]	2.88
Total	227,000		38.37

[1] fob Australia (Mining Journal 305 No. 7831 p. 231, Sept. 20, 1985)
[2] 60% of fob Sorel, Que. (Mining Annual Review-1985 p. 76)
[3] Mining Engineering 37, No. 5 p. 482 1985
[4] Canadian Mining Journal, 106 p. 27 Feb. 1985 (Ore grade)

5.2 HYDRODYNAMIC STUDY OF TWO PHASE (GAS-LIQUID) FLOTATION

Two phase (gas-liquid) flotations are of practical importance. An example of this includes the removal of emulsified oil by flotation (Takahashi et al., 1979; Van Ham et al., 1982), Another example is the separation of proteins and enzymes and other foam fractionation techniques (Lemlich, 1972). In all of these operations, it is widely recognized that the aeration rate influences the separation efficiency. As a result of this, hydrodynamic data on such systems will be useful for design and scale-up purposes.

5.2.1 Gas Hold-Up and Flow Regime Mapping

Gas hold-up in a bubble column represents an important design parameter. It is required in the calculation of the gas interfacial area which is directly related to the flotation rate constant (see 2.5). The effect of liquid and gas flow rates and frother concentration (pine oil) on the individual phase hold-ups has been determined and the results are summarized below.

The variation of gas hold-up with gas and liquid velocities is shown in Figures 5.8 and 5.9. These results show that the gas hold-up was independent of liquid velocity. The results obtained here are similar to those reported earlier by Schulman and Molstad (1950), Kolbel et al. (1972), Deckwer et al. (1974) and Kumar et al. (1976).

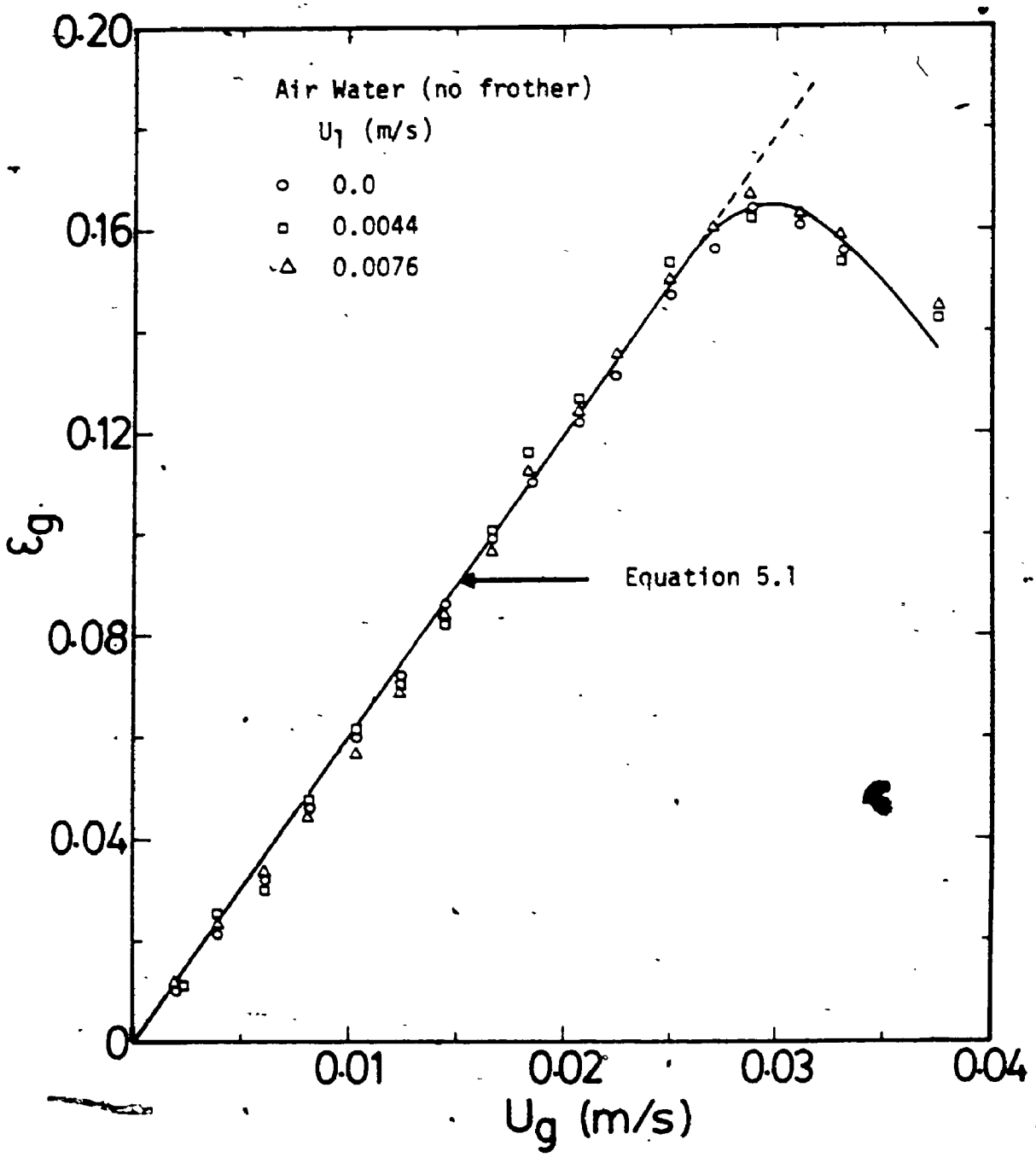

Figure 5.8 Effect of liquid and gas velocities on gas hold-up

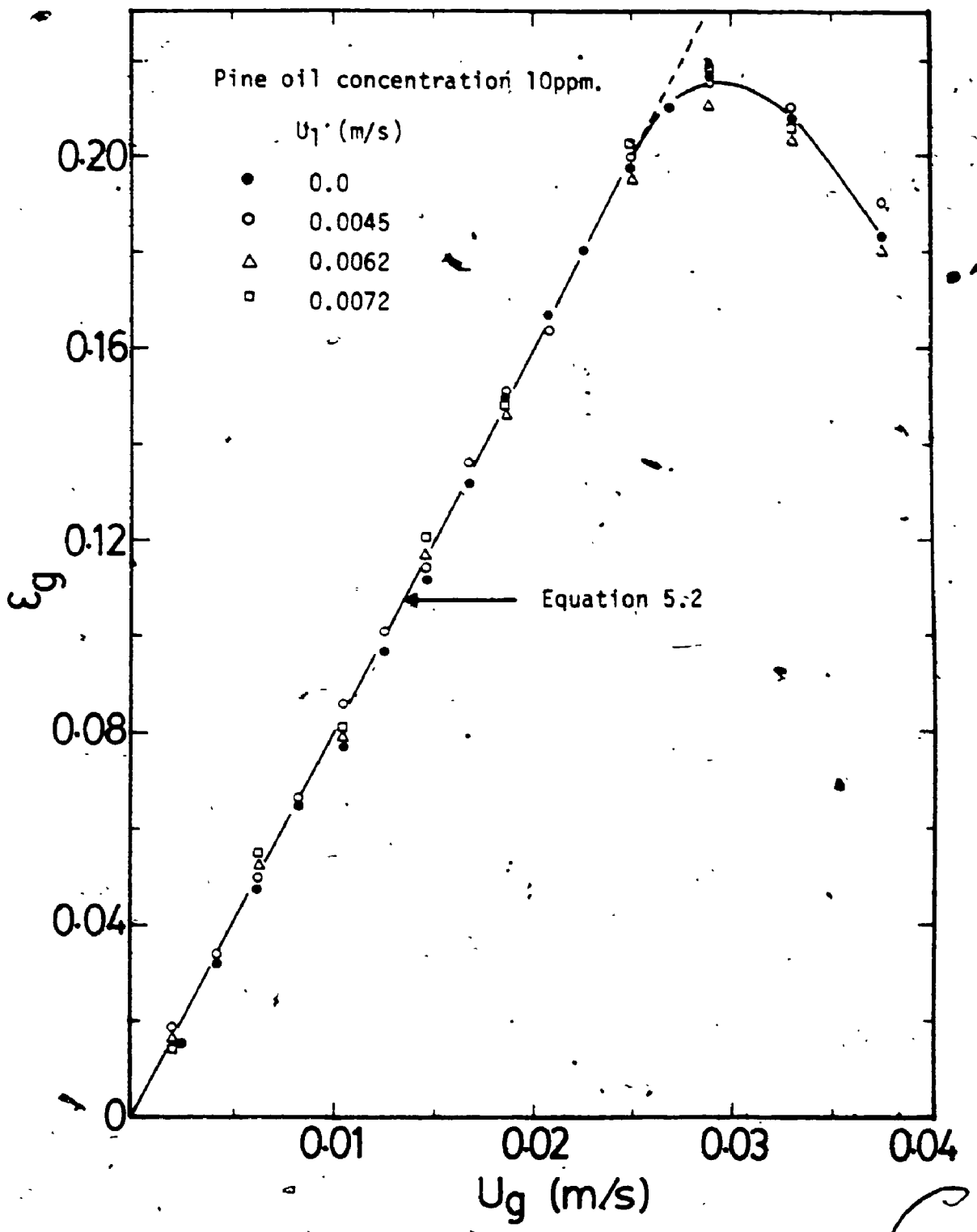

Figure 5.9 Effect of gas and liquid velocities on gas hold-up.

At low gas velocities (U_g < 0.025 m/s), the gas hold-up increases linearly with gas velocity. For gas velocities in the range of 0.025 to 0.031 m/s, the gas hold-up increases only moderately with gas velocity. Beyond a gas velocity of 0.031 m/s, the gas hold-up decreases with increasing gas velocity. The existence of a gas hold-up maxima with the porous plate distributor used in this study is consistent with the observation of others as well (Schulman and Molstad, 1950; Kolbel et al., 1972; Deckwer et al., 1974). This maxima is attributed to the transition from the homogeneous (bubbly) flow regime to the heterogeneous (churn turbulence) flow regime.

The effect of frother concentration on the gas hold-up is shown in Figure 5.10. At the pH at which these gas hold-up measurements were carried out (4.00 ± 0.10), considerable foaming was observed for pine oil concentrations exceeding 50 ppm. In general, the gas hold-up was found to increase with frother concentration. The increase in gas hold-up with frother concentration can not be explained on the basis of liquid surface tension changes (Shah et al., 1982) since no detectable changes in the liquid surface tension were observed at the levels reported here (Figure 5.11). The increase in gas hold-up with frother addition however may be explained on the basis of surface tension gradient present on the bubble surface (Levich, 1962; Davis and Acrivos, 1966). The dipole orientation which takes place on the

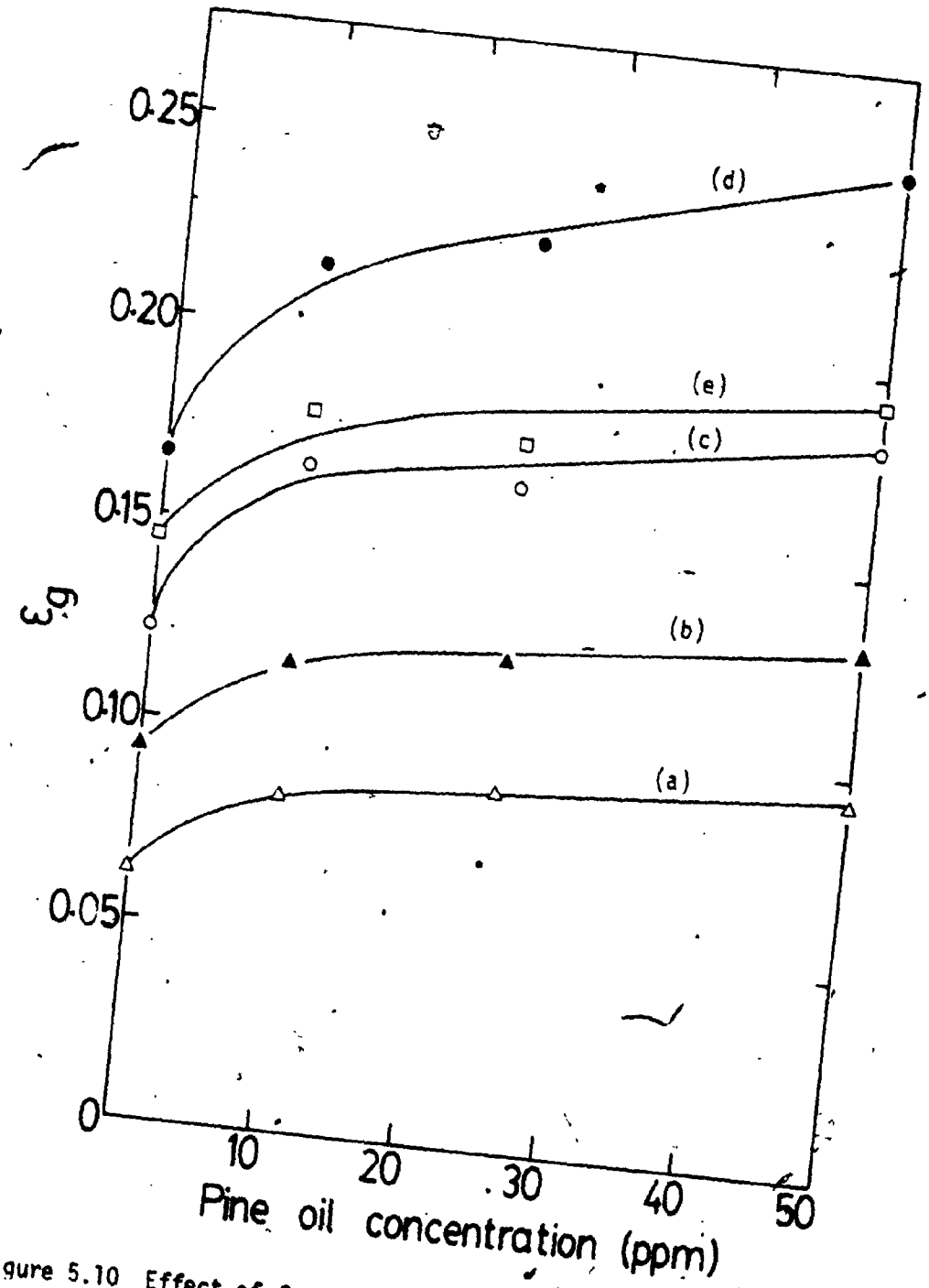

Figure 5.10 Effect of frother concentration on gas hold-up.
(a) U_g = 0.011 m/s; (b) U_g = 0.015 m/s; (c) U_g = 0.029 m/s;
(d) U_g = 0.029 m/s; (e) U_g = 0.037 m/s.

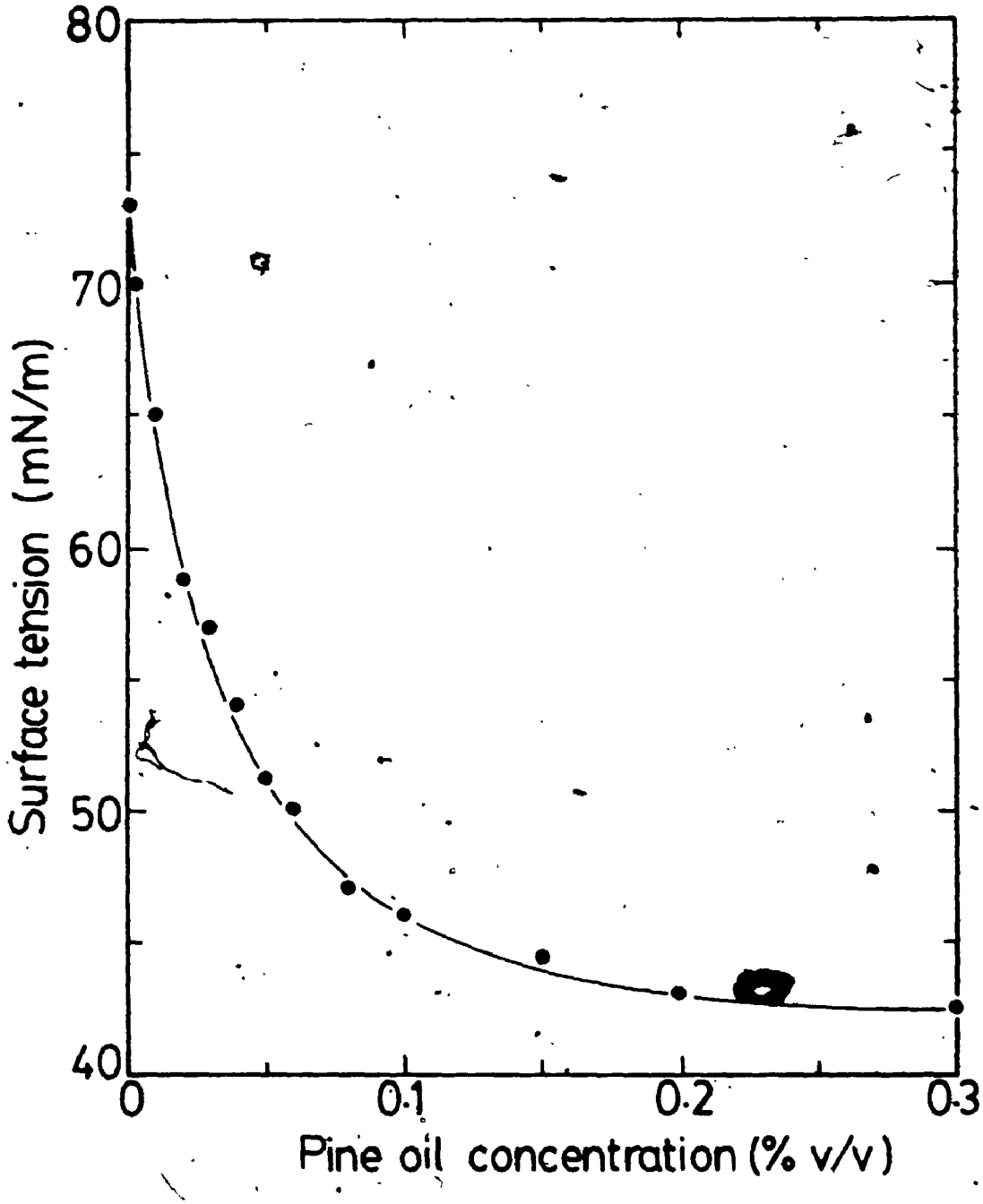

Figure 5.11 Variation of liquid surface tension with frother concentration.

bubble surface (with the polar head of the frother molecule extending into the water) prevents bubble coalescence (Raymond and Zieminski, 1971). Photographic evidence obtained (Figure 5.12) has confirmed that the bubble size was reduced in the presence of pine oil. In general, the gas hold-up was found to increase with frother concentration. However, the increase was not directly proportional to the frother concentration.

A correlation of the gas hold-up measurements gave the following relationships:

i) Air water

$$\varepsilon_g = 5.9\ U_g \qquad (5.1)$$

ii) Air water pine oil (10 ppm)

$$\varepsilon_g = 8.0\ U_g \qquad (5.2)$$

iii) Air water pine oil (25 ppm)

$$\varepsilon_g = 8.3\ U_g \qquad (5.3)$$

iv) Air water pine oil (50 ppm)

$$\varepsilon_g = 8.8\ U_g \qquad (5.4)$$

5.2.1.1 Flow Regime Mapping

In bubble column reactors, the hydrodynamics, transport and mixing properties such as fluid-fluid interfacial areas

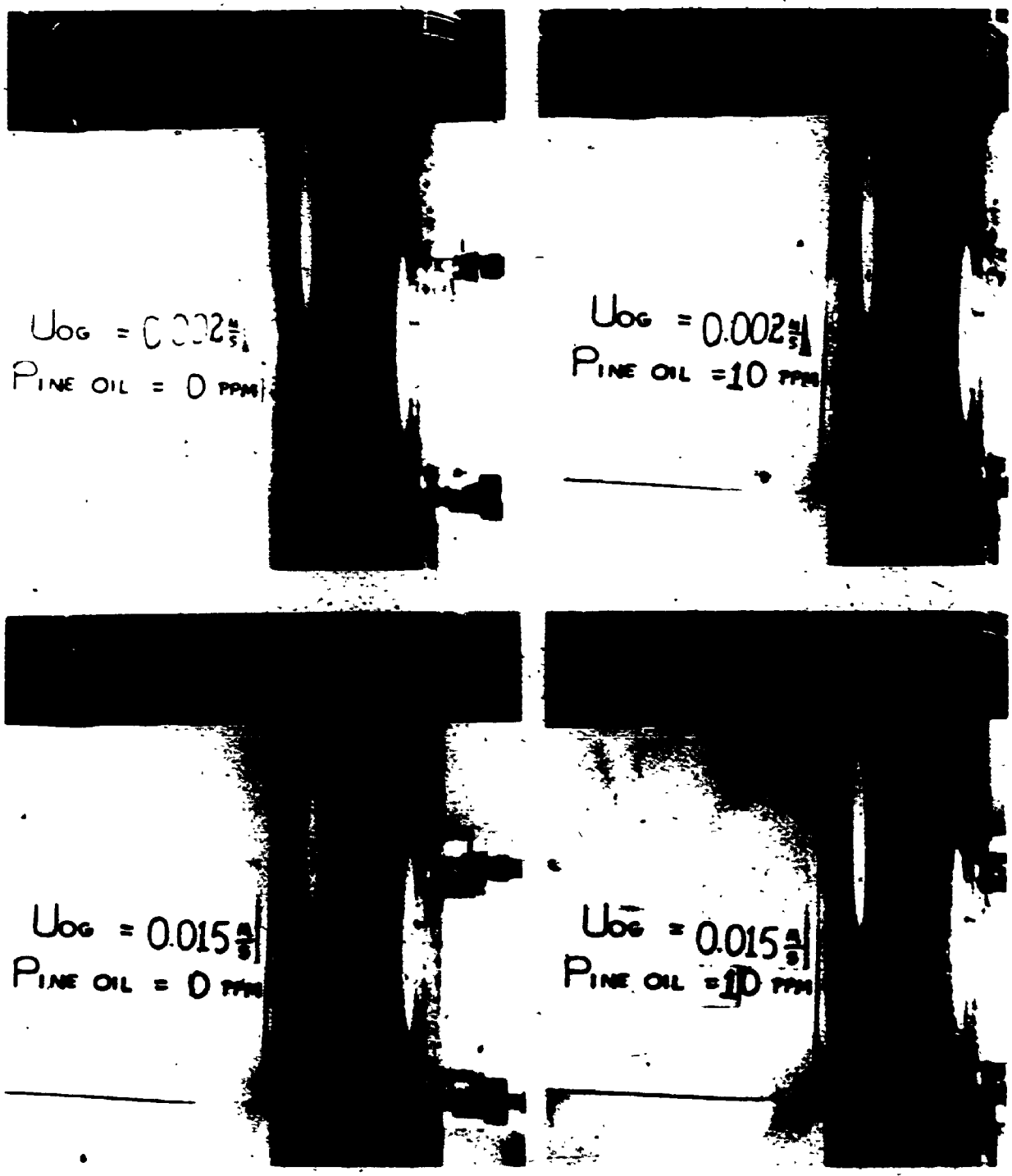

Figure 5.12. PHOTOGRAPH. Effect of frother on bubble size.

and interface heat and mass transfer coefficients depend strongly on the prevailing flow regime. The identification of the applicable gas flow regimes is therefore important for bubble column reactor design and scale-up. Generally, the gas flow can take the form of a homogenous or heterogenous dispersion. The former is characterized by a fairly uniform gas dispersion in the liquid with the resultant fluid behaving as a single fluid. By contrast, the two phases behave differently under heterogeneous flow conditions.

A review of the methods commonly used to characterize flow regimes in bubble column reactors has been given by Shah et al. (1982) and Shah and Deckwer (1985). In the present study, the flow regimes were characterized using the changes in the bubble rise velocity with gas velocity as shown in Figure 5.13. For clarity, the effect of frother concentration on the bubble rise velocity and consequently the flow regime mapping is shown separately in Figure 5.14.

For the air water system (Figure 5.13a), the bubble rise velocity decreases initially with increasing gas velocity which is in agreement with the results of others (Kolbel et al., 1972). This flow regime corresponds to the chain bubbling regime where the bubbles leave the pore openings independently. The initial decrease in the bubble rise velocity is attributed to the "crowding effect" similar to that reported for solid sedimentation (Richardson and Zaki,

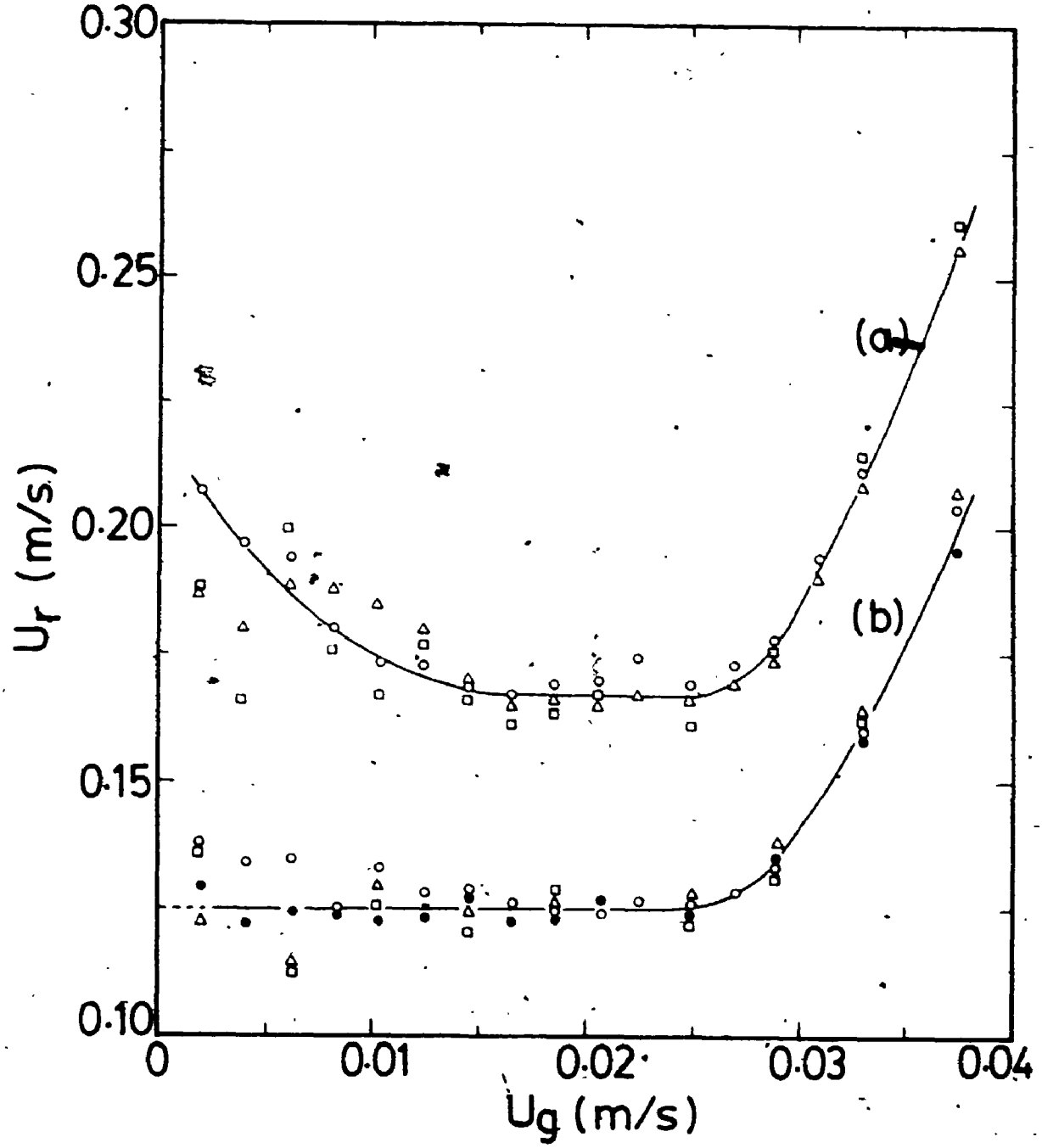

Figure 5.13 Effect of frother addition on bubble rise velocity.
(a) No frother (symbols same as in Figure 5.8)
(b) 10 ppm pine oil (symbols same as in Figure 5.9)

1954). With increasing gas velocity (U_g in the range of 0.01-0.021 m/s), the bubble rise velocity remains fairly constant. This flow regime corresponds to the fully developed bubble flow regime. For gas velocities exceeding 0.021 m/s, the bubble rise velocity increases rapidly with increasing gas velocity. In this flow regime, large bubbles were observed rising in a spiral manner in the column. This flow regime is therefore ascribed to the churn-turbulence flow regime.

The effect of frother addition on the flow regime mapping is shown in Figure 5.13b. Addition of pine oil at a level of 10 ppm resulted in a decrease in bubble size which gave a relatively high bubble density even at the low gas velocities. As a result, the chain bubbling flow regime was not observed. However, at gas velocities exceeding 0.21 m/s, the bubble rise velocity increased rapidly with gas velocity. The presence of the frother resulted in a drop in the bubble rise velocity in the bubbly flow and churn turbulence flow regimes when compared to the air water system.

The effect of increasing the frother concentration is shown in Figure 5.14. It can be seen that increasing the frother concentration from 10 ppm to 50 ppm only resulted in marginal decreases in the bubble rise velocity which is in agreement with the results of Lindland and Terjesan (1965) and Raymond and Zieminski (1971). These authors found that

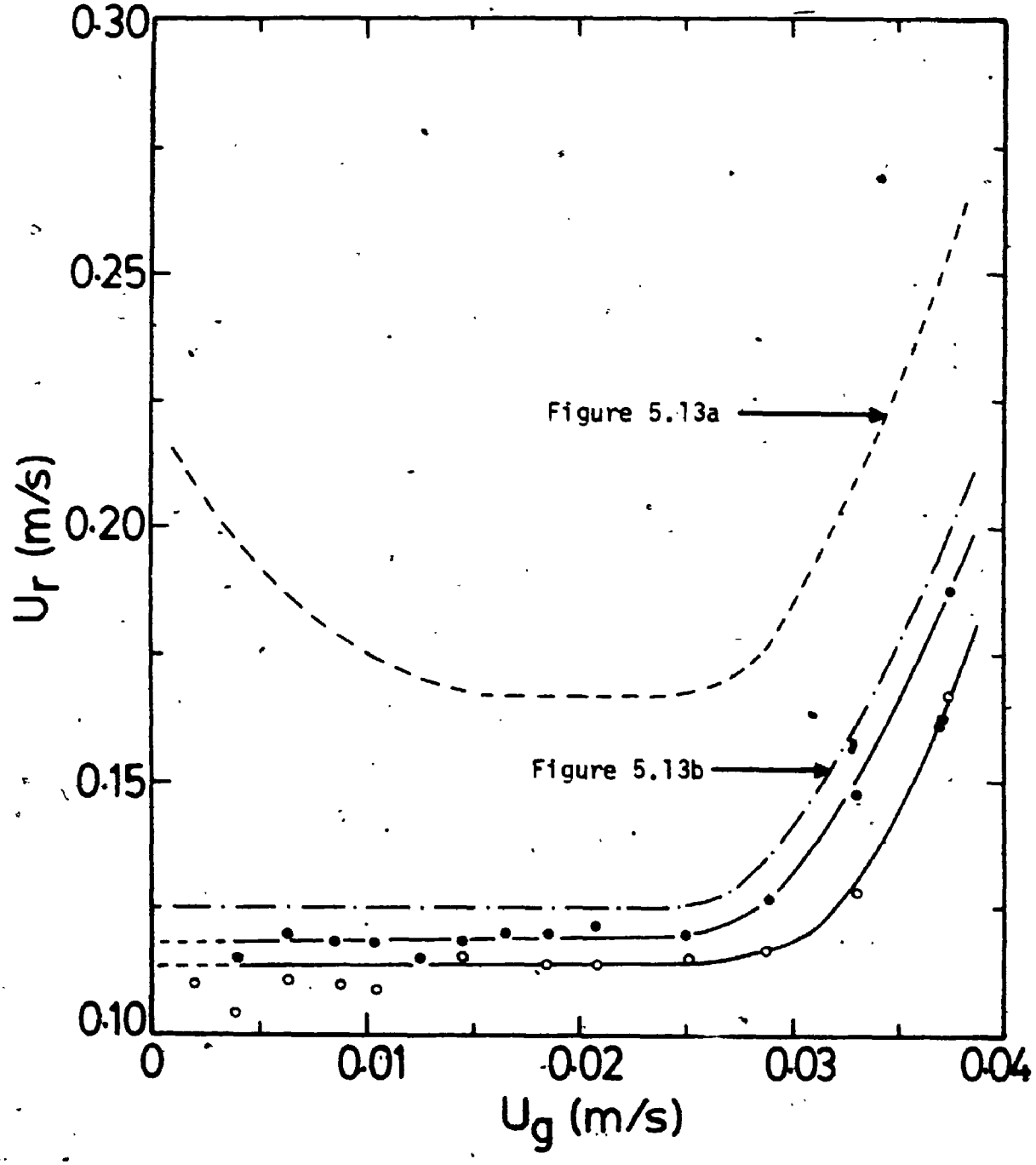

Figure 5.14 Effect of frother concentration on the bubble rise velocity. (●) 25 ppm; (○) 50 ppm.

after a small amount of surfactant has been added, further addition caused insignificant changes in the terminal rise velocity. However, the transition from the fully developed bubbly flow regime to the churn turbulence flow regime shifts to higher gas velocities with increasing frother concentration which is also consistent with the results of Kelkar et al. (1983).

5.2.2 Liquid Phase Dispersion

The extent of liquid mixing in a bubble column reactor also represents another important design and scale-up parameter. For example, in two phase flotation, the degree of separation and the enrichments obtained will depend on the extent of mixing of the liquid phase (Lemlich, 1966; Pinford, 19). The effect of liquid and gas velocities and frother concentration on the liquid phase mixing has been studied and the results are summarized in Figures 5.15 and 5.16.

For the air water system, three distinct mixing regions are clearly evident. At low gas velocities (U_g < 0.01 m/s), The liquid dispersion coefficient increases moderately with gas velocity. With increasing gas velocity the dispersion coefficient remains fairly constant over the gas velocity range 0.01 to 0.021 m/s. Beyond a gas velocity of 0.021 m/s, the liquid dispersion coefficient increases rapidly with gas velocity. The different mixing regimes identified

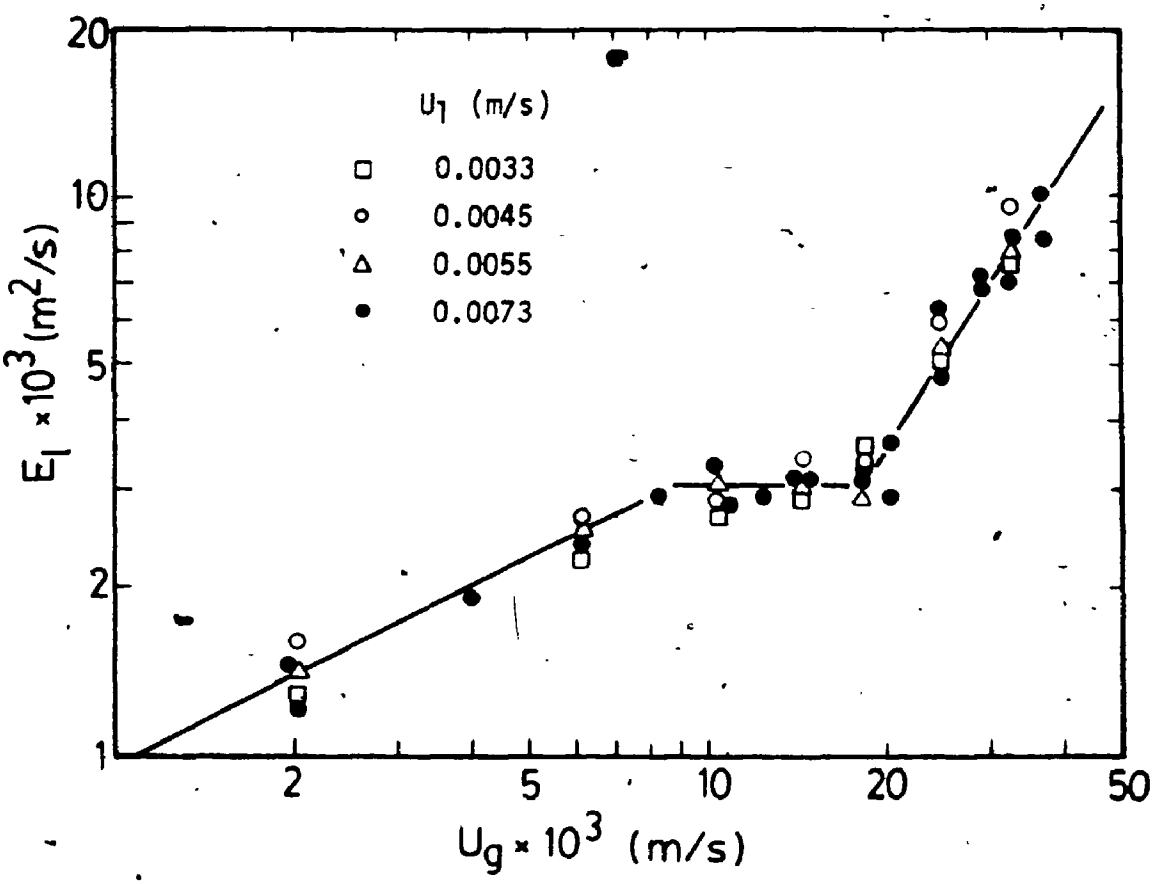

Figure 5.15 Effect of liquid and gas velocities on the liquid dispersion coefficient.

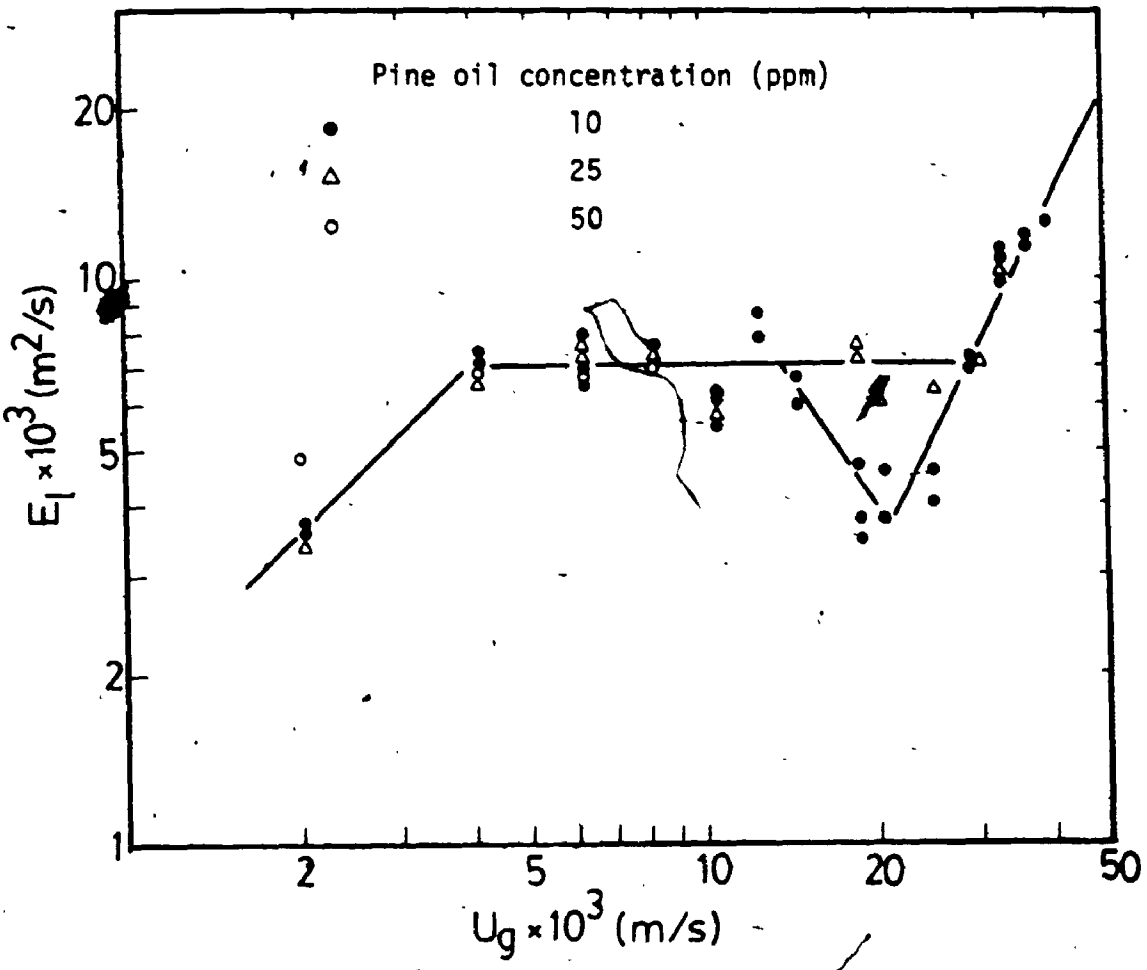

Figure 5.16 Effect of frother concentration on the liquid dispersion coefficient.

from Figure 5.15 agree rather well with those from the flow regime diagram for this system (Figure 5.13a). The trend obtained here is consistent with that reported by Gondo et al. (1973). The rapid increase in the liquid dispersion coefficient with gas velocity in the churn turbulence flow regime is also consistent with the experimental observation of Schumpe et al. (1979) who reported a rapid decline in the conversion of CO_2 for gas velocities corresponding to this flow regime.

The effect of frother concentration on the liquid dispersion coefficient is shown in Figure 5.16. Three distinct mixing regions are also observed from Figure 5.16. However, the initial increase in the liquid dispersion coefficient with gas velocity occurred over a narrower gas velocity range when compared to the air water system. This is also consistent with the flow regime diagram for these systems (Figures 5.13b and 5.14). In general, the addition of a frother resulted in an increase in the liquid dispersion coefficient. However, at a frother concentration of 10 ppm, the liquid dispersion coefficients decreased to the values obtained for the air water system. This effect was not observed for frother concentrations exceeding 10 ppm. The liquid dispersion data also shows that with increasing frother concentration, the bubbly flow regime could be maintained to higher gas velocities which is also in agreement with the flow regime diagrams for these systems.

5.2.2.1 Correlation of the Liquid Dispersion Data

A regression analysis of the liquid phase dispersion data gave the following correlations:

Air water system (no frother)

Region I: $U_g < 0.009$ m/s

$$E_L = 0.036\ U_g^{0.53} \qquad (5.5)$$

RegionII: $0.009 < U_g < 0.021$ m/s

$$E_L = (0.0031 \pm 0.0003)\ m^2/s \qquad (5.6)$$

Region III: $U_g > 0.021$ m/s

$$E_L = 2.02\ U_g^{1.63} \qquad (5.7)$$

The regression coefficients for equations 5.5 and 5.7 were 0.969 and 0.933 respectively. The gas velocity exponents obtained in this study agree rather well with those reported by Gondo et al. (1973) and Houzelot et al. (1985) for Region I and by Gondo et al. (1973) and Sangnimnuan et al. (1984) for regions II and III respectively. The close agreement between equation 5.7 and that presented by Sangnimnuan et al. (1984) suggests that for Region III, the liquid phase dispersion coefficient does not depend on the column diameter.

The following asymptotic relationships were obtained for the air-water (with frother) system:

Region II: $U_g < 0.025$ m/s

$$E_L = (0.0070 \pm 0.0011) \text{ m}^2/\text{s} \quad (5.8)$$

and for Region III: $U_g > 0.025$ m/s

$$E_L = 0.904\ U_g^{2.02} \quad (5.9)$$

In order to provide dimensionally consistent correlations the isotropic turbulence model of Baird and Rice (1975) was used. In the case of eddy diffusivity, dimensional analysis provides the following relationship for the liquid dispersion coefficient

$$E_L \propto K\ l^{4/3}\ P_m^{1/3} \quad (5.10)$$

where l is the characteristic length, P_m is the specific energy dissipation rate, and K is a dimensionless constant. The characteristic length used in equation 5.6 is assumed to be the column diameter since Joshi (1980) and Viswanathan and Rao (1984) have shown that the height of a circulation cell is proportional to the column diameter. For vertical bubble columns, the specific energy dissipation rate is given by

$$P_m = U_g\ g \quad (5.11)$$

where g is the acceleration due to gravity. On substituting for P_m and l, the following relationships are obtained:

$$Pe_{LG} \propto Fr^{1/3} \tag{5.12}$$

where

$$Pe_{LG} = \frac{U_g D}{E_L} \tag{5.13}$$

and

$$Fr = \frac{U_g^2}{gD} \tag{5.14}$$

By using equation 5.12, the liquid phase dispersion coefficient may be expressed as a dimensionless function of the Froude number. When this is done, equations 5.5 to 5.9 reduce to:

$$E_L = 0.675\ D^{1.235}\ g^{0.235}\ U_g^{0.53} \tag{5.15}$$

$$E_L = 0.0675\ D^{1.5}\ g^{0.5} \tag{5.16}$$

$$E_L = 28.5\ D^{0.69}\ g^{-0.31}\ U_g^{1.63} \tag{5.17}$$

$$E_L = 0.151\ D^{1.5}\ g^{0.5} \tag{5.18}$$

$$E_L = 11.5\ D^{0.51}\ g^{-0.49}\ U_g^{2.02} \tag{5.19}$$

respectively.

Since the isotropic turbulence model predicts a column diameter dependence even for Region III, its use under these conditions is not recommended.

Quite recently, Dobby and Finch (1985, 1986) have suggested that the liquid phase dispersion coefficient under

flotation conditions (bubbly flow regime) may be approximated by

$$E_L = 0.063\ D \qquad (5.20)$$

Equation 5.20 was derived from published literature data as well as from these authors' own measurements on industrial flotation columns. Table 5.7 shows a comparison of the predicted liquid phase dispersion coefficients using equations 5.16 and 5.20 with those obtained experimentally for the fully developed bubbly flow regime.

It is clear from Table 5.7 that the use of equation 5.16 gave better agreement with the experimentally determined values than equation 5.20. Furthermore, the utility of equation 5.20 has been questioned recently (Ityokumbul et al., 1986b,c). For example, these authors used literature data which showed strong gas velocity dependence and/or were determined with wrong boundary conditions (Rice et al., 1974; 1981; Magnussen and Schumacher, 1978; Dobby and Finch, 1985). In addition, the use of Dobby and Finch's data (which was determined in square columns) in the correlation for equation 5.20 does not appear to be valid since Alexander and Shah (1976) have shown that the non-uniform flow patterns that are established in non-circular columns gives rise to higher liquid dispersion values. Moreover, Dobby and Finch did not vary the gas velocity in their studies to determine its effect on the liquid dispersion coefficient.

TABLE 5.7 COMPARISON OF OBSERVED AND CALCULATED VALUES OF E_L IN REGION II FOR AIR WATER SYSTEM (no frother)

Author	D (m)	E_L, m^2/s		
		Observed	Eqn. 5.16	Eqn. 5.20
Gondo et al. (1973)	0.10	0.0068	0.0067	0.0063
This work (1986)	0.06	0.0031	0.0031	0.0038

The variation of the liquid phase dispersion coefficient with gas velocity shows an almost identical trend as the bubble rise velocity. Since the isotropic turbulence model adequately represents the liquid dispersion data for the chain bubbling and bubbly flow regimes, its use in characterizing the applicable flow regimes is suggested with the gas phase Froude number representing a useful parameter for the establishment of flow regimes in vertical bubble columns. The liquid phase dispersion data obtained in this study suggests the following demarcations for flow regimes in vertical bubble columns:

(i) For chain bubbling,

$$Fr < 1.25 \times 10^{-4} \qquad (5.22)$$

(ii) For bubbly flow regime,

$$1.25 \times 10^{-4} < Fr < 7.2 \times 10^{-4} \qquad (5.23)$$

and

(iii) For churn turbulence flow regime,

$$Fr > 7.2 \times 10^{-4} \qquad (5.24)$$

Since similar Froude numbers were estimated from the data of Gondo et al. (1973), it appears that the use of equations 5.22 to 5.24 for the estimation of flow regimes in vertical columns with diameters exceeding 0.06 m appears to be justified.

5.3 THREE PHASE SYSTEMS

Phase hold-ups, liquid phase dispersion and particle settling characteristics under flotation conditions have been determined as a function of solid concentration and gas velocity. In the presence of the solids used in this study, considerable foaming was observed for frother concentrations exceeding 10 ppm. As a result of this, the frother concentration in these studies was fixed at 10 ppm.

5.3.1 Solid Hold-Up and Particle Settling Velocity

For mineral flotation, it is the hold-up of the gas and solid phases that is required for design purposes. Since attempts to carry out continuous flotation experiments with the oilsand tailings were hampered by the presence of residual bitumen which easily clogged the narrow tubings, experiments were performed to simulate the behaviour of gangue particles (mostly silica sand) under flotation conditions. The hold-up of the nonfloatable sand particles of varying size has been determined as a function of gas and liquid velocities, solid concentration of the feed and frother addition. The results are summarized in Figure 5.17. Each of the points shown in Figure 5.17 represents the flat portion of Figure 4.7. Similar results have been obtained by Bhaga and Weber (1972). The concentration of solids in the reactor does not depend on the gas hold-up

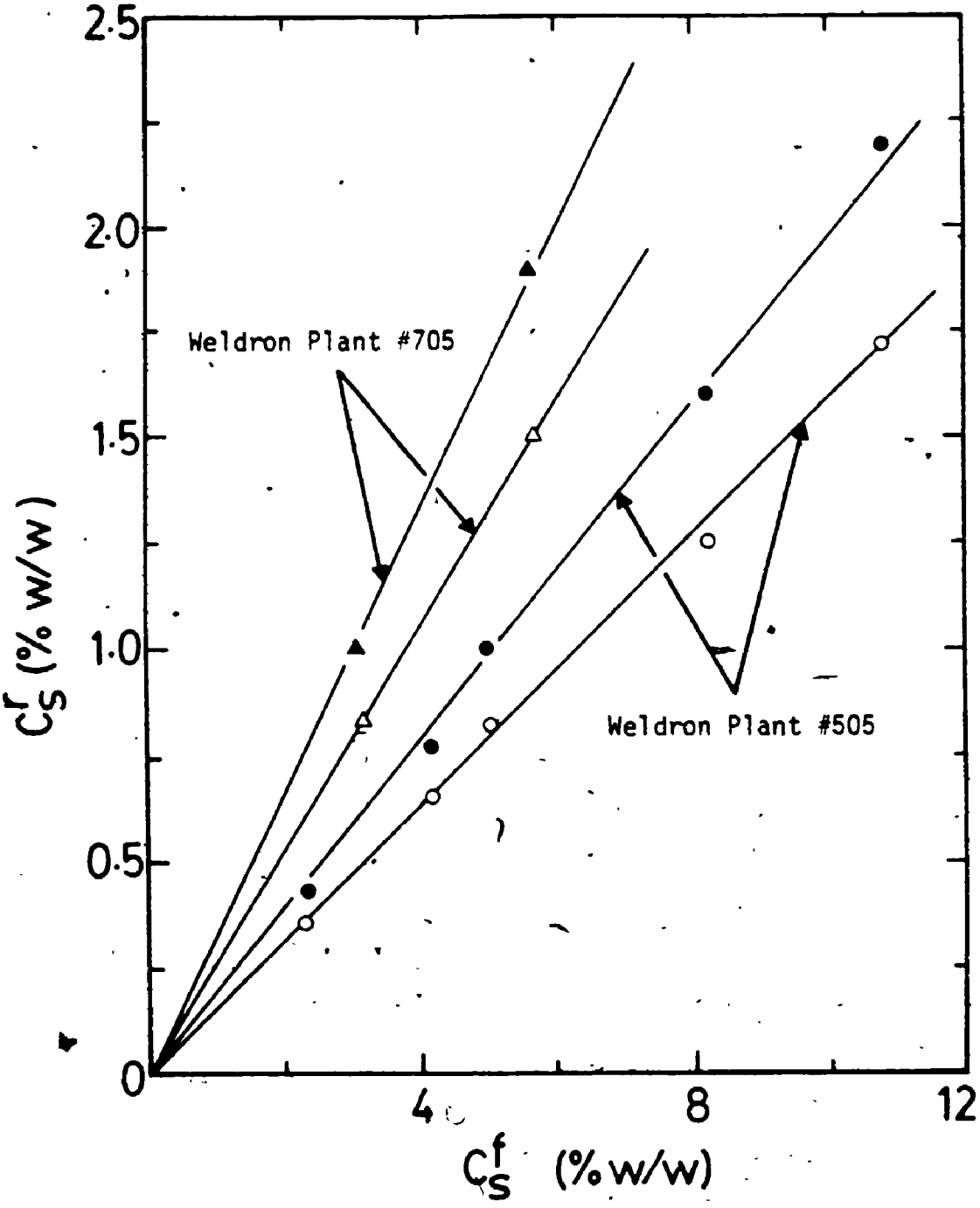

Figure 5.17 Effect of particle size and liquid velocity on solid hold-up. (The open and closed symbols represent liquid superficial velocities of 0.0043 and 0.0063 m/s respectively)

which is in agreement with the results of Bhaga and Weber (1972).

It is important to establish what the slopes of these lines actually represent. In Chapter 3, it was assumed that the transport of solids was by sedimentation and convection only. The data of Bhaga and Weber (1972) has shown that for particle settling outside the Stoke's regime, their settling velocity in the presence of gas bubbles was well represented by equation 2.22. Since Bhaga and Weber used mono-dispersed solid particles, it is assumed that the same theory can be extended to the poly-dispersed solids sand particles used here. The theoretical values of the slopes were calculated using

$$\sum_i \left(\frac{U_L x_{F_i}}{U_L + V_{P_i}}\right) \qquad (5.25)$$

where x_{F_i} is the relative proportion of fraction i in the feed (see Figure 4.1) and V_{P_i} is the terminal settling velocity of fraction i in the presence of gas bubbles calculated using equation 2.22 and U_L is the superficial liquid velocity. The superficial liquid velocity was used since the plots in Figure 4.7 as well as the data of Bhaga and Weber (1972) show that the solid to liquid ratio in the column does not depend on the gas hold-up. For particles settling in the Stoke's regime, it was assumed that the presence of gas bubbles did not change their settling characteristics

(Ramchandran and Chaudhari, 1983). A comparison of the calculated values of the slope (by equation 5.25) with those experimentally determined is shown in Table 5.8.

The close agreement between the calculated and predicted values suggests that the sedimentation convection model offers a good description of particle behaviour in a bubble column.

5.3.1.2 Effect of Calming Zone On Gangue Recovery

Contamination of the froth product in mineral flotation depends on the gangue concentration at the froth-pulp interface. In conventional mechanical flotation cells where highly turbulent conditions exist, gangue recovery is usually high. It is also for this reason that the present designs for industrial bubble column flotation cells introduce wash water near the froth-pulp interface. However, this practice may be detrimental to the particle collection process as particle detachment is likely to be promoted as a result of the increased turbulence near the wash water entry point. In order to test if gangue concentration in the calming section can be altered by varying the height of the calming section, several solid hold-up experiments were carried out as described in Chapter 4. The total fluid volume in these experiments was fixed while the feed inlet point was varied. The results obtained are shown in Figure 5.18. The results

TABLE 5.8 COMPARISON OF SOLID HOLD-UP PARAMETERS

Sand #	U = 0.0063 m/s		U = 0.0043 m/s	
	Expt.	Calc*	Expt.	Calc*
Weldron #705	0.333	0.328	0.264	0.260
Weldron #505	0.198	0.20	0.156	0.151

* Detailed calculations are shown in Appendix 6.

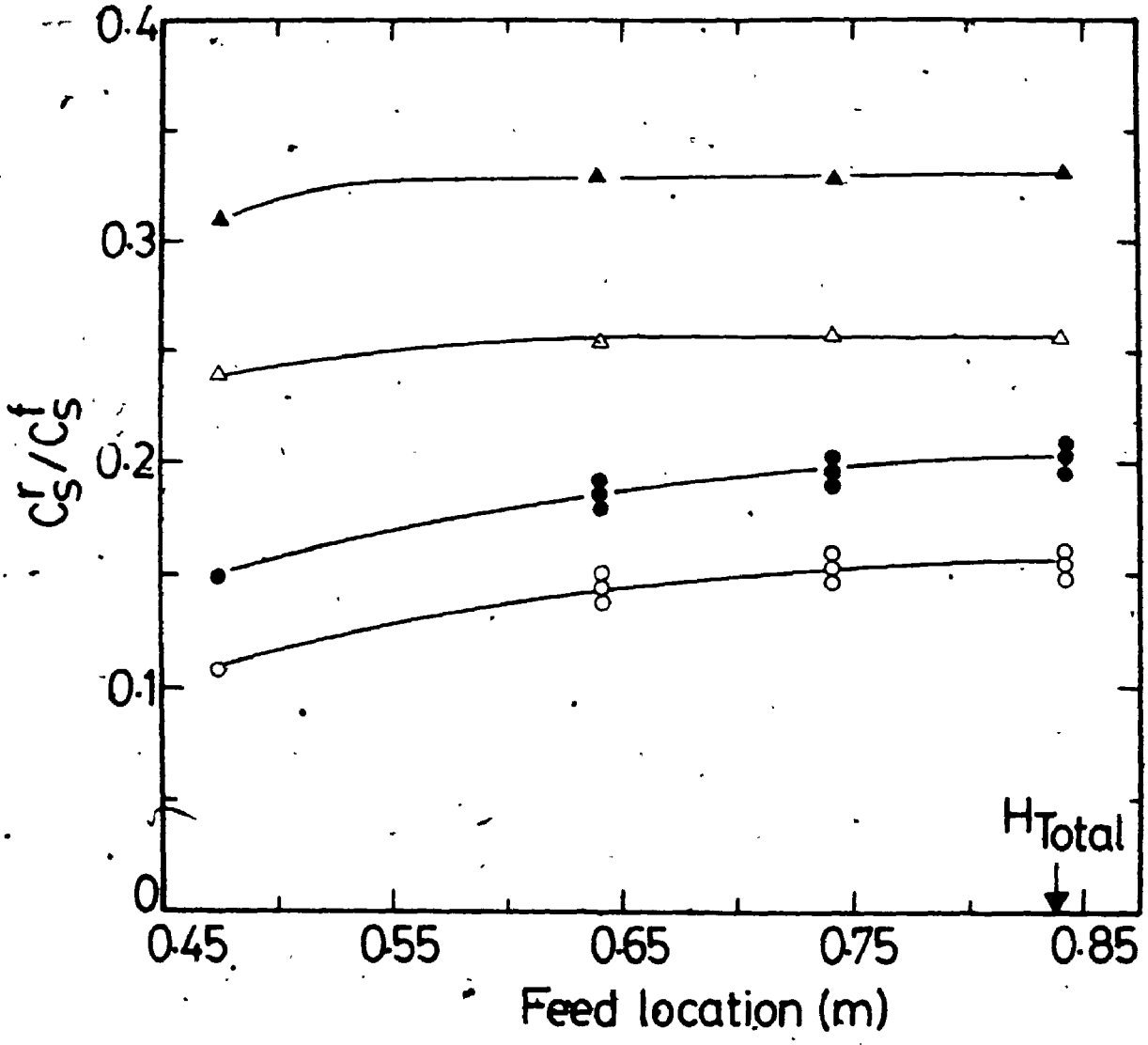

Figure 5.18 Variation of average solid concentration in the column with feed location (symbols same as in Figure 5.17).

presented here represent the worst case scenario since fines would tend to accumulate in the calming section. In an actual flotation experiment, the constant removal of concentrate at the top will reduce the accumulation of fines. It can be readily seen from Figure 5.18 that for the coarser sand particles, gangue concentration in the calming zone may be reduced considerably by introducing the feed at a distance of 0.20 m from the interface. For the same separation, there was no significant change in the average concentration of the finer sand. This explains why for fine particle flotation, the wash water tonnage may even be larger than the feed rate (Wheeler, 1966). Since the major component of the gangue minerals in the centrifuge tailings is sand with a particle size distribution similar to that of the coarser sand (Trevoy et al., 1978), the calming section may be used to control gangue recovery.

5.3.2 Gas and Liquid Hold-Up

The variation of gas and liquid hold-ups with solid concentration is shown in Figures 5.19 to 5.22. The solid lines on these figures represent the corresponding values for the two phase systems. It can be seen that the differences between the two and three phase systems were pronounced only at the lower gas velocities. Visual observations revealed that at these low gas velocities, some solids settled on the gas distributor. When this happened, the

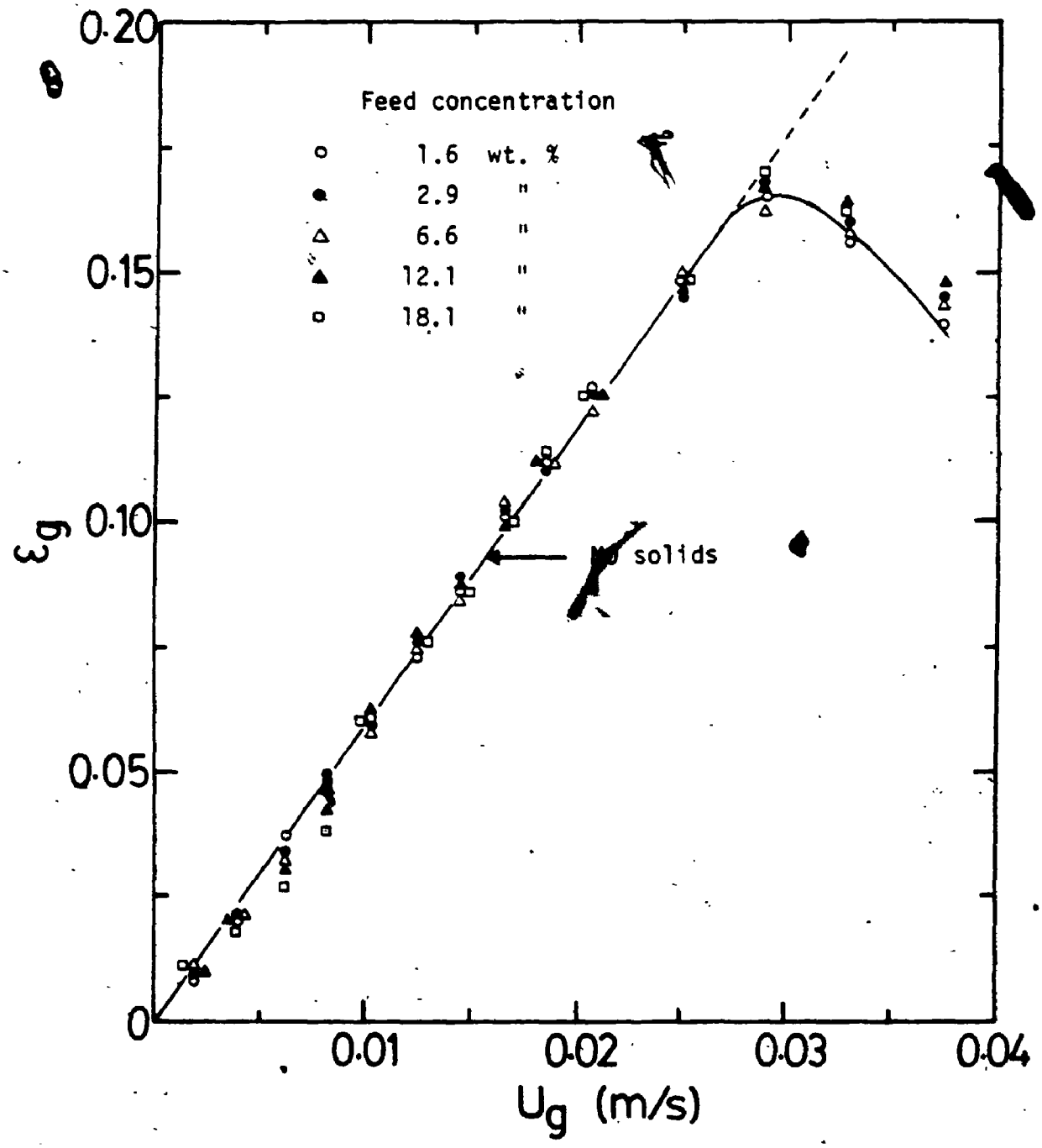

Figure 5.19 Effect of solid concentration on gas hold-up.

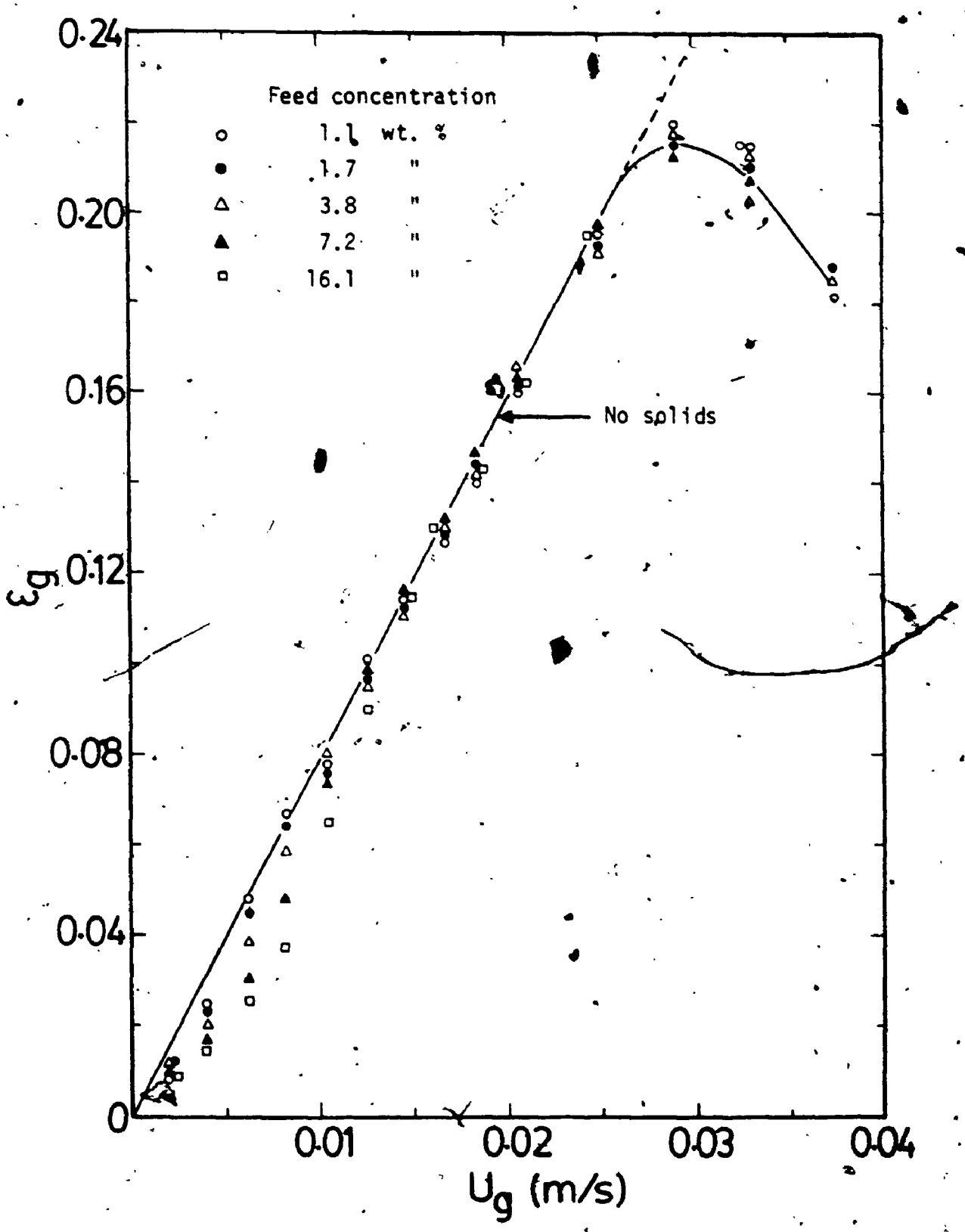

Figure 5.20 Effect of solid concentration and frother on gas hold-up. (pine oil concentration 10 ppm).

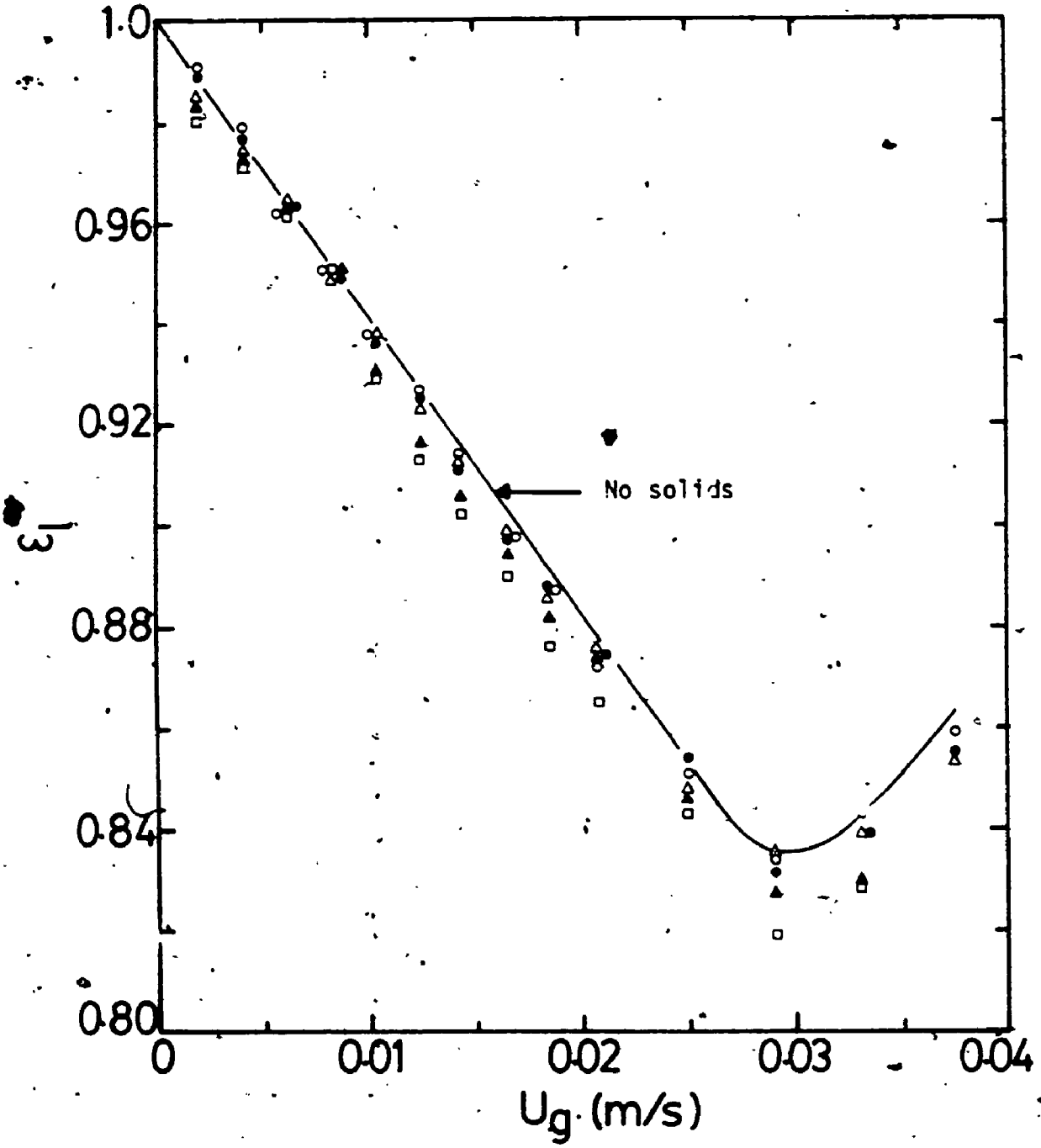

Figure 5.21 Effect of solid concentration on liquid hold-up.
(symbols same as in Figure 5.19)

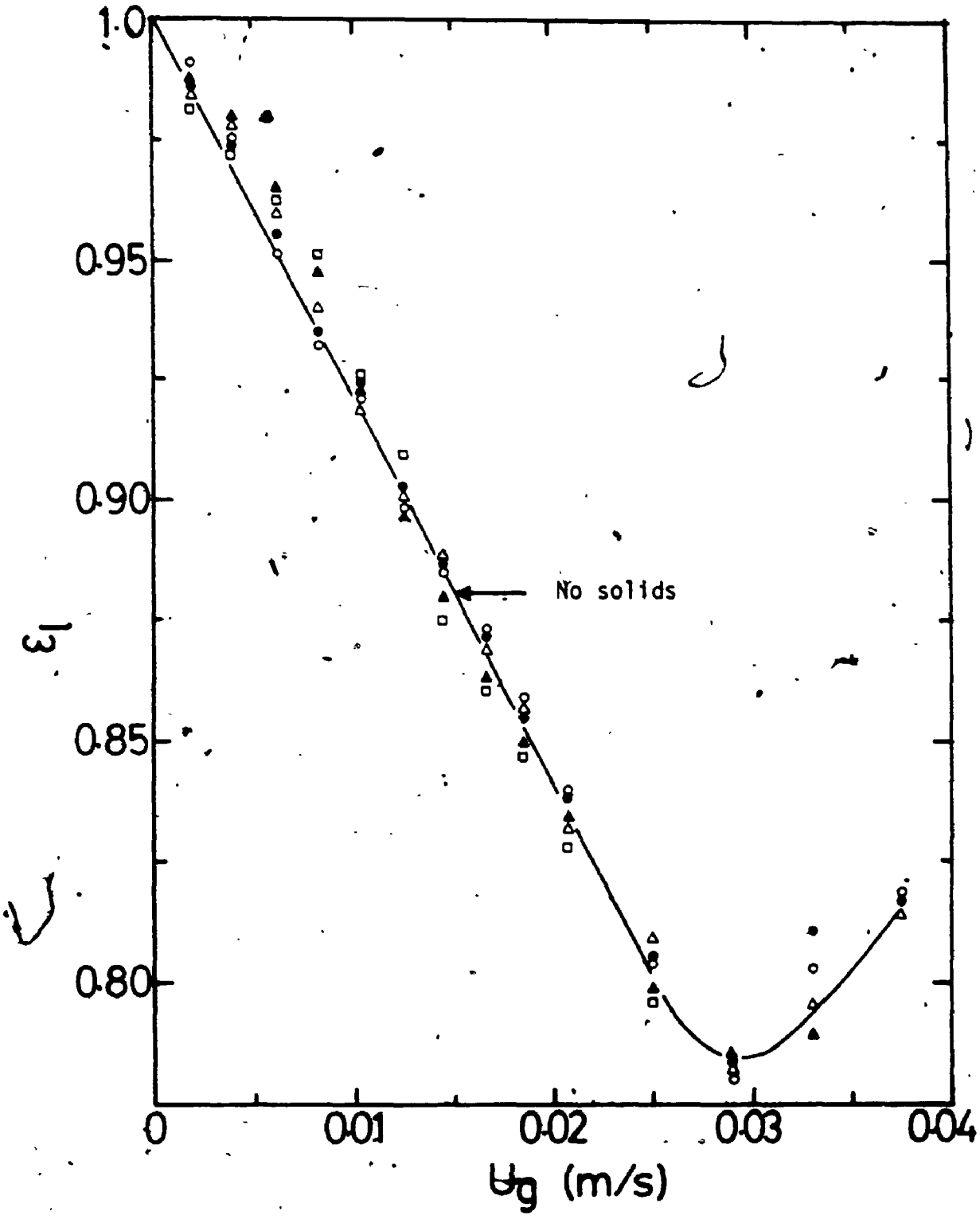

Figure 5.22 Effect of solid concentration on the liquid hold-up. (symbols same as in Figure 5.20)

bubbles leaving the bed of sand particles were considerably larger than those observed in the two phase systems (see Figure 5.23). When solids were observed on the grid, the presence of frother was not effective in controlling the bubble size. The same effect is obtained when the bubble rise velocity is plotted as shown in Figures 5.24 and 5.25.

For the range of feed solid concentrations used here, the effect of solids on the gas hold-up was not observed except when the solids settled on the gas distributor. Since the maximum solid depth in these experiments was 0.004 m, the increase in bubble size can not be attributed to liquid viscosity effects as has been postulated for three phase fluidization (Muroyama and Fan, 1985).

5.3.3 Liquid Phase Mixing

The effect of solid concentration, frother and gas velocity on the liquid dispersion coefficient is shown in Figures 5.26 and 5.27. A comparison with the corresponding values for two phase systems will reveal that the presence of solids reduced the liquid dispersion coefficients for gas velocities in the bubbly flow regime except when solids were observed on the gas distributor. When this happened, the effect of frother was not observed which is in agreement with the gas hold-up and bubble rise velocity results already discussed in section 5.3.2. In the churn turbulence

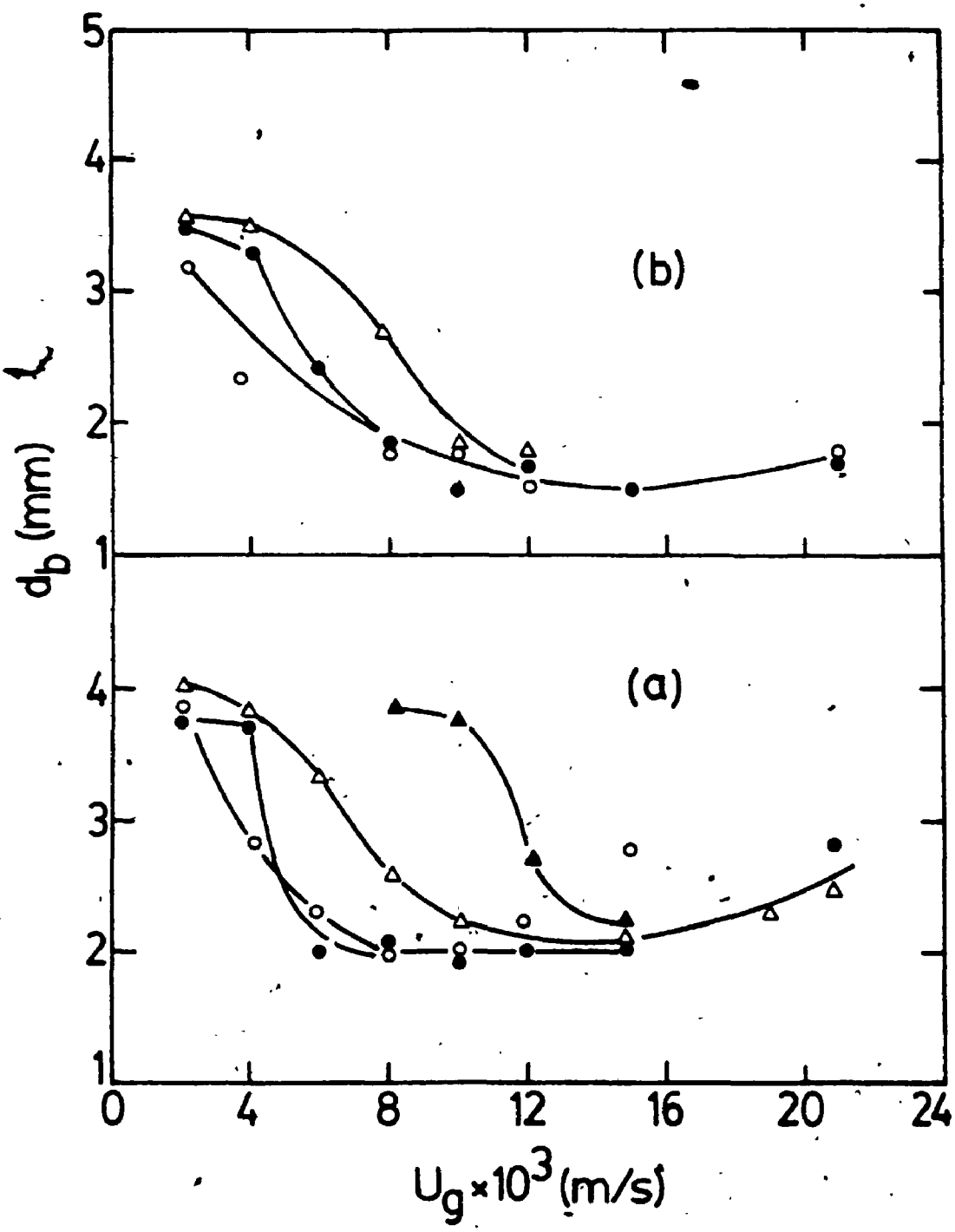

Figure 5.23 Variation of bubble size with gas velocity in the presence of solids: (a) No frother; symbols same as in Figure 5.19 (b) 10 ppm; symbols same as in Figure 5.20

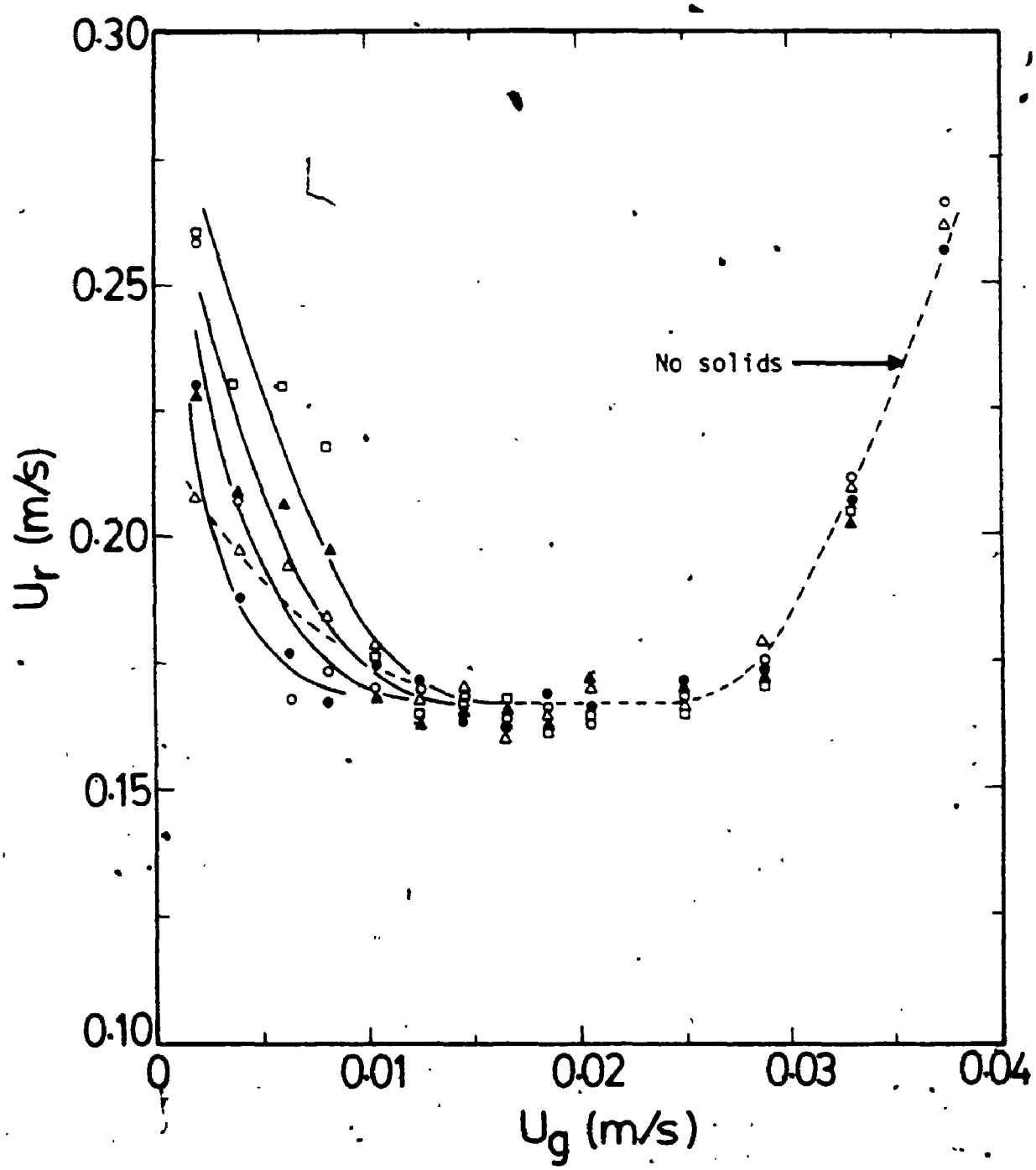

Figure 5.24 Effect of solid concentration on the bubble rise velocity. (symbols same as in Figure 5.19)

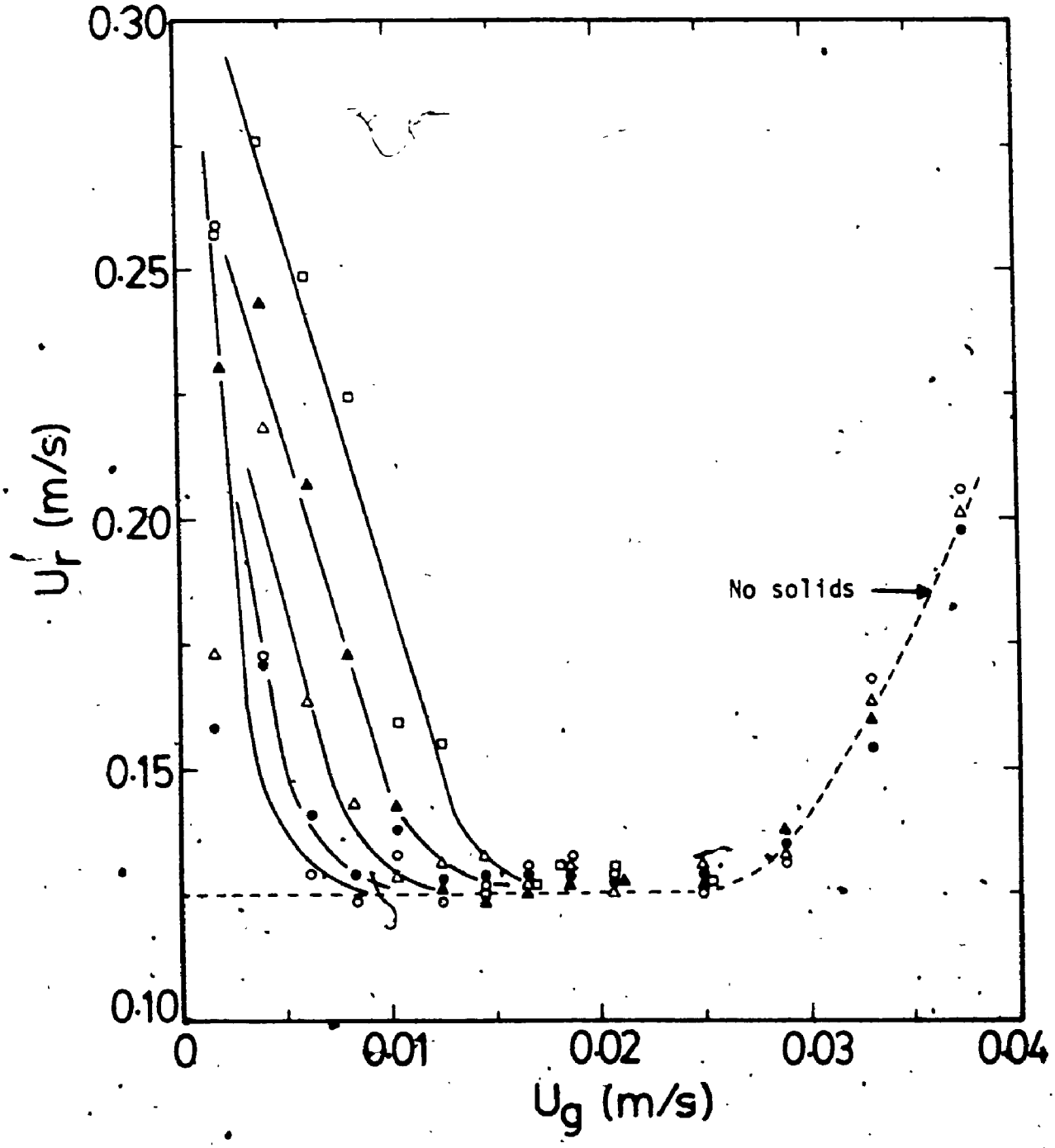

Figure 5.25 Effect of solid concentration and frother on bubble rise velocity. (symbols same as in Figure 5.20)

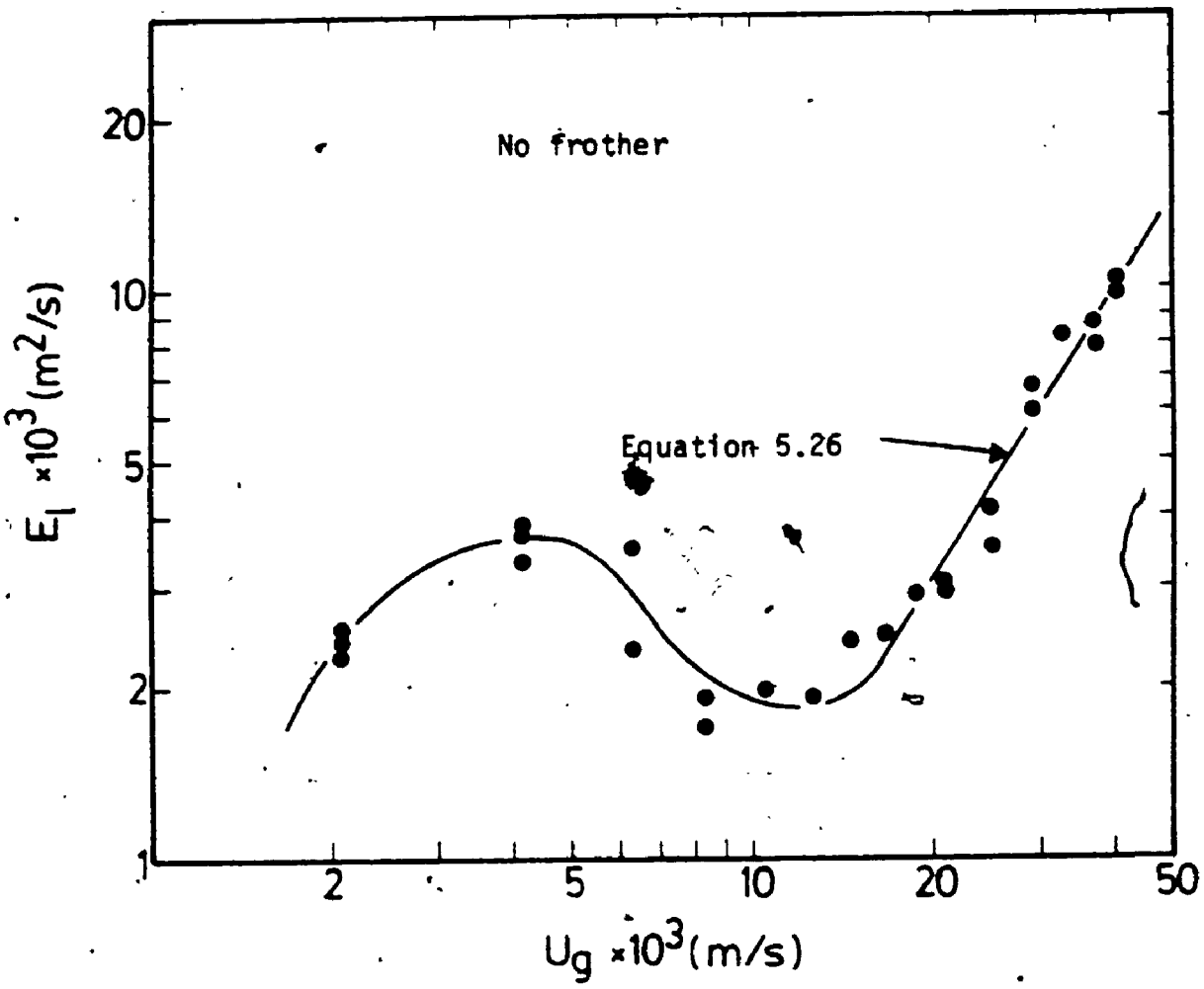

Figure 5.26 Liquid dispersion coefficient in the presence of solids (5 wt. %)

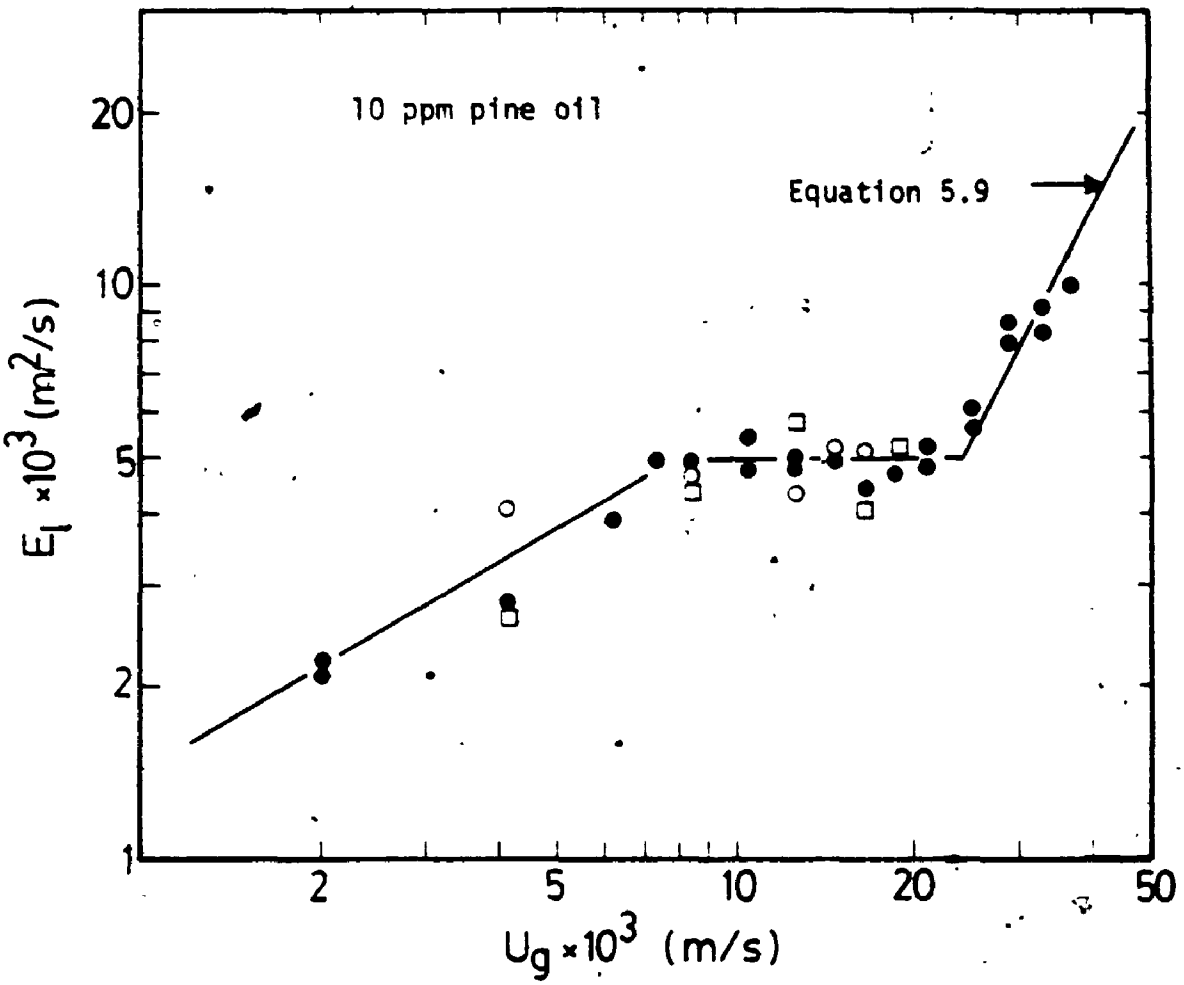

Figure 5.27 Effect of feed solid concentration on the liquid dispersion coefficient in the presence of frother (●) 5 wt. %; (○) 10 wt. %; (□) 15 wt. %.

flow regime, the effect of solids was not significant as seen from Figures 5.26 and 5.27. For example, a correlation of the liquid dispersion data for the air water solid system gave the following correlation

$$E_L = 2.12\ U_g^{1.67} \qquad (5.26)$$

which agrees rather well with equation 5.7. Increasing the feed solid concentration from 5% to 11% does not appear to have any significant effect on the liquid dispersion coefficient. The decrease of the liquid dispersion coefficient in the presence of solids can not be adequately explained at the present time. However, it is assumed to be related to the increase in radial mixing which has been reported for three phase systems (Bhaga and Weber, 1972).

CHAPTER 6

CONCLUSIONS AND RECOMMENDATIONS

6.1 FLOTATION AND HEAVY MINERALS BENEFICIATION PROCESS

The froth flotation recovery of heavy minerals from oilsand centrifuge tailings has been studied. The results obtained indicate that:

(I) The optimum pH for heavy minerals recovery is in the range of 8.3 to 11.7. The effect of pH is explained on the basis of collector removal and ionization, and the adsorption of H^+ and OH^- ions on the mineral surfaces.

(II) The optimum frother dosage was found to be 0.15% (v/v) of pine oil. The effect of frother can best be understood by considering the effects of its adsorption at the air liquid and solid liquid interfaces.

(III) With a feed containing 10-12% TiO_2 and 4-5% ZrO_2SiO_2 a 28-30% TiO_2 and 10-12% $ZrO_2 \cdot SiO_2$ concentrate is considered attainable at 85-95% recoveries of both minerals if frothers are used.

(IV) The use of causticized starch to depress iron recovery resulted in depression of the heavy minerals as well. As the heavy minerals and iron minerals have different physical

properties, separation between them must be left to the subsequent upgrading operations (gravity, magnetic and high tension separations).

(V) The use of flotation for the recovery of these heavy minerals offers several significant cost savings when compared to the processes that have been developed and patented to date.

(VI) The upgrading process developed for the froth product from the flotation stage has the added advantage of permitting the recovery of the traces of rare earth minerals which also occur in the centrifuge tailings. None of the processes that have been developed and patented has been successful in recovering these rare earth minerals. It also permits the recovery of an iron oxide product.

6.2 HYDRODYNAMIC STUDY OF BUBBLE COLUMN FLOTATION

6.2.1 Two-Phase Systems

A hydrodynamic study of two phase (gas-liquid) bubble column has been carried out. The results obtained indicate that:

(I) The gas hold-up for air water system is given by equation 5.1. In the presence of frother, the gas hold-up increases and bubbly flow conditions are maintained to higher gas velocities. The different flow regimes in

vertical bubble columns of diameters exceeding 0.06 m may be characterized by the gas phase Froude numbers as given by equations 5.22 to 5.24.

(II) The dependence of liquid phase mixing on the gas velocity agrees well with the flow regimes determined using the variation of bubble rise velocity with gas velocity. For the air-water system studied, the use of equations 5.15 to 5.17 for the chain-bubbling, bubbly and churn turbulence flow regimes respectively is recommended. For the fully developed bubbly flow regime, the liquid phase dispersion coefficient is independent of gas velocity, since the column diameter does not appear to have an effect on the liquid phase dispersion data in the churn turbulence flow regime (based on a comparison of this work with the data of Sangnimnuan et al., 1984), the use of the isotropic turbulence model to provide dimensionally consistent correlations in this flow regime is not recommended. The isotropic turbulence model may however be used in the chain bubbling and bubbly flow regimes. The addition of frothers generally resulted in increased dispersion of the liquid phase.

6.2.2 Three-Phase Systems

A hydrodynamic study of three-phase bubble columns operating under flotation conditions gave the following results:

(I) The particle settling velocity in a bubble column is well predicted by equations 2.22. For particles settling in the Stoke's regime, the effect of gas bubbles appears to be minimal.

(II) The presence of solids does not alter the gas hold-up and flow regimes except when the solids were observed on the grid.

(III) The "calming" zone (that is the section above the feed inlet point to the froth-pulp interface) may be used to control gangue recovery instead of the present practice of introducing wash water near the froth-pulp interface. As explained earlier, wash water addition may be detrimental to the particle collection process as the increased turbulence near the water inlet point will likely promote particle detachment.

(IV) The liquid dispersion coefficient in the presence of solid particles is reduced by about 40% when compared to the corresponding air-water system. This effect is attributed to the increase in radial mixing which has been reported for these systems (Bhaga and Weber, 1972).

6.3 RECOMMENDATIONS FOR FUTURE STUDIES

The use of the "calming" section to control gangue recovery in bubble column flotation is a relatively new concept

which will need to be verified with a real flotation feedstock. Future studies in this area should address this important operational change in bubble column flotation which when adopted, promises to enhance the advantages of using this device.

The results obtained may be applied to other two and three phase systems as well. For example, the liquid phase dispersion data obtained here may be used in the design of gas-liquid reactors. Future studies should therefore be carried out on systems other than the air and water used in the present study.

The use of the isotropic turbulence model for flow regime mapping in vertical bubble columns offers some distinct advantages over the present application of the drift-flux analysis as the gas hold-up data is not required. The extension of this model to other gas-fluid contacting systems (for example different gas distributor design, different liquids, etc.) needs to be investigated further.

APPENDIX A

CALIBRATION OF ROTAMETER

Two rotameters were used to measure the air flow rates. For calibrating these rotameters, the air line was pressurized by compressed air at 116 KPa. Air was then metered with a wet-test gas meter for a period of 1-3 minutes. The calibration curves so obtained are shown in Figure A.1.

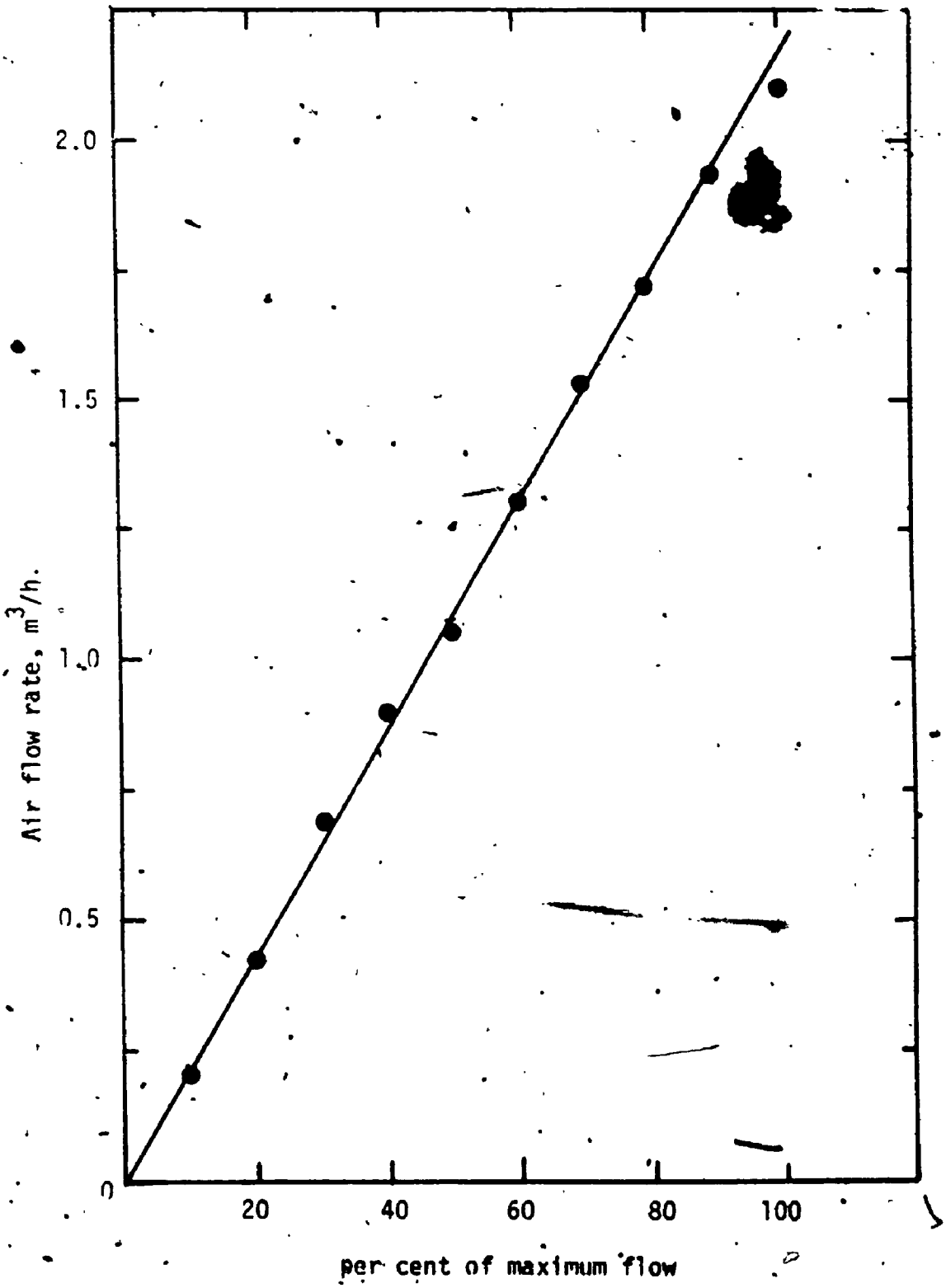

Figure A.1. Calibration curve for air flow meter

APPENDIX B

B.1 FREQUENCY RESPONSE OF AXIAL DISPERSION EQUATION FOR CLOSED BOUNDARY CONDITIONS

The one-dimensional dispersion model is described by the dimensionless equation

$$\frac{1}{Pe}\frac{\partial^2 C}{\partial z^2} - \frac{\partial C}{\partial z} = \frac{\partial C}{\partial \theta} \qquad (B.1)$$

The boundary conditions necessary for solving equation B.1 are

$$C_i(\theta) = C(0^+,\theta) - \frac{1}{Pe}\frac{\partial C}{\partial z} \qquad (B.2)$$

$$\left.\frac{\partial C}{\partial z}\right|_{z=1} = 0 \qquad (B.3)$$

$$C(z,0) = 0 \qquad (B.4)$$

The system transfer function $\bar{g}(j\omega)$ which is obtained from a Laplace transformation of equations B.1 to B.4 is given below

$$\bar{C} = \frac{4q\ \exp(\frac{Pe}{2})}{(1+q)^2\exp(\frac{Pe}{2}\ q) - (1-q)^2\exp(-\frac{Pe}{2}\ q)} \qquad (B.5)$$

The frequency response of equation B.5 has been given by Clements (1969). If we define

$$a = \frac{4\omega\tau}{Pe} \qquad (B.6)$$

and

$$b = \frac{1}{2} \arctan a \quad \text{(principal value)} \tag{B.7}$$

the magnitude of $\bar{G}(j\omega)$ is given by

$$|\bar{G}(j\omega)| = (R^2 + I^2)^{1/2} \tag{B.8}$$

with the phase angle of $\bar{G}(j\omega)$ being

$$\text{angle}[\bar{G}(j\omega)] = \arctan\left(\frac{I}{R}\right) \tag{B.9}$$

where R and I represent the real and imaginary components of $\bar{G}(j\omega)$.

$$R = \frac{(B\alpha_1 + D\alpha_2)}{\alpha_1^2 + \alpha_2^2} \exp(Pe/2) \tag{B.10}$$

$$I = \frac{D\alpha_1 - B\alpha_2}{\alpha_1^2 + \alpha_2^2} \exp(Pe/2) \tag{B.11}$$

and

$$\alpha_1 = (1+B^2-D^2)\sinh\left(\frac{PeB}{2}\right)\cos\left(\frac{PeD}{2}\right) - 2BD\cosh\left(\frac{PeB}{2}\right)\sin\left(\frac{PeD}{2}\right)$$

$$+ 2B\cosh\left(\frac{PeB}{2}\right)\cos\left(\frac{PeD}{2}\right) - 2D\sinh\left(\frac{PeB}{2}\right)\sin\left(\frac{PeD}{2}\right) \tag{B.12}$$

$$\alpha_2 = 2BD\sinh\left(\frac{PeB}{2}\right)\cos\left(\frac{PeD}{2}\right) + (1+B^2-D^2)\cosh\left(\frac{PeB}{2}\right)\sin\left(\frac{PeD}{2}\right)$$

$$+ 2D\cosh\left(\frac{PeB}{2}\right)\cos\left(\frac{PeD}{2}\right) + 2B\sinh\left(\frac{PeB}{2}\right)\sin\left(\frac{PeD}{2}\right) \tag{B.13}$$

$$B = (1+a^2)^{1/4}\cos b \tag{B.14}$$

$$D = (1+a^2)^{1/2}\sin b \tag{B.15}$$

B.2 FOURIER TRANSFORMATION USING FILON'S QUADRATURE

The data curve $G_d(t)$ was numerically Fourier transformed using Filon's quadrature. Filon developed a quadrature formula for the following integrations

$$\int_a^b f(t)\sin\omega t\, dt \quad \text{and} \quad \int_a^b f(t)\cos\omega t\, dt \qquad (B.16)$$

which is based on approximation by parabolic segments as in Simpson's rule. However, in Filon's method, the numerical values of the coefficients of Simpson's rule are replaced by trigonometric functions of $\omega\Delta t$. To apply Filon's formula, the curve is divided into an odd number, 2n+1, of points at intervals of Δt. If we denote these points by I_o, I_1, I_2..., I_{2n}, where

$$I_o = f(a)\sin\omega a \qquad (B.17)$$

and

$$I_{2n} = f(b)\sin\omega b \qquad (B.18)$$

Let

$$S_{2n} = \frac{1}{2} I_o + I_2 + \ldots + I_{2n-2} + I_{2n} \qquad (B.19)$$

$$S_{2n-1} = I_1 + I_3 + \ldots + I_{2n-1} \qquad (B.20)$$

$$\theta = \omega\Delta t \qquad (B.21)$$

$$\alpha = \frac{1}{\theta} + \frac{\sin 2\theta}{2\theta^2} - \frac{2\sin^2\theta}{\theta^3} \qquad (B.22)$$

$$\beta = 2\left(\frac{\cos^2\theta + 1}{\theta^2} + \frac{\sin 2\theta}{\theta^3}\right) \qquad (B.23)$$

and

$$\gamma = 4\left(\frac{\sin\theta}{\theta^3} - \frac{\cos\theta}{\theta^2}\right) \qquad (B.24)$$

α, β and γ must be computed from Taylor's series expansions of equations B.22 through B.24 when θ is small, to prevent loss of significant digits. Then

$$\int_a^b f(t)\sin\omega t\, dt \approx \Delta t\{\alpha[f(a)\cos\omega a - f(b)\cos\omega b] + \beta S_{2n} + \gamma S_{2n-1}\} \qquad (B.25)$$

For the integration of the cosine form, the same procedure as in the $\sin\omega t$ is repeated recalling that

$$\sin(\omega t + \pi/2) = \cos\omega t \qquad (B.26)$$

If I_o is now denoted by $f(a)\cos\omega a$ and I_{2n} by $f(b)\cos\omega b$,

$$\int_a^b f(t)\cos\omega t\, dt \approx \Delta t\{\alpha[f(a)\cos(\omega a+\pi/2) - f(b)\cos(\omega b+\pi/2)] + \beta S_{2n} + \gamma S_{2n-1}\} \qquad (B.27)$$

The computer program used for these computations and the estimation of the liquid phase Peclet number, Pe_L (or liquid dispersion coefficient) and τ is shown in Appendix B.3.

B.3 Computer Program Used.

The following is a replica of the computer program used for parameters estimation in the frequency domain for the closed-closed boundary conditions.

```
CCCCCCCCCCCCCCCCCCCCCCCCCCCCCCCCCCCCCCCCCCCCCCCCCCCCCCCCCCCCCCCCCCCCCCCCCC
C
C     SIMPLEX DIRECT SEARCH MINIMIZATION AS OUTLINED BY NEDLER AND MEAD
C     (REFERENCE: COMPUTER JOURNAL 7(4),308 1964)
C
C     DIMENSIONED FOR 10 PARAMETERS
C     **** DEFINATION OF SYMBOLS ****
C
C     NV          NUMBER OF PARAMETERS IN THE OBJECTIVE FUNCTION
C     NP          NUMBER OF VERTICES OF THE SIMPLEX
C     ALPHA       REFLECTION COEFFICIENT
C     BETA        CONTRACTION COEFFICIENT
C     GAMMA       EXPANSION COEFFICIENT
C     DELTA       STEP LENGTH
C     MAXIT       MAXIMUM NUMBER OF ITERATIONS
C     FY(J)       VALUE OF OBJECTIVE FUNCTION AT POINT J
C     P(J,I)      PARAMETERS I=1,NV FOR POINT J
C     P(NC,I)     PARAMETERS FOR CENTROID
C     P(NC+1,I)   PARAMETERS FOR REFLECTED POINT
C     OBJFN(J)    SUBROUTINE TO DEFINE THE OBJECTIVE FUNCTION AT POINT J
C
C     NWHER       COUNTER TO DEFINE CONVERGENCE METHOD
C     NWHER=1     REFLECTION SUCCESS
C     NWHER=2     EXPANSION FAILURE
C     NWHER=3     EXPANSION SUCCESS
C     NWHER=4     CONTRACTION SUCCESS
C     NWHER=5     CONTRACTION FAILURE
C
C     RUN#        EXPERIMENT IDENTIFICATION
C
C
CCCCCCCCCCCCCCCCCCCCCCCCCCCCCCCCCCCCCCCCCCCCCCCCCCCCCCCCCCCCCCCCCCCCCCCCCC


      PROGRAM TEST(INPUT,OUTPUT,DATA,RUN#,TAPE5=DATA,TAPE6=RUN#)
      COMMON Y(100),PP(10,6),FY(10),SIG(2,10),VAL(100),FTN(2),DVN(2),CO
     *UNT,MO,NM,DM,N,DT,NV,T(100),RT(100),RD(50),CD(50),BD(50),W(50)
      DIMENSION R(50),C(50),B(50)
      GAMMA=2.0
      ALPHA=1.0
      BETA=0.5
      COUNT=0.0
C
      READ(5,*)MAXIT
      READ(5,*)NV
      NP=NV+1
      NC=NP+1
```

```
      XNV=FLOAT(NV)
      XNP=FLOAT(NP)
C
C     READ INITIAL SIMPLEX VERTICES P(J,I) FOR ALL POINTS J
C
C     INITIAL SIMPLEX
C
      READ(5,*)DELTA
      READ(5,*)(PP(1,I),I=1,NV)
      Q1=DELTA/(XNV*SQRT(2.))*(SQRT(XNP)+XNV-1.0)
      Q2=DELTA/(XNV*SQRT(2.))*(SQRT(XNP)-1.0)
      DO 5 J=2,NP
      DO 35 I=1,NV
      IF(I.EQ.(J-1)) GO TO 20
      PP(J,I)=PP(1,I)+Q2
      GO TO 35
   20 PP(J,I)=PP(1,I)+Q1
   35 CONTINUE
    5 CONTINUE
C
C     READING OF THE INPUT DATA AND NORMALISATION OF THE CONCENTRATION-
C     TIME CURVE
C
      READ(5,*)WO,NW,DW,N,DT
      READ(5,*)(Y(J),J=1,N)

      Z=88.0
      PI=3.1415927
      TD=PP(1,I)
      PE=PP(1,2)

      T(1)=0.0
      DO 400 J=2,N
      T(J)=T(J-1)+DT
  400 CONTINUE
      W(1)=WO
      DO 420 J=2,NW
      W(J)=W(J-1)+DW
  420 CONTINUE

C
C     AREA UNDER THE CONCENTRATION-TIME CURVE MEASURED IN THE TAILINGS
C     STREAM USING THE TRAPEZOIDAL APPROXIMATION
C
C     RT(J) REPRESENTS THE E(T) CURVE OF THE TRACER RESPONSE
C

      SUM=(Y(1)+Y(N))/2.0
      N2=N-2
      N1=N-1
      DO 430 J=2,N1
      SUM=SUM+Y(J)
```

```
  430 CONTINUE
      RR=SUM*DT
      DO 440 J=1,N
      RT(J)=Y(J)/RR
  440 CONTINUE

C
C     CALCULATION OF THE MEASURED FREQUENCY RESPONSE
C     THE NUMERICAL INTEGRATION OF THE FOURIER TRANSFORMS IS DONE USING
C     FILON'S QUADRATURE.
C

      DO 450 K=1,NW
      S2N=(RT(1)*SIN(W(K)*T(1))+RT(N)*SIN(W(K)*T(N)))/2.
      DO 470 J=3,N2,2
      S2N=S2N+RT(J)*SIN(W(K)*T(J))
  470 CONTINUE
      S2N1=0.0
      DO 480 J=2,N1,2
      S2N1=S2N1+RT(J)*SIN(W(K)*T(J))
  480 CONTINUE
      TH=W(K)*DT
      AL=1./TH+SIN(2.*TH)/(2.*TH**2.)-2.*(SIN(TH))**2./(TH**3.)
      BET=2.*(((COS(TH))**2.+1.)/(TH**2.)-SIN(2.*TH)/(TH**3.))
      GAM=4.*(SIN(TH)/(TH**3.)-COS(TH)/(TH**2.))
      CD(K)=-DT*(AL*(RT(1)*COS(W(K)*T(1))-RT(N)*COS(W(K)*T(N)))+BET*S2N
     **+GAM*S2N1)
      S2N=(RT(1)*COS(W(K)*T(1))+RT(N)*COS(W(K)*T(N)))/2.0
      DO 490 J=3,N2,2
      S2N=S2N+RT(J)*COS(W(K)*T(J))
  490 CONTINUE
      S2N1=0.0
      DO 500 J=2,N1,2
  500 S2N1=S2N1+RT(J)*COS(W(K)*T(J))
      RD(K)=DT*(*(AL*(RT(1)*COS(W(K)*T(1)+PI/2.)-RT(N)*COS(W(K)*T(N)+PI/
     *2.))+BET*S2N+GAM*S2N1)
      MD(K)=(RD(K)**2.+CD(K)**2.)**0.5
  450 CONTINUE

C
C     THE OBJECTIVE FUNCTION IS EVALUATED FOR ALL POINTS
C

      DO 10 J=1,NP
   10 CALL OBJFN(J)

      WRITE(6,200)
      WRITE(6,220)
      DO 15 J=1,NP
   15 WRITE(6,340)(PP(J,I),I=1,NV),FY(J)
C
C     FIND POINTS WITH MAXIMUM AND MINIMUM OBJ.FUNCTIONS
C
      ITN=0
   45 WRITE(6,260)NUMBER
```

```
      IF(ITN.GT.MAXIT) GO TO 125
      ITN=ITN+1
      KMAX=1
      KSMX=1
      KMIN=1
      DO 48 I=2,NP
      IF(FY(KMAX).LT.FY(I)) KMAX=I
   48 CONTINUE
      IF(KMAX.EQ.1) KSMX=2
      DO 50 I=2,NP
      IF(FY(KMIN).GT.FY(I)) KMIN=I
      IF(FY(KSMX).LT.FY(I).AND.I.NE.KMAX) KSMX=I
   50 CONTINUE
      WRITE(6,350)ITN,FY(KMIN),(PP(KMIN,I),I=1,NV)

C
C     ESTIMATE CENTROID OF SIMPLEX WITH POINT KMAX EXCLUDED
C

      DO 53 I=1,NV
      PP(NC,I)=0.0
      DO 52 J=1,NP
      IF(J.NE.KMAX) PP(NC,I)=PP(NC,I)+PP(J,I)
   52 CONTINUE
   53 PP(NC,I)=PP(NC,I)/XNV
C
C     OBJFN FUNCTION AT CENTROID IS AVERAGE AT VERTICES
C

      FY(NC)=0.0
      DO 54 I=1,NP
   54 FY(NC)=FY(NC)+FY(I)
C
C     CONVERGENCE TEST
C
      SUM=0.0
      DO 55 I=1,NP
      XX=0.0
      X=FY(NC)-FY(I)
      IF(ABS(X).GT.1.E-7) XX=X*X
   55 SUM=SUM+XX
      SE=SQRT(SUM/XNP)
      IF(SE.LE.1.E-4) GO TO 135
C
C     REFLECTION
C
      DO 60 I=1,NV
   60 PP(NC+1,I)=(1.0+ALPHA)*PP(NC,I)-ALPHA*PP(KMAX,I)
      CALL OBJFN(NC+1)
      IF(FY(NC+1).GT.FY(KSMX)) GO TO 90
      IF(FY(NC+1).LT.FY(KMIN)) GO TO 80
      NUMBER=1
   65 NEW=NC+1
   70 DO 75 I=1,NV
   75 PP(KMAX,I)=PP(NEW,I)
```

```
      FY(KMAX)=FY(NEW)
      GO TO 45
C
C     EXPANSION
C
   80 DO 85 I=1,NV
   85 PP(NC+2,I)=GAMMA*PP(NC+1,I)+(1.0-GAMMA)*PP(NC,I)
      CALL OBJFN(NC+2)
      NWHER=2
      IF(FY(NC+2).GT.FY(KMIN)) GO TO 65
      NWHER=3
      NEW=NC+2
      GO TO 70
C
C     CONTRACTION
C

   90 IF(FY(NC+1).GE.FY(KMAX)) GO TO 100
      DO 95 I=1,NV
   95 PP(KMAX,I)=PP(NC+1,I)
      FY(KMAX)=FY(NC+1)
  100 DO 105 I=1,NV
  105 PP(NC+1,I)=BETA*PP(KMAX,I)+(1.0-BETA)*PP(NC,I)
      CALL OBJFN(NC+1)
      NWHER=4
      IF(FY(NC+1).LT.FY(KMAX)) GO TO 65
C
C     CONTRACTION FAILURE
C
      DO 120 J=1,NP
      IF(J.EQ.KMIN) GO TO 120
      DO 110 I=1,NV
  110 PP(J,I)=(PP(J,I)+PP(KMIN,I))/2.0
      CALL OBJFN(J)
  120 CONTINUE
      NWHER=5
      GO TO 45
  125 WRITE(6,305)
      GO TO 145
  135 WRITE(6,300)
  145 WRITE(6,350)ITN,FY(KMIN),(PP(KMIN,I),I=1,NV)
      WRITE(6,250)COUNT
      COUNT=-10.0
      CALL OBJFN(KMIN)

  200 FORMAT(1H1,///)
  220 FORMAT(///20X,30HOPTIMIZATION BY SIMPLEX METHOD////)
  250 FORMAT(F8.3)
  260 FORMAT(I3)
  300 FORMAT(///20X,11HCONVERGENCE////)
  305 FORMAT(///20X,14HNO CONVERGENCE////)
  310 FORMAT(12X,9(1PE11.4,2X))
  350 FORMAT(2X,6HITN =,I4,5X,21HOBJECTIVE FUNCTION =,1PE14.7,/20X,11H
     *PARAMETERS =,2(10X,1PE11.4))
      END
```

```
      SUBROUTINE OBJFN(M)
      COMMON Y(100),PP(10,6),FY(10),SIG(2,10),VAL(100),FTN(2),DVN(2),CO
     *UNT,WO,NW,DW,N,DT,NV,T(100),RT(100),RD(50),CD(50),GD(50),W(50)
      DIMENSION R(50),C(50),G(50)
      TD=PP(M,1)
      PE=PP(M,2)
      Z=88.0
      UG=Z/TD
      DG=UG*Z/PE
C
C     CALCULATE THE THEORITICAL FREQUENCY RESPONSE
C
      DO 50 K=1,NW
      A=4.0*W(K)*TD/PE
      B=0.50*ATAN(A)
      BB=(1.+A*A)**0.25*COS(B)
      D=(1.+A*A)**0.25*SIN(B)
      X0=1.+BB*BB-D*D
      X1=SINH(PE*BB/2.)
      X2=COS(PE*D/2.)
      X3=COSH(PE*BB/2.)
      X4=SIN(PE*D/2.)
      AL1=X0*X1*X2-2.*BB*D*X3*X4+2.*BB*X3*X2-2.*D*X1*X4
      AL2=2.*BB*D*X1*X2+X0*X3*X4+2.*D*X3*X2+2.*BB*X1*X4
      R(K)=2.*EXP(PE/2.)*(BB*AL1+D*AL2)/(AL1**2.+AL2**2.)
      C(K)=2.*EXP(PE/2.)*(D*AL1-BB*AL2)/(AL1**2.+AL2**2.)
      IF(K.GT.1) GO TO 50
      WRITE(6,1000)X0,X1,X2,X3,X4,A,B,BB,D,AL1,AL2,R(K),C(K)
 1000 FORMAT(2X,13F9.5)
   50 CONTINUE
      DO 60 K=1,NW
   60 G(K)=(R(K)**2.+C(K)**2.)**0.5
C
C     CALCULATE THE ERROR BETWEEN THE CALCULATED AND OBSERVED RESPONSES
C
      SUM=((R(1)-RD(1))**2.+(C(1)-CD(1))**2.+(R(N)-RD(N))**2.+(C(N)-CD(
     *N))**2.)/2.
      SUM=SUM*2.
      NW1=NW-1
      DO 120 K=2,NW1
  120 SUM=SUM+(R(K)-RD(K))**2.+(C(K)-CD(K))**2.
      PHI=SQRT(SUM/NW)
      FY(M)=PHI
      IF(COUNT.NE.-10) GO TO 250
C
C     OUTPUT
C
      WRITE(6,1100)Z,UG,DG,PE,TD
```

```
1100 FORMAT(5X,3HZ= ,G10.4,5X,4HUG= ,F6.3,5X,4HDG= ,G10.4,5X,4HPE= ,F8.
     *3,5X,4HTD= ,F8.4)
     WRITE(6,1200)
1200 FORMAT(//,6X,4HC(T),8X,4HE(T),3X,4HTIME,//)
     DO 130 J=1,N
 130 WRITE(6,1300)Y(J),RT(J),T(J)
1300 FORMAT(5X,F6.3,5X,F6.4,2X,F5.2)
     WRITE(6,1400)
1400 FORMAT(///,6X,4HGCAL,5X,5HGEXPT,4X,4HFREQ,/)
     DO 140 J=1,NW
 140 WRITE(6,1500)G(J),GD(J),W(J)
1500 FORMAT(1X,2F10.6,1X,F6.3)
     WRITE(6,1600)PHI
1600 FORMAT(//,1X,16HRESIDUAL ERROR= ,F14.9)
     WRITE(6,1700)
1700 FORMAT(///)
 250 CONTINUE
     RETURN
     END
```

APPENDIX C

The flux of solids in the column relative to the stationary wall is given by

$$\text{Flux} = \left(\frac{V_p + U_L}{1-\varepsilon_g}\right) C_s \qquad (C.1)$$

where V_p and U_L are the contributions to the average solid velocity due to sedimentation and convection respectively, and C_s is the solid concentration at any point in the column. It should be noted that V_p is not the solid slip velocity but a solid settling velocity in the presence of gas bubbles. The superficial velocities are used here because the results of Bhatia and Weber (1972) as well as those of the author (Figure 4.7) revealed that the average solid concentration in the column does not depend on the gas hold-up.

The solid settling velocity in the presence of gas bubbles was calculated using the following relationships (Ramachandran and Chaudhari, 1983):

$$V_p = \frac{g\, d_p^2\, (\rho_p - \rho_L)}{18 \mu_L} \quad \text{for } Re_p < 0.4 \qquad (C.2)$$

and

$$V_p = \left[0.0178\, \frac{g^2 (\rho_p - \rho_L)^2}{\rho_L \mu_L}\right]^{1/3} d_p \quad 0.4 < Re_p < 500 \qquad (C.3)$$

where

$$Re_p = \frac{V_p\, \rho_L\, d_p}{\mu_L} \qquad (C.4)$$

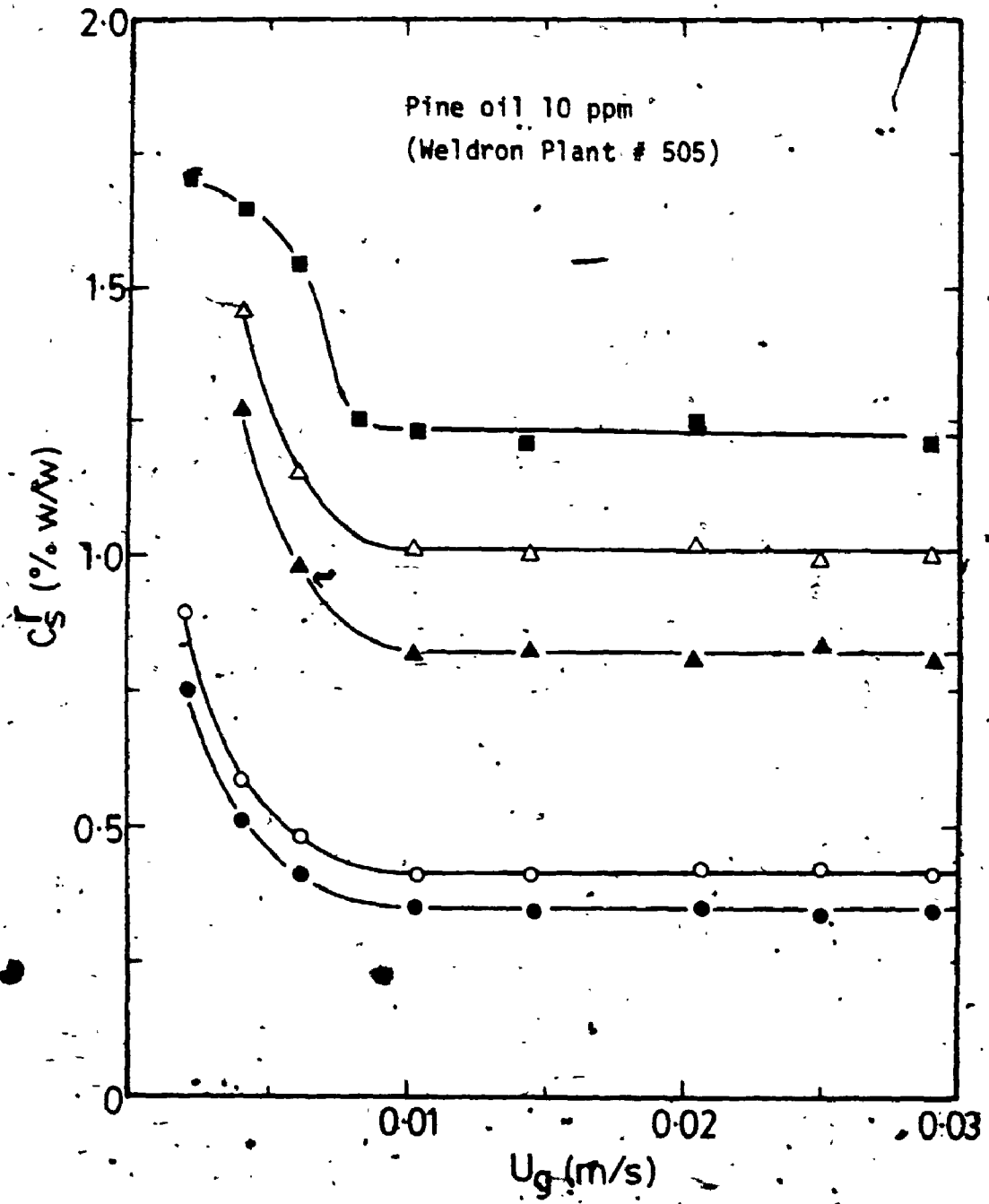

Figure 4.7 Variation of solid to liquid ratio in the column with feed solid concentration: (○, ●) 2.4 wt. %; (△, ▲) 5.0 wt. % and (■) 8.4 wt. %. The open and closed symbols represent liquid velocities of 0.0043 m/s and 0.0063 m/s respectively.

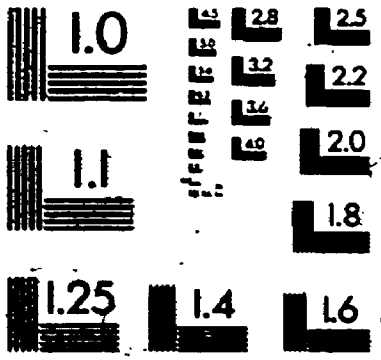

If the gas hold-up does not vary with height, the solid concentration C_s may be assumed to be constant since the flux at steady state will be the same over the column height. The average solid concentration is therefore given by

$$C_s^r = \left(\frac{U_L}{U_L + V_p}\right) C_s^f \qquad (C.5)$$

For poly-dispersed solids, equation C.5 may be rewritten as

$$C_s^r = \sum_i \left(\frac{U_L C_i^f}{U_L + V_{p_i}}\right) \qquad (C.6)$$

$$= C_s^f \sum_i \left(\frac{U_L x_i^f}{U_L + V_{p_i}}\right) \qquad (C.7)$$

where x_i^f is the weight ratio of fraction i in the feed. For the sand used in this study (Weldron Plant Designation 505 and 705), particle settling velocities of the various size fractions were estimated and the results are shown in Table C.1.

Size Fraction (μm)	$\bar{d}_p$ (μm)	$V_p * 10^2$ (m/s)	Weight Fraction 505*	705*
-63	44	0.16	0.005	0.05
-88 +63	75	0.48	0.038	0.19
-106 +88	96	1.54	0.067	0.19
-125 +106	115	1.84	0.07	0.17
-150 +125	137	2.20	0.17	0.27
-177 +150	163	2.62	0.18	0.03
-210 +177	193	3.09	0.16	0.07
-250 +210	230	3.69	0.17	0.02
-350 +250	300	4.81	0.10	0.008
+350	400	6.41	0.04	0.002

* Weldron, Plant Designation for the sand.

On substituting the values for x_i^f and V_{p_i} into equation C.7, the values shown in Table 5.8 were obtained.

BIBLIOGRAPHY

Afschar, A.S. and K. Schügerl (1968). Eigenschaften von dreiphasen - fließbetten mit gleichstrom von wasser und luft. Chem. Eng. Sci. 23, 267.

Akita, K. and F. Yoshida (1974). Bubble size, interfacial area, liquid-phase mass transfer coefficients in bubble columns. Ind. Eng. Chem. Process Design Develop. 13(1), 84-91.

Alexander, B.F. and Y.T. Shah (1976). Axial dispersion coefficients in bubble columns. Chem. Eng. J., 11, 155.

Anfruns, J.J. and J.A. Kitchner (1977). Rate of capture of small particles in flotation. Trans. Inst. Min. Metall. 86, C9.

Anon. (1965). Flotation column due for mill scale tests in Canada. Engng. Min. J., 166, 76.

Anon. (1974). Syncrude Canada modifies Mildred Lake Scheme. Canadian Petroleum 14, 28.

Aoyama, Y., K. Ogushi, K. Koide and H. Kubata (1968). Liquid mixing in concurrent bubble columns. J. Chem. Eng. Japan, 1(2), 158.

Argo, W.B. and D.R. Cova (1965). Longitudinal mixing in gas sparged tubular reactors. Ind. Eng. Chem. Process Design Develop., 4(4), 352.

Awasthi, R.C. and K. Vasudeva (1983). On mean residence times in flow systems. Chem. Eng. Sci. 38, 313.

Baird, M.H.I. and R.G. Rice (1975). Axial dispersion in large unbaffled columns. Chem. Eng. J., 9, 171.

Barton, D.R. and R.R. Wallace (1979). The effects of an experimental spillage of oilsands tailings sludge on benthic invertebrates. Environmental Pollution, 18, pp. 305.

Baptista, M.V. and C.W. Bowman (1969). The flotation mechanism of solids from the Athabasca oil sands. Proceedings 19th Can. Chem. Conf. Edmonton.

Bhaga, D. and M.E. Weber (1972). Holdup in vertical two and three phase flow. Can. J. Chem. Eng. 50, 323.

Bowman, C.W. (1967). Molecular and interfacial properties of Athabascas tar sands. In Proceedings: 7th World Petrol. Congress, Mexico 3, 583.

Brown, D.J. (1965). A photographic study of froth flotation. Fuel Society J., Univ. Sheffield, 16, 22.

Bushell, C.H.G. (1962). Kinetics of flotation. Trans. Soc. Min. Eng., AIME, 223, 266.

Camps, F.W. (1976). Processing Athabasca tar sands, tailings disposal. Proceedings, 26th Can. Chem. Engr. Conference, Toronto, October, paper 9a.

Chen, B.H. and A.F. McMillan (1982). Heat transfer and axial dispersion in batch bubble columns. Can. J. Chem. Eng. 60, 436.

Cienski, T. and V. Coffin (1981). Column flotation operations at Mines Gaspe Molybdenum circuit. Can. Min. J. 102, 28.

Clark, K.A. (1944). Hot water separation of Alberta bituminous sands. Trans. Can. Inst. Mining Met. 47, 257-274.

Clements, W.C. Jr. and K.B. Schnelle (1963). Pulse testing for dynamic analysis: An investigation of computational methods and difficulties. Ind. Eng. Chem. Process Design Develop. 2, 94.

Cova, D.R. (1966). Catalyst suspension in gas-agitated tubular reactors. Ind. Eng. Chem. Process Des. Develop. 5, 20.

Davis, R.E. and A. Acrivos (1966). The influence of surfactants on the creeping motion of bubbles. Chem. Eng. Sci. 21, 681.

Danckwerts, P.V. (1953). Continuous flow systems, distribution of residence times. Chem. Eng. Sci. 2, 1.

Deckwer, W.D., U. Graeser, H. Langemann and Y. Serpemen (1973). Zones of different mixing in the liquid phase of bubble columns. Chem. Eng. Sci. 28, 1223.

Devine, W.D., Y.T. Shah and B.I. Morsi (1985). Liquid phase axial mixing in a bubble column with viscous non-Newtonian liquids. Can. J. Chem. Eng. 63, 195.

Dobby, G.S. (1984). A fundamental flotation model and flotation column scale-up. Ph.D. Thesis, McGill University, Montreal, Canada.

Dobby, G.S. and J.A. Finch (1985). Mixing characteristics of industrial flotation columns. Chem. Eng. Sci. 40, 1061.

Dobby, G.S. and J.A. Finch (1986). Flotation column scale-up and modelling. CIM Bulletin, 78, 89.

Eigeles, M.A. (1950). Theoretical basis of the flotation of non-sulphide minerals. In "An introduction to the theory of flotation" V.I. Klassen and V.A. Mokrousov, Chapter 14, Butterworths, London, 1963.

Engelbrecht, J.A. and E.T. Woodburn (1975). The effects of froth height, aeration rate, and gas precipitation on flotation. J. South African Inst. Min. Metal. 75, 125.

Environment Canada (1984). Dry tailings disposal from oil-sands mining. Vols. I and II with appendices A-D. Unpublished report of the Industrial Programs Branch, Environment Protection Services, Ottawa.

Epstein, N. (1981). Three phase fluidization: some knowledge gaps. Can. J. Chem. Eng. 59, 649.

Fahim, M.A. and Wakao, N. (1982). Parameter estimation from tracer response measurements. Chem. Eng. J. 25, 1.

Farkas, E.J. and P.F. LeBlond (1969). Solids concentration profile in the bubble column slurry reactor. Can. J. Chem. Eng. 47, 215.

Finch, J.A. and G.W. Smith (1975). Bubble-solid attachment as a function of bubble surface tension. Can. Metall. Quarterly 14(1), 47-51.

Finch, J.A. and G.W. Smith (1981). In 'Anionic surfactants - physical chemistry of surfactant action'. Reynders, E.H. (ed.), Marcel Dekker, New York, Chapter 8.

Flint, L.R. (1971). Bubble column flotation. Ph.D. Thesis, University of Queensland, Australia.

Flint, L.R. (1973). Factors influencing the design of flotation equipment. Miner. Sci. Eng. 5, 232.

Fuerstenau, D.W. and T.W. Healy (1972). In 'Adsorptive bubble fractionation techniques' R. Lemlich (ed.), Academic Press, New York, Chapter 6.

Gaudin, A.M. (1930). Selectivity index: a yardstick of the segregation accomplished by concentrating operations. Trans. Inst. Min. Metall. Eng. 87, 483.

Gaudin, A.M. (1957). Flotation. 2nd Edition. New York: McGraw Hill.

Gewers, C.W.W. (1968). Colloid and surface chemical problems in non-conventional heavy oil recovery. Journal of Can. Petrol. Techn. 7, 85.

Glembotskii, V.A., V.I. Klassen and I.N. Plaskin. (1963). Flotation, p. 595. Primary Sources, N.Y.

Gondo, S., S. Tanaka, K. Kazuyoshi and K. Kusunoki (1973). Liquid mixing by large gas bubbles in bubble columns. Chem. Eng. Sci. 28, 1437.

Guillemin, E.A. (1963). Theory of linear physical systems. J. Wiley, New York.

Hocking, M.B. (1977). Physical characteristics and microbiological settling-rate modification of aqueous suspensions from hot-water-process oil-sands extraction. Fuel 56(7), 334.

Holcombe, N.T., D.N. Smith, H.N. Knickle and W. O'Dowd. (1983). Thermal dispersion and heat transfer in non-isothermal bubble columns. Chem. Eng. Commun. 21, 135.

Houghton, G., A.M. McLean and P.D. Ritchie (1957). Mechanism of formation of gas bubble-beds. Chem. Eng. Sci. 7, 40.

Houzelot, J.L., M.F. Thiebaut, J.C. Charpentier and J. Schiber (1985). Contribution to the hydrodynamic study of bubble columns. Intern. Chem. Eng. 25(4), 645.

Imafuku, K., T.Y. Wang, K. Koide and H. Kubota (1968). The behaviour of suspended solid particles in the bubble column. J. Chem. Engr. Japan 1, pp. 153.

Imaizumi, T. and T. Inoue (1963). Kinetic consideration of froth flotation. Proc. 6th Intern. Mineral Processing Congress, Cannes. A. Robert (ed.). Pergamon Press, Oxford.

Ityokumbul, M.T., N. Kosaric, W. Bulani, and W.L. Cairns (1985a). Froth flotation for the beneficiation of heavy minerals from oil sand tailings. AOSTRA J. Res. 2(1), 59-66.

Ityokumbul, M.T., N. Kosaric, W. Bulani and W.L. Cairns (1985b). Factors affecting the recovery of heavy minerals from oil sand tailings by flotation. Paper presented at the 20th Can. Symp. on Water Pollution Research, Toronto, Feb. 21. Also published in Water Poll. Res. J. Canada 21, 21 (1986).

Ityokumbul, M.T., W. Bulani, N. Kosaric and W.L. Cairns (1985c). Flotation process invention. Internal Report of an Invention to The University of Western Ontario Research Office.

Ityokumbul, M.T., W. Bulani and N. Kosaric (1986a). Economic and environmental benefits from froth flotation recovery of titanium, zirconium, iron and rare earth minerals from oilsand tailings. Paper accepted for the 13th Biennial International Conference of the IAWPRC to be held in Rio de Janeiro, August 17-22. Also published in Water Sci. Tech. 19, 323.

Ityokumbul, M.T., N. Kosaric and W. Bulani (1986b). A note on experimental methods for parameters estimation for bubble columns reactors. Submitted to Chem. Eng. Sci.

Ityokumbul, M.T., W. Bulani and N. Kosaric (1986c). Estimation of true moments from truncated data. An experimental evaluation. Submitted to Canadian Journal of Chemical Engineering.

Jameson, G.J., S. Nam and M. Moo Young (1977). Physical factors affecting recovery rates in flotation. Miner. Sci. Eng. 9, 103.

Joshi, J.B. (1980). Axial-mixing in multiphase contactors a unified correlation. Trans. Inst. Chem. Eng. 58, 155.

Kara, S., B.G. Kelkar, Y.T. Shah and N.L. Carr (1982). Hydrodynamics and axial mixing in a three-phase bubble column. Ind. Eng. Chem. Process Des. Dev. 21, 584.

Kato, Y., A. Nishiwaki, T. Fukuda and S. Tanaka (1972). The behaviour of suspended solid particles and liquid in bubble columns. J. Chem. Eng. Japan 5, 112.

Kato, Y., S. Morooka, T. Kago, T. Saruwatari and S. Yang (1985). Axial holdup distributions of gas and solid particles in three phase fluidized bed for gas-liquid (slurry)-solid systems. J. Chem. Eng. Japan 18, 308.

Kelkar, B.G., S.P. Godbole, M.F. Honath, Y.T. Shah, N.L. Carr and W.D. Deckwer (1983). Effect of addition of alcohols on gas holdup and backmixing in bubble columns. AIChE J. 29(3), 361.

Kelkar, B.G., Y.T. Shah and N.L. Carr (1984). Hydrodynamics and axial mixing in a three phase bubble column, effects of slurry properties. Ind. Eng. Chem. Process Des. Develop. 23, 308.

Kessick, M.A. (1979a). Structure and properties of oil sands clay tailings. J. Can. Petrol. Technology 18(1), 49.

Kim, S.D. (1974). Hydrodynamic properties of two and three phase fluidized beds. Ph.D. Thesis, University of Western Ontario, London, Canada.

King, R.P., T.A. Hatton and D.G. Hulbert (1975). Bubble loading during flotation. Trans. Inst. Min. Met. 83, C112.

Klassen, V.I. and V.A. Mokrousov (1963). An introduction to the theory of flotation. Butterworths, London, p. 304.

Klimpel, R.R. (1984). Use of chemical reagents in flotation. Chem. Eng. 91(19), 75.

Koide, K., T. Yasuda, S. Iwamoto and E. Fukuda (1983). Critical gas velocity required for complete suspension of solids particles in solid-suspended bubble columns. J. Chem. Engr. Japan 16(1), 7.

Kojima, H. and K. Asano (1981). Hydrodynamic characteristics of a suspension-bubble column. Intern. Chem. Eng. 21, 473.

Kolbel, H., R. Beinhauer and H. Langemann (1972). Dynamische messung des relativen gasgehaltes in blassensaulen mittels adsorption von rontgenstrahlen. Chem. Ing. Tech. 44, 697.

Konig, B., R. Bucholz, J. Lucke and K. Schugerl (1978). Longitudinal mixing of the liquid phase in bubble columns. Ger. Chem. Eng. 1, 199.

Kosaric, N., N.C.C. Gray, A.L. Stewart and W.L. Cairns (1981). Bacteria-induced deemulsification of complex petroleum emulsions. Report prepared for Alberta Oil Sands Technology and Research Authority under AOSTRA Agreement #211, p. 67.

Kramers, J.W. and Brown, R.A.S. (1976). Survey of heavy minerals in the surface-mineable area of the Athabasca oilsand deposits. CIM Bull. 69, 92.

Kruyt, H.R. (1954). Colloid Science, Vol. I. Elsevier, Amsterdam.

Kubota, K., S. Hayashi and Y. Bitoh (1986). Optical measurement of slurry concentration profile in a concurrent-flow gas-slurry column. Ind. Eng. Chem. Fundam. 25, 181.

Kulkarni, R.D. and P. Somasundaran (1975). Kinetics of collector adsorption at the liquid/air interface and its role in hematite flotation. AIChE. Symp. Series 71(150), 124.

Kumar, A., T.T. Dagaleesan, G.S. Laddha and H.E. Hoelscher (1976). Bubble swarm characteristics in bubble columns. Can. J. Chem. Eng. 54, 503.

Laplante, A.R., J.M. Toguri and H.W. Smith (1983). The effect of air flow rate on the kinetics of flotation. Part 2: The transfer of material from the froth over the cell lip. Int. J. Min. Process. 11, 227.

Lehrer, I.H. (1984). Turbulent and dispersion coefficients in the liquid in a two-phase bubble column. AIChE J. 30, 654.

Leja, J. and J.H. Schulman (1954). Flotation theory: molecular interactions between frother and collectors at solid/liquid/air interfaces. Trans. Amer. Inst. Min. (Metall.) Engrs., Min. Engng. 221.

Lemlich, R. (1966). A theoretical approach to nonfoaming adsorptive bubble fractionation. AIChE. J. 12, 802.

Lemlich, R. (1972). Adsorptive bubble separation techniques. Academic Press, New York, pp. 331.

Levenspiel, O. (1972). Chemical reaction engineering: An introduction to the design of chemical reactors. Chap. 9, pp. 242-308, J. Wiley, New York.

Levenspiel, O. (1978). The chemical reactor Omnibook. Oregon State University Bookstores, Inc.

Levich, V.G. (1962). Physicochemical hydrodynamics. Prentice-Hall, Englewood Cliffs, N.J.

Lindland, K.P. and S.G. Terjesen (1965). The effect of a surface-active agent on mass transfer in falling drop extraction. Chem. Eng. Sci. 5, 1.

Magnussen, P. and V. Schumacher (1978). Axial mixing of liquid in packed bubble columns and perforated plate columns of large diameter. Chem. React. Eng. ACS Symp. Ser., Houston, V.W. Weekman and D. Luss (eds), 65, 337.

Mashelkar, R.A. (1970). Bubble columns. Brit. Chem. Eng. 15(10), 1297.

Mackenzie, J.M.W. (1970). Interactions between oil drops and mineral surfaces. Trans. AIME 247(3), 202-208.

Mackinnon, M.D. (1981). A study of chemical and physical properties of Syncrude's tailing pond, Mildred Lake. Syncrude Environmental Research Monograph, pp. 1-81 and Appendix.

Mackinnon, M.D. and H. Boerger (1986). Description of two treatment methods for oil sands tailings water. Paper presented at 21st Can. Symp. on Water Pollution Research, CCIW, Burlington, April 30.

Michelsen, M.L. (1972). A least squares method for residence time distribution analysis. Chem. Eng. J. 4, 171.

Moschopedis, S.E., J.F. Fryer and J.G. Speight (1977). Water soluble constituents of Athabasca bitumen. Fuel 56, 109-110.

Muroyama, K. and L.S. Fan (1985). Fundamentals of gas-liquid-solid fluidization. AIChE. J. 31, 1.

Murphy, K.L. and P.L. Timpany (1967). Design and analysis of mixing for an aeration tank. J. Sanitary. Eng. Div. 93(SA5), 1.

Nelder, J.A. and R. Mead (1964). A simplex method for function minimization. Computer J. 7, 304.

Oels, U., J. Lucke, R. Buchholz and K. Schugerl (1978). Influence of gas distributor type and composition of liquid on the behaviour of a bubble column bioreactor. Ger. Chem. Eng. 1, 115.

Pinford, T.A. (1972). Precipitate flotation in "Adsorptive bubble separation techniques", R. Lemlich (ed.), Chapter 5. Academic Press, New York.

Ramachandran, P.A. and R.V. Chaudhari (1983). Three phase catalytic reactors. Gordon and Breach Science Publishers, New York.

Raymond, D.R. and S.A. Zieminski (1971). Mass transfer and drag coefficients on bubbles rising in dilute aqueous solutions. AIChE J. 17, 57.

Reay, D. (1973). Ph.D. Thesis, McGill University, Montreal, Canada.

Reith, T., S. Renken and B.A. Isreal (1968). Gas hold-up and axial mixing in the fluid phase of bubble columns. Chem. Eng. Sci. 23, 619.

Rice, R.G., A.D. Oliver, J.P. Newman and R.J. Wiles (1974). Reduced dispersion using baffles in column flotation. Powder Techn. 10, 201.

Rice, R.G., J.M.I. Tupperainen and R.M. Hedge (1981). Dispersion and hold-up in bubble columns. Comparison of rigid and flexible spargers. Can. J. Chem. Eng. 59, 677.

Richardson, J.F. and W.N. Zaki (1954). Sedimentation and fluidization: Part I. Trans. Inst. Chem. Eng. 32, 35.

Riquarts, H.-P. (1981). A physical model for axial mixing of the liquid phase for heterogenous flow regime in bubble columns. Ger. Chem. Eng. 4, 18.

Robinson, B.A. and J.W. Tesler (1986). Characterization of flow maldistribution using inlet-outlet tracer techniques: an application of internal residence time distributions. Chem. Eng. Sci. 41, 469.

Sada, E., H. Kumazawa and C.H. Lee (1986). Influences of suspended fine particles on gas holdup and mass transfer characteristics in a slurry bubble column, AIChE J. 32, 853.

Sangnimnuan, A., G.N. Prasad and J.B. Agnew (1984). Gas holdup and backmixing in a bubble column reactor under coal hydroliquefaction conditions. Chem. Eng. Commun. 25, 193.

Schugerl, K. (1967). Wechselwirkung zwischen stromung und vermishung des anstromgases in gasdurchstromtem fliepbetten. Chem. Eng. Sci. 22, 793.

Schugerl, K., U. Oels and J. Lucke (1977). Bubble column bioreactors. Tower bioreactors without mechanical agitation, in Advances in Biochemical Engineering. Ghose, T.K., A. Fiechter and N. Blakebrough (Eds.), 7, 1.

Schumpe, A., Y. Serpemen and W.D. Deckwer (1979). Effective use of bubble column reactors. Ger. Chem. Eng. 2, 234.

Shah, Y.T. and W.D. Deckwer (1985). Fluid-fluid reactors, in "Scale-up in chemical process industries", ed. R. Kabel and A. Bisio. J. Wiley, New York.

Shah, Y.T., G.J. Stiegel and M.M. Sharma (1978). Backmixing in gas-liquid reactors. AIChE. J. 24(3), 369.

Shah, Y.T., B.G. Kelkar, S.P. Godbole and W.D. Deckwer (1982). Design parameters estimations for bubble column reactors. AIChE. J. 28(3), 353.

Shulman, H.L. and M.C. Molstad (1950). Gas bubble columns for gas-liquid contacting. Ind. Eng. Chem. 42, 1058.

Smith, D.N. and J.A. Ruether (1985). Dispersed solid dynamics in a slurry bubble column. Chem. Eng. Sci. 40, 741.

Smith, D.N., J.A. Ruether, Y.T. Shah and M.N. Badgujar (1986). Modified sedimentation-dispersion model for solids in a three phase slurry column. AIChE. J. 32, 426.

Taggart, A.F. Ed. (1945). Handbook of mineral dressing: ores and industrial minerals. J. Wiley and Sons, New York, Chapter 12.

Takahashi, T., T. Miyahara and Y. Nishizaki (1979). Separation of oily water by bubble column. J. Chem. Engr. Japan 12(5), 394-399.

Tomlinson, H.S. and M.G. Fleming (1963). Flotation rate studies. Proc. 6th International Mineral Processing Congress, Cannes. A. Roberts (ed.). Pergamon Press, Oxford, p. 563.

Towell, G.D. and G.H. Ackerman (1972). Axial mixing of liquid and gas in large bubble reactors. Proc. 5th European/2nd Intern. Symp. on Chem. React. Engr., Amsterdam.

Trevoy, L.W., R. Schutte and R.R. Goforth (1978). Development of the heavy minerals potential from the Athabasca tar sands. CIM Bulletin 71, 175.

Van Ham, N.J.M., L.A. Behie and W.Y. Svrcek (1983). The effect of air distribution on the induced air flotation of fine oil in water emulsions. Can. J. Chem. Eng. 61, 541.

Viswanathan, K. and D.S. Rao (1984). Inviscid liquid circulation in bubble columns. Chem. Eng. Commun. 25, 133.

Wendt, R., A. Steiff and P.M. Weinspach (1984). Liquid phase dispersion in bubble columns. Ger. Chem. Eng. 7, 267.

Westerterp, K.R., W.P.M. van Swaaij and A.A.C.M. Beenackers (1984). Chemical reactor design and operation, 2nd Edition. J. Wiley, Chichester.

Wheeler, D.A. (1966). Big flotation column mill tested. Eng. Min. J. 167, 98.

Wheeler, D.A. (1984). Private communication.

Zisman, W.A. (1964). In "Contact angle, wettabilities and adhesion, Advances in Chemistry, Series 43." Fowkes, F.M. and R.F. Gould (Eds.). American Chemical Society, Washington.